INSTRUMENTATION AND PERFORMANCE OF GEOSYNTHETICS BENEATH FLEXIBLE PAVEMENTS IN WINTERPORT AND FRANKFORT, MAINE

FINAL REPORT
TECHNICAL REPORT ME 97-14
DECEMBER 1998

PB99-165201

Research

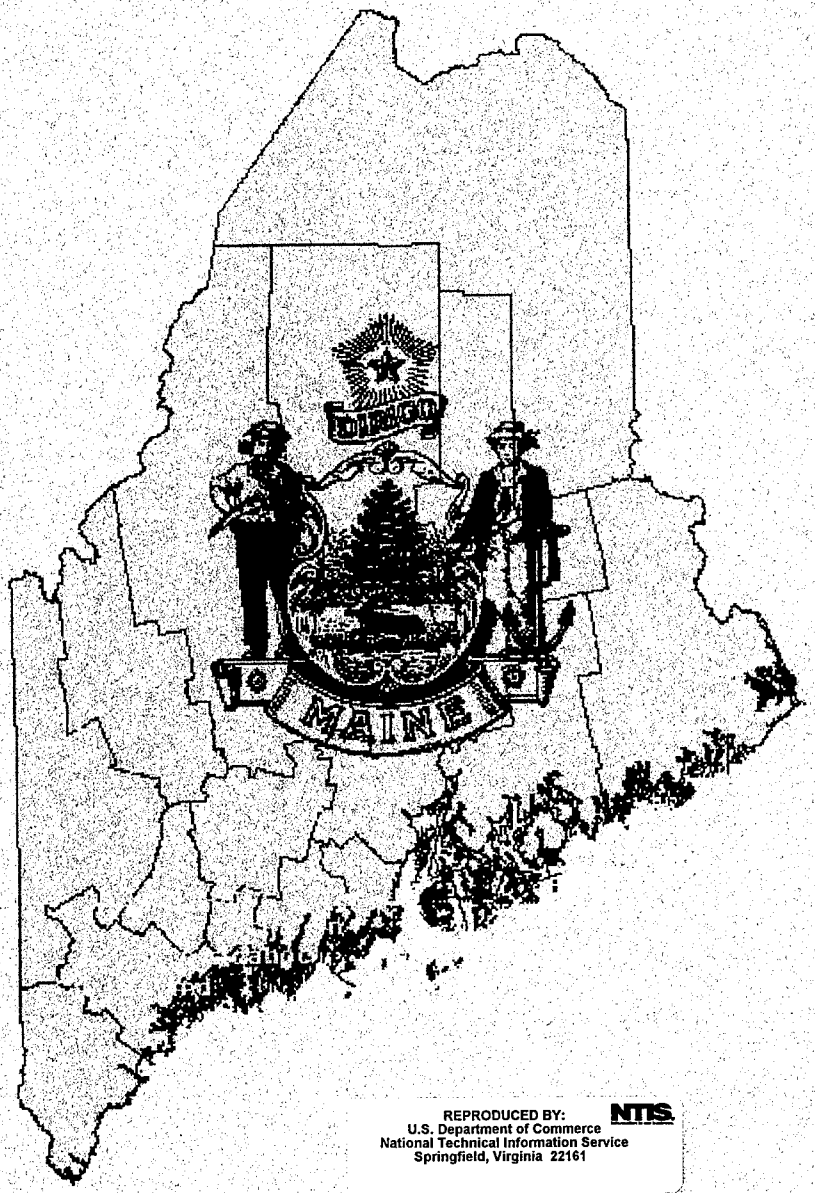

Technical Report Documentation Page

1. Report No.	2.	3. Recipient's Accession
ME 97-14		PB99-165201

4. Title and Subtitle	5. Report Date
Instrumentation and Performance of Geosynthetics Beneath Flexible Pavements in Winterport and Frankfort, Maine	December 1998
	6.

7. Author(s)	8. Performing Organization Report No.
Christine P. Fetten Dana N. Humphrey	

9. Performing Organization Name and Address	10. Project/Task/Work Unit No.
Department of Civil and Environmental Engineering University of Maine at Orono 5711 Boardman Hall Orono, ME 04469-5711	11. Contract (C) or Grant (G) No.

12. Sponsoring Organization Name and Address	13. Type of Report and Period Covered
Maine DOT 16 State House Station Augusta, ME 04469-0016	Final Report
	14. Sponsoring Agency Code

15. Supplementary Notes

16. Abstract (Limit 200 words)

The objective of this study was to evaluate the effectiveness of geosynthetics in terms of reinforcement, separation, and drainage for roadways constructed in cold regions where the aggregate base course is thicker than investigated in previous studies. This project goes beyond previous work by evaluating the effectiveness of geosynthetics as reinforcement, separation, and drainage layers in paved roadway sections with subbases ranging from 580 to 640 mm thick (23 to 25 in.).

The study was performed on a 3.0 km (1.9 mile) portion of U.S. Route 1A in the towns of Frankfort and and Winterport, Maine. The subsurface exploration revealed weak subgrade soil with an AASHTO classification of A-6 and an average laboratory CBR value of 3. The project evaluated four different geosynthetics: reinforcement geogrid, high strength geotextile; heavy weight nonwoven geotextile, and drainage geocomposite. The project was instrumented to monitor the performance 'of the geosynthetics. Loadcells attached to the geogrid showed that most of the force developed during placement and compaction of the first lift of overlying aggregate. Strain gages attached to the high strength geotextile showed similar results, although there was some evidence that the force per unit width increased somewhat with time. Overall the force in the geogrid and high strength geotextile was only a small fraction of the ultimate strengths of the materials. Piezometer readings showed that a drainage geocomposite placed 450 mm (18 in.) below subgrade may have been effective in reducing pore water pressures. Falling weight deflectometer results were inconclusive in evaluating the effects of the geosynthetics. Further monitoring will be conducted to evaluate long term performance.

17. Document Analysis/Descriptors	18. Availability Statement
Keywords: geotextile, geogrid, drainage geocomposite, geosynthetics, reinforcement, separation, drainage, frost penetration	

19. Security Class (this report)	20. Security Class (this page)	21. No. of Pages	22. Price

GENERAL DISCLAIMER

This document may be affected by one or more of the following statements:

- This document has been reproduced from the best copy furnished by the sponsoring agency. It is being released in the interest of making available as much information as possible.
- This document may contain data which exceeds the sheet parameters. It was furnished in this condition by the sponsoring agency and is the best copy available.
- This document may contain tone-on-tone or color graphs, charts and/or pictures which have been reproduced in black and white.
- The document is paginated as submitted by the original source.
- Portions of this document are not fully legible due to the historical nature of some of the material. However, it is the best reproduction available from the original submission.

A STUDY FOR THE
MAINE DEPARTMENT OF TRANSPORTATION

INSTRUMENTATION AND PERFORMANCE OF GEOSYNTHETICS BENEATH FLEXIBLE PAVEMENTS IN WINTERPORT AND FRANKFORT, MAINE

Bureau of Planning, Research, & Community Services
Transportation Research Division
Technical Report 97-14
December 1, 1998

Prepared by:
Christine P. Fetten
Dana N. Humphrey

Department of Civil and Environmental Engineering
University of Maine
Orono, Maine

INSTRUMENTATION AND PERFORMANCE OF GEOSYNTHETICS BENEATH FLEXIBLE PAVEMENTS IN WINTERPORT AND FRANKFORT, MAINE

Christine Fetten and Dana N. Humphrey
Department of Civil and Environmental Engineering
University of Maine, Orono, Maine

-EXECUTIVE SUMMARY -

The Maine Department of Transportation is evaluating the reinforcing, separation and filtration potential of geosynthetics in a 3.0 km (1.9 mile) portion of U.S. Route 1A in the towns of Frankfort and Winterport. Previous studies of geosynthetic reinforcement in flexible pavement systems have examined subbase thickness ranging from 50 to 305 mm (2 to 12 in.). This project goes beyond previous work by evaluating the effectiveness of geosynthetics as reinforcement, separation, and drainage layers in paved roadway sections with subbases ranging from 580 to 640 mm thick (23 to 25 in.).

The objective of this study was to evaluate the effectiveness of geosynthetics in terms of reinforcement, separation, and drainage for roadways constructed in cold regions where the aggregate base course is thicker than investigated in previous studies. Primary emphasis was given to the reinforcement application. To perform this evaluation the following tasks were accomplished:

1. A literature review was conducted of laboratory tests, field work, and computer analyses of geosynthetics used beneath unpaved and paved roads.

2. A 3.0 km (1.9 mile) portion of U.S. Route 1A was instrumented with strain gages, loadcells, piezometers, and thermocouples to evaluate the reinforcing and drainage effectiveness of the geosynthetics.

3. The roadway was monitored from construction during summer and fall, 1997 through August, 1998. The stress in the geogrid and geotextile, pore water pressures in the drainage section, and the frost depth in several sections were investigated.

4. Pavement performance was measured before and after construction with a falling weight deflectometer (FWD). Structural numbers were then obtained by processing the FWD results in the Darwin Pavement Design and Analysis System. The performance of each section was evaluated by comparing the improvement of the before and after structural numbers as well as direct comparison of the after structural numbers obtained from the sections.

The literature review included studies on unpaved temporary or haul roads, and flexible pavements with reinforcing geosynthetics in the substructure. Possible reinforcement mechanisms included: providing confinement for aggregates in the subbase course, confinement of the subgrade layer, increases in the effective shear strength, and improved load distribution. The geosynthetic must be deformed to mobilize the tensile force needed to obtain a reinforcing benefit. This presents a problem for paved roads, since the pavement cannot tolerate large deformations.

There have been few studies evaluating the use of geosynthetics in flexible pavement systems. Laboratory studies that related load cycles to rut depth and pavement performance were conducted at the University of Waterloo, Montana State University, Georgia Institute of Technology, and Virginia Polytechnic Institute. Many of these studies quantify the benefits of geosynthetics by measuring the increased load applications and/or reduced aggregate thickness made possible by the geosynthetics. The laboratory studies applied loads to a circular plate. This could overestimate the potential benefits of the geosynthetic since the applied force will be in all directions (axisymmetric), in comparison to an actual roadbed, which is plane strain loading, where there is negligible strain in the direction parallel to the centerline. Observed improvement was dependent on sectional properties such as subgrade strength, aggregate thickness, geosynthetic location and geosynthetic stiffness. Results have shown some benefits of geogrid/geotextile reinforcement in flexible pavements. However, the maximum subbase thickness in these studies was 300 mm (12 in.) and the maximum pavement thickness was 160 mm (6.3 in.) thick. In general the reinforcing benefit decreased as the aggregate subbase thickness, pavement thickness, and subgrade strength increased. No literature was found that studied the effects of geosynthetic reinforcement in cold region areas with the subbase and asphalt layers that are as thick as used in Maine.

A computer analysis conducted at the Georgia Institute of Technology showed that sections with an asphalt layer greater than 65 to 90 mm (2.5 to 3.5 in.) thick were not expected to show improvement with reinforcement geosynthetics, even if they were placed on weak subgrades. The study also showed that the effect of geosynthetics beneath flexible pavements in terms of stress, strain and deflection are relatively small for geosynthetic reinforced sections designed to carry more than about 200,000 equivalent 80-kN (18-kip) single axle loads. The reconstructed section of Route 1A is designed to carry 1.5 million equivalent 80-kN (18-kip) single axle loads.

A design procedure was proposed for geosynthetic reinforcement in flexible pavements by Penner, et al. (1985). It uses a layer coefficient ratio or equivalence factor that is applied to the reinforced layer to reflect the improved structural characteristics of the base. This analysis procedure predicts that geosynthetic reinforcement would provide no benefit for subbase aggregate layers greater than 300 mm (12 in.).

A full-scale field trial evaluating the use of reinforcement geogrid and geotextile, separation geotextile, and drainage geocomposite in the reconstruction of US Route 1A in the towns of Winterport and Frankfort was begun in May 1997 and completed in June 1998. Historically, this area has had poor pavement performance. The subsurface exploration revealed weak subgrade soil with an AASHTO classification of A-6 and an

average laboratory CBR value of 3. The project was divided into five test sections. Each section was divided into two or three subsections each with a different position of the geosynthetic.

The project evaluated four different geosynthetics. Tenax M330 reinforcement geogrid and Mirafi 67809 high strength geotextile were used in different sections (A-1, A-2, E-3, B-1, and B-2) for reinforcement. Mirafi 180N, a heavy weight nonwoven geotextile, was used for separation in Sections C-2 and E-2. Tenax Tendrain 100-2 drainage geocomposite was used in Sections D-1, D-2, and D-3 as a drainage layer. The road section consisted of a 580 to 640-mm (23 to 25-in.) layer of subbase aggregate overlain by a 180-mm (7-in.) asphalt layer. The reinforcement geogrid was placed at different depths in Sections A-1, A-2, and E-3. In Section A-1, the geogrid was placed at the bottom of a 580-mm (23-in.) subbase aggregate layer. Section A-2 had two layers of geogrid, one place at the bottom of a 640-mm (25-in.) subbase aggregate layer and the other at mid-thickness of that layer. In Section E-3, the geogrid was placed 250 mm (10 in.) below the asphalt layer. Reinforcement geotextile was placed at the bottom of a 580-mm (23-in.) subbase aggregate layer in Section B-1, and at the bottom of a 640-mm (25-in.) subbase aggregate layer in Section B-2. The drainage geocomposite was placed 460 mm (18 in.) below the subgrade layer in Section D-1, at the bottom of a 640 mm (25 in.) subbase aggregate layer in Section D-2, and at the top and bottom of a 640 mm (25 in.) subbase layer in Section D-3.

A control section was also included. It was originally constructed with 640 mm (25 in.) of subbase aggregate, however, traffic loading on the exposed aggregate surface quickly caused the section to fail. The contractor had to re-excavate this section, undercutting an additional 610 mm (24 in.) into the weak subgrade soils. The contractor then placed a total of 1250 mm (49 in.) of subbase aggregate to bring the road back to its indented grade. This problem did not occur in any of the sections with geosynthetics even though the contractor and resident engineer thought that undercutting was needed at several locations. This confirms that geosynthetics can be used to expedite construction of roads on soft subgrades.

The University of Maine instrumented sections of this project to monitor the performance of the geosynthetics. Custom-made loadcells were attached to the geogrid at five different stations. Strain gages were attached to the geotextile to monitor the tensile forces in two sections. The loadcells or strain gages were attached at offsets that positioned the instruments in the outside wheel path of the right (northbound) lane. Three piezometers were placed at each of five stations to monitor pore water pressures in sections with drainage geocomposite as well as adjacent sections for comparison. Frost penetration was measured at four stations with thermocouples. Instrument measurements were taken from installation until August 1998.

Seven loadcells were attached to geogrid in each instrumented section. In a given section, the loadcells mounted on the geogrid had a survival rate that ranged from zero to 57%. Fortunately, sufficient loadcells remained to allow evaluation of geogrid performance. Results indicate that little force was induced in the geogrid with the majority gained during placement and compaction of the first lift of overlying subbase

aggregate. There was little subsequent change in force. In Sections A-1 and A-2 the geogrid is covered by 580 mm (23 in.) and 250 mm (10 in.) of gravel, respectively. In these sections the loadcells showed a force between about 0.75 and 1.0 kN/m (50 and 70 lb/ft). Two loadcells showed higher forces of up to 1.7 kN/m (116 lb/ft) which is only 5% of the ultimate tensile strength of the geogrid. One loadcell was in compression suggesting that there are localized areas of compression. This could have been created by a wave of geogrid that generally advanced ahead of aggregate placement being locally trapped beneath the aggregate. The force in the geogrid was essentially the same when placed at depths of 250, 580, and 640 mm (10, 23, and 25 in.) in a flexible road section with a 180 mm (7 in.) asphalt layer.

Strain gages were mounted on the reinforcement geotextile in subsections B-1 and B-2 to measure the tension during and after construction. Gages were placed in pairs, one on each side of the geotextile, to eliminate the effects of bending by averaging the reading from each pair. These gages were reliable and had 76% survival. Forces ranged from zero to 5 kN/m. For most gages, the majority of force was induced during construction. In addition, there was an apparent increase in force in most strain gages that coincided with spring thaw. The possibility that the increase could be due to temperature change or creep was examined, but stable readings during frost penetration and the force being only a small fraction of the ultimate tensile strength, suggests that these are not reasons for the force increase. Some strain gages also showed continued slow force increase after spring thaw.

Piezometers were installed in Sections C-2, D-1, D-2, D-3, and in the control section. These instruments were used to determine if the drainage geocomposite aided in dissipating pore water pressures. Pressures were averaged for the months of October through November, 1997 and June through August, 1998. Due to a malfunctioning readout box, readings were not taken at the critical period of spring melt. The Fall, 1997 readings in the subbase layer of drainage sections (D-1, D-2 and D-3) ranged from 10 to 118 mm (0.4 to 4.6 in.) of water head, while the control section had 414 mm (16 in.) of head and Section C-2 had 138 mm (5.4 in) of head. Theses readings also showed that the amount of head in the subgrade soil of the drainage sections had lower levels (-15.4 to 74 mm (0.6 to 3.0 in)) in comparison to the control section (149 mm; 6.0 in.) and Section C-2 (210 mm; 8.0 in.). Readings taken in summer, 1998 show negative head in many piezometers. This could be due to damage to the piezometers during the winter.

A substantial amount of water has come out of outlet pipes. The flow rate was highest during the spring thaw (March). After March, periods of increased flow coincided with precipitation events. Section D-1, which had a geocomposite placed 460 mm (18 in.) below the subgrade, removed the most water followed by Section D-2 with a geocomposite placed at subgrade. Section D-3 was located in a fill section. Outlet E in this section, which drained the geocomposite placed on subgrade, had less flow than in Sections D-1 and D-2. Outlet F in Section D-3, which drained a geocomposite located directly under the pavement, had no flow. This suggests that the new pavement did not allow ingress of water or that any water that penetrated the pavement was drained away by the subbase course.

Pavement performance has been measured with a falling weight deflectometer (FWD). Readings were taken prior to reconstruction and after reconstruction in April of 1998. The FWD readings were processed with the DARWin Pavement Design and Analysis System. The pavement thickness prior to reconstruction ranged from 127 to 254 mm (5 to 10 in.), making comparison of data from before reconstruction to after reconstruction difficult and possibly misleading. The highest structural number (SN) was obtained in the control sections that had to be under cut 610 mm (24 in.) due to poor subgrade conditions encountered during construction. Since the control section could not be used it for its intended purpose, Section C-2, which only had a separation geotextile placed 640 mm (25 in.) below the asphalt layer, was used as the basis for comparison with the other sections. The April 1998 structural numbers of Section C-2 were higher than the geotextile and geogrid reinforced sections. Thus, reinforcement did not increase the SN as backcalculated from Falling Weight Deflectometer tests. It is possible that the FWD was incapable of detecting the beneficial effects of the geosynthetics. The amount of improvement from the original FWD testing and post construction readings show that the greatest improvement is in the undercut section with drainage geocomposite (Section D-1). Overall, the small magnitude of induced force in the geogrid and geotextile, and little improvement in structural number suggest little reinforcing benefits for the thick subbase course used in this study. However, monitoring of the test sections should continue to fully evaluate the effects of the geosynthetics.

The structural number (SN) in the Section D-1 with drainage geocomposite placed 460 mm (18 in.) below subgrade was 7% higher than the SN in a section with only separation geotextile. However, the SN of sections with drainage geocomposite on subgrade was 7% lower than the section with only the separation geotextile. This suggests that the drainage geocomposite may slightly improve the SN when placed below the subgrade.

A STUDY FOR THE
MAINE DEPARTMENT OF TRANSPORTATION

INSTRUMENTATION AND PERFORMANCE OF GEOSYNTHETICS BENEATH FLEXIBLE PAVEMENTS IN WINTERPORT AND FRANKFORT, MAINE

Bureau of Planning, Research, & Community Services
Transportation Research Division
Technical Report 97-14
December 1, 1998

Prepared by:
Christine P. Fetten
Dana N. Humphrey

Department of Civil and Environmental Engineering
University of Maine
Orono, Maine

ACKNOWLEDGEMENTS

The authors thank the Maine Department of Transportation for their support of this research. Special thanks are given to Scott Hayden and Phil Dunn of the Maine Department of Transportation, and Tom Jewell and Jeff Wardwell from Wardwell and Sons Construction Company for all their help during the project. Karen Henry from the U.S. Army Corps of Engineers Cold Regions Research and Engineering Laboratory and Barry Christopher are thanked for their help and advice on many aspects of the project.

TABLE OF CONTENTS

LIST OF FIGURES

LIST OF TABLES

1. INTRODUCTION

1.1 BACKGROUND

The towns of Winterport and Frankfort, Maine have a history of poor subgrade soils. The soils are frost susceptible, moist silty clays and very silty fine sands. The water content is in excess of 20% in some areas and the California Bearing Ratio is low (CBR≈3). Route 1A in Winterport and Frankfort has been plagued with cracking, rutting and potholes. The rutting was so severe in some sections that water was observed coming up through the cracks (Hayden, 1996).

A subsurface investigation (Hayden, 1996) reported poor subgrade soil conditions along the entire length of the project. Water seepage was encountered above proposed subgrade at several locations. The samples indicate plastic soils with liquid limits as high as 37 and plasticity indexes of 17. These soils have poor load bearing characteristics. Three CBR tests were conducted on representative samples. These tests produced values of 2.6, 3.2, and 3.6. Due to these poor soil conditions it was calculated that a 810-mm (32-in.) structural section consisting of 180 mm (7 in.) asphalt surface and 640 mm (25 in.) of aggregate subbase would be needed. An additional, 150 mm (6 in.) of underlying granular soil was recommended as a stabilization platform. However, reinforcement geosynthetics were proposed as an alternative to the 150 mm (6 in.) stabilization lift.

Geosynthetics are used on many projects for reinforcement, separation, and drainage applications. The use of geosynthetics as reinforcement is known to be

beneficial for unsurfaced roads. However, relatively little research has been devoted to study the effects of geosynthetic reinforcement in paved roads. The Maine Department of Transportation has been using geosynthetics since the 1980's without any conclusive studies about the performance of geosynthetics as reinforcement. Moreover, the benefits to Maine roads that are derived from the drainage function of geosynthetics have not been examined. This federal highway reconstruction project (project no. F-STP-026(109)) was used to evaluate the use of geosynthetics in Maine on a 3.0 km (1.9 mile) of section of Route 1A in the towns of Winterport and Frankfort. Measurements of force in the reinforcement geogrid and geotextile section, and pore water pressure in the drainage section were compared to previous studies to evaluate the effectiveness of the different geosynthetics placed in the roadbed.

Geogrids and high strength geotextile have shown great promise in the construction of unpaved roadways or temporary construction roads. "Since soil has compressive strength but not tensile strength and geotextiles/geogrid have tensile strength but not compressive strength, the performance of a soil mass can be improved by using a geotextile/geogrid to impart tensile strength to the mass" (Rollings and Rollings, 1996). These materials can provide tensile resistance to restrain lateral movement through friction or interlocking developed between the aggregate and the geosynthetic (Holtz, et al., 1995). High strength geosynthetics can also provide membrane type support of wheel loads where the vertical component of this membrane stress helps support the applied wheel loads (Holtz, et al., 1995). In addition, Holtz, et al. (1995) state that geosynthetics can increase the bearing capacity of the system by forcing the potential bearing capacity

failure surface to develop along an alternate surface with a higher shear strength. The tension that is developed in the geotextile is achieved through wheel path rutting. However, the effectiveness of wheel path rutting for paved roads with thick pavement and subbase sections, such as used in Maine, must be examined.

Geotextiles used in separation/stabilization applications can provide the combined functions of separation and filtration and reduce the intensity of stress on the subgrade (Holtz, et al., 1995). Geotextiles can act as a separation layer to prevent the pumping of the fine grained subgrade soil into the clean base layer. This has two benefits: to prevent localized bearing failures, and potentially reduce heave and loss of strength due to thawing since overlying aggregate is kept clean. Geotextiles can also maintain the permeability in the aggregate and/or the shear strength of the granular material under a pavement (Rollings and Rollings, 1996). Contamination of the subbase materials is prevented by the separation geotextile. The geotextile also allows for drainage and water pressure dissipation in the subgrade. This will enable the subgrade to have improved strength over time.

The incorporation of a high compressive strength, high flow rate geocomposite drainage net placed along subgrade can provide positive drainage for water to escape the pavement system (Zhao and Banks, 1997). When placed below subgrade the drainage geocomposite can act as a capillary break to mitigate frost heaving (Henry, 1996). The incorporation of a geonet drainage composite within the pavement system can help reduce the time the pavement system is saturated. However the effectiveness of a

horizontal geocomposite drainage layer placed within the subbase at the subgrade/subbase interface or in the subgrade has not been investigated for the type of field conditions encountered in Maine (Hayden, et al., 1998).

The purpose of this project is to provide a rational means to judge the performance improvement and cost savings that could be derived from the use of geosynthetic reinforcement and geocomposite drainage layers in highway projects with weak subgrade soils (Hayden, 1996). Instruments installed in sections containing reinforcement geogrid and geotextile, and drainage geocomposite will measure force and pore pressure. These values will be compared to previous experiments and field studies to determine the effectiveness of the different geosynthetics.

1.2 SCOPE OF STUDY

A 3 km (1.9 mile) section of Route 1A was used to study the performance of three different geosynthetics: geogrid, geotextile, and geocomposite drainage net. The project was separated into six test sections (A-E). The test sections concentrate on different applications of the geosynthetics such as reinforcement, separation/stabilization, drainage and control section. The sections were instrumented to monitor the behavior of the different types of geosynthetics. The geogrid was instrumented with loadcells, strain gages were used on the reinforcement geotextile, piezometers were used to monitor the water pressure in the geocomposite drainage geonet sections, and thermocouples were installed in several sections to determine the depth of frost penetration.

There have been a few studies that investigated the performance of geosynthetic reinforcement in flexible pavements. However, no studies have been performed on road sections that are as thick as the ones found in Maine. This project evaluated the reinforcement, separation, and filtration properties of geosynthetics in road sections up to 820 mm (32 in.) thick. The loadcells and strain gages attached to the geogrid and geotextile will monitor the force induced in these materials. The piezometers monitored the water pressure to determine how long the road section stays saturated with water. This project will allow the Maine DOT to determine if using geosynthetics is beneficial to road construction for thicker flexible pavement systems.

1.3 ORGANIZATION OF REPORT

This report contains six chapters and one appendix. Chapter 2 is a literature review of laboratory and field studies, computer analyses of potential benefits, and design methods for unsurfaced roads and flexible pavements with geosynthetics.

Chapter 3 describes the project, different design sections, material properties of different geosynthetics, and construction procedures.

Chapter 4 contains instrumentation and field measurement procedures for the reinforcement geogrid, reinforcement geotextile, thermocouples, and piezometers. It also describes calibration procedures for loadcells and strain gages attached to the reinforcement geogrid and geotextile.

Chapter 5 gives the results of loadcell, strain gage, piezometer, and Falling Weight Deflectometer (FWD) field measurements. The Darwin pavement analysis computer program was used to determine structural numbers from FWD results. Section performance was related to the structural numbers of instrumented sections and the control section.

Chapter 6 summarizes the findings of this research and gives conclusions and recommendations for further research. The Appendix contains instrument calibration and testing data.

2. LITERATURE REVIEW

2.1 INTRODUCTION

Geosynthetics have been used since the early 1970's. Their use has increased markedly in recent years. The reinforcing benefits of geosynthetics in unsurfaced roads have been studied and proven. In the past few years studies to determine the potential benefits of using geosynthetics as reinforcement in paved permanent roads have been performed by a few organizations. Geosynthetics is a term that includes geogrids, geotextiles, and geocomposites. This chapter will concentrate on research done on these materials and factors that affect performance.

Geosynthetics have the potential to provide several mechanisms that can lead to improved road performance. Confinement of the subbase and subgrade layers, distribution of load to a larger area of the subgrade, filtration, separation, and tensioned membrane effect are the major modes of possible improvement. The effectiveness of these mechanisms are dependent on the road section properties. Geosynthetic placement, subgrade strength, aggregate size, pavement and subbase thickness, and geosynthetic stiffness are all factors that determine the amount of improvement that can be achieved with the use of geosynthetics.

There have been many studies that have evaluated the use of geosynthetics for unpaved temporary or haul roads but only a limited number of studies for flexible pavement systems. Both laboratory and field trials have studied geosynthetics by varying

the road section properties. In addition, numerical and computer analyses have shown the effects that geosynthetics can have on flexible pavements.

2.2 MECHANISMS THAT CAN LEAD TO IMPROVED ROADWAY PERFORMANCE

There are several factors that can make geogrids and geotextiles beneficial to roadway performance. In a typical road profile, there is the subgrade, subbase, aggregate base and then asphaltic-concrete pavement. This pavement system is very effective in compression, but cannot carry a significant tensile load. The use of a high stiffness geogrid or geotextile can provide reinforcement by adding tensile strength to the system. According to Barksdale, et al. (1989), there is a significant difference between the behavior of geogrids and geotextiles. Several authors believe that geogrids provide superior performance to geotextiles when used as reinforcement beneath paved roads because of interlock between the geogrid and the aggregate (Barksdale, et al., 1989; Haas, et al., 1985). This interlocking is thought to utilize the tensile strength of the geogrid and allow it to resist lateral movement, which is a typical failure mode of roadways. Moreover, the use of geogrid within the base layer can reduce the stress on the subgrade by distributing the concentrated loads of the wheels over a larger area in unpaved and thin flexible pavement sections (less than 700 mm (28 in.)). "The dual mechanisms of reinforcement are a further spreading of the load to the subgrade, providing a more stable support condition; and development of an appreciable amount of tensile stress resistance in the fabric" (Al-Qadi, et al., 1994). This action has been shown to increase the bearing capacity of the soil (Barksdale, et al., 1989). Confinement of both the subgrade and subbase sections prevents lateral spreading of the road section. A

decrease in permanent deformations and more even rutting patterns have also been benefits observed from geogrid/geotextile performance in unpaved and thin flexible paved roads (Bathurst and Raymond, 1987; Montanelli, et al., 1997).

Geosynthetics can also act as separation layers between the subbase aggregate and the subgrade. Geotextiles inhibit the pumping of subgrade fines into the aggregate subbase and also prevent aggregate penetration into the subgrade. These two mechanisms prevent reduction in effective base course thickness (Al-Qadi, et al., 1994). Certain geotextiles and geocomposites can aid in drainage of the roadway section, thus removing water quickly away from the roadway. Use of geotextiles as a capillary barrier was studied by Henry (1996), but more recent unpublished studies by Henry have shown that geotextiles are unlikely to act as capillary barriers for long term field conditions. However, it is likely that thicker geocomposites will act as a capillary barrier.

Results of one study conducted by Henry (1996) indicate "geotextiles possibly reinforced soil during freezing to reduce frost heave". It has been found that geosynthetics that absorb water "do not reduce frost heave" and may cause added damage to the road system (Henry, 1996).

2.3 GEOSYNTHETICS IN UNPAVED HAUL AND TEMPORARY ROADS

Research began in the 1970's on using geosynthetics to reinforce and improve unpaved haul and temporary roads. Field trials, computer modeling, and design methods

have been established for soil-fabric-aggregate (SFA) systems. The mechanisms of improvement for unpaved roads shed light on possible improvement mechanisms for paved roads. Possible mechanisms are: confinement and reinforcement of the aggregate layer; confinement of the subgrade soil; separation of the subgrade soil and the aggregate layers; and introduction of a filter medium to aid in separation and drainage (Bender and Barenberg, 1978).

2.3.1 Laboratory Studies in Soil Fabric Aggregate Systems

In a study conducted by the University of Illinois (Bender and Barenberg, 1978), laboratory research showed that SFA systems could take an increase volume of traffic compared to the same section of road with no reinforcement. Soil-fabric-aggregate systems also have a more spread-out rutting pattern and have less maximum permanent deflections than unreinforced sections. Test sections with fabric at the subgrade interface have less mixing of the fine subgrade particles with the aggregate base layer. Moreover, free flow of the water from the soil into the aggregate layer is maintained. When loads are applied to aggregate over a weak subgrade, the development of shear stress at the interface of the aggregate and subgrade limits the effectiveness of load distribution. The fabric or geogrid can confine the aggregate thus increasing the effective shear strength and the load distribution effectiveness of the fabric. SFA systems have been shown to increase the load-bearing capacity of the soil. Bender, et al. (1978) also showed that the tensile forces in the fabric tended to restrain upheaval of the soil mass contained within the slip planes both under the load and away from the loaded area. In a three-dimensional

laboratory test no significant difference was observed between the SFA and the soil aggregate because the stress applied was much lower than stresses occurring on a haul road. The results of a two-dimensional test performed by Bender, et al. (1978) showed a decrease in permanent deformation in SFA compared to an unreinforced section.

A laboratory study conducted by Lai and Robnett (1982), showed that when a fabric is included between the subgrade and aggregate layer the compressive stress decreased under simulated wheel loading as seen in Table 2.1. The testing apparatus, shown in Figure 2.1, had pressure cells located at different depths from the surface that measured the compressive stress. The reduction of stress can be attributed to either the membrane effect or to "increased load-spreading capability of the confined aggregate" (Lai and Robnett, 1982). The membrane effect describes a mechanism where deformation of the system causes the stretched fabric to develop in-plane tensile stress. Tolerable levels of imposed subgrade stresses are typically determined by the theory of plasticity and work done by Rodin (1965) and Whitman (1966).

Table 2.1. Stresses measured by pressure cells in 2.4-m (8-ft) pit tests (Lai and Robnett, 1982).

			Stress Normal to Pressure Cell (psi)	
Pressure Cell No.	Depth from Surface (in.)	Offset from C/L of Load (in.)	With Typar 3401	Without Fabric
9	16	0	12.0	15.5
3	20	0	11.0	15.5
4	30	0	---	---
7	42	0	5.5	6.5
8	20	6	8.2	13.0
6	20	12	7.0	7.5
5	20	18	1.6	0.8
2[a]	16	18	3.4	5.0
1[a]	32	30	3.4	3.4

[a]Radial stress; all other stresses are vertical

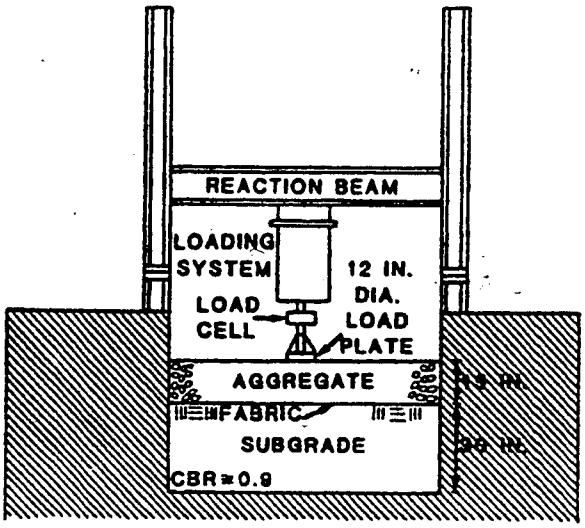

Figure 2.1. Schematic diagram of 2.4-m (8ft) deep test apparatus.

2.3.2 Computer Modeling of Soil Fabric Aggregate Systems in Unsurfaced Roads

Computer modeling, in conjunction with laboratory and field testing, is a very useful way of investigating mechanisms of improvement and the amount of improvement that is achieved by using fabric to reinforce road sections. To better understand the mechanisms of structural improvement, theoretical behavior models (ILLI-PAVE, LSTRN3, BISAR, and a simple confinement model) were used to assess low deformation systems (rut depths less than 38 mm (1.5 in.)) in a study by Thompson and Raad (1981). Results of an elastic-based finite-element computer model (LSTRN3) "indicated that lateral strains in the fabric, vertical subgrade stresses and strains, and surface deflections are not affected if the transformed section has a thickness that is at least 12 times the thickness of the original fabric" (Thompson and Raad, 1981). A transformed section is when a fabric-reinforced section is designed to have the same stiffness as an unreinforced section of

subgrade and stone base. The modulus of the transformed section is a function of the modulus of the fabric, the thickness of the original fabric, and the transformed section. A stress dependent finite-element model (ILLI-PAVE) was used to study the potential effect of a fabric layer in a soil-aggregate system. The parameters were a soft subgrade, a fabric that would not slip on the subgrade or crushed stone (no slip), and 203 mm (8 in.) of crushed stone. The analysis showed that there is "no fabric effect on vertical stress distribution, failure zones in the granular base, and deflection pattern in the pavement section" (Thompson and Raad, 1981). The reason could be that there was only 17.8 mm (0.70 in.) of surface deflection, which was not enough to mobilize the fabric tensile reinforcement effect.

An elastic layered program (BISAR) analyzed the effects of slippage of the fabric at the interface between the subgrade and aggregate. There is lower vertical deformation within the thickness of the section for the case with no fabric slippage. The results of a finite element analysis conducted by Bender, et al. (1987) show that the fabric reinforces the aggregate layer by restricting the horizontal strains in the aggregate layer, which reduces the critical horizontal strains at the soil-aggregate interface. The results were consistent with observed behavior.

Lateral confinement pressures increase when the SFA deforms. If the aggregate layer is incompressible and the deformed shape of the fabric is approximated by a circular arc (see Figure 2.2), and ignoring the confining effect of the shear stresses at the

interface between subgrade and aggregate, and the tensile stresses in the fabric (they act in opposite directions), the following can be determined:

$$\Delta\sigma/\sigma = [P_o (r) / K_s K_o h (h+r)] (1+ \alpha) \qquad \text{Equation 2.1}$$

where:

$$\alpha = \Delta_p / \Delta_r \qquad \text{Equation 2.2}$$

P_o = applied surface pressure

r = radius of loaded area

K_s = modulus of subgrade reaction

K_o = coefficient of earth pressure at rest

h = thickness of granular layer

$\Delta\sigma / \sigma$ = increase in confinement at interface due to deformation of fabric, expressed in terms of original confinement (σ) before fabric deforms

Δp = permanent deformation

Δr = resilient deformation

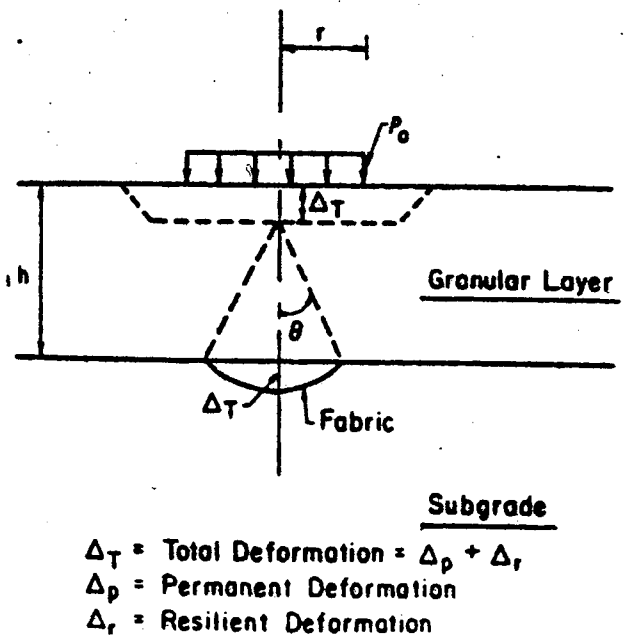

Figure 2.2. Increased confinement-effect model.

This demonstrates that significant improvement in shear strength, stiffness and permanent deformation behavior in the granular material can be correlated to small increases in confining pressure (Thompson and Raad, 1981). The results of the computer analysis confirmed that the benefits of fabric reinforced soil are only realized when the fabric deforms sufficiently for confining pressures to develop.

2.4 LABORATORY STUDIES OF GEOGRIDS AND GEOTEXTILES BENEATH FLEXIBLE PAVEMENTS

Researchers have conducted both laboratory and field investigations to determine the reinforcing mechanisms of geogrid and geotextiles beneath paved roads. From these studies, factors that affect performance have been determined. Some research has found that use of geogrid can either increase the road life or reduce the amount of aggregate base. In contrast, other research has found little benefit from geosynthetics or that it is dependent on specific soil properties and location of the geogrid or geotextile in the road cross section.

2.4.1 Laboratory Results

There have been several laboratory and full-scale experimental tests done on geosynthetics to study their reinforcing mechanisms. Studies by Barksdale, et al. (1989), Penner, et al. (1985), Kennepohl, et al. (1985), Haas, et al. (1988), Al-Qadi, et al. (1994), Cancelli, et al. (1996), Perkins, et al. (1996), and Montanelli, et al. (1997) have shown that there are some benefits to geosynthetic reinforcement in flexible pavements. However, no literature was found that studied the effects of geosynthetic reinforcement in

cold regions where the subbase and asphalt layers are as thick as used in Maine. The road section that was reconstructed in the Frankfort-Winterport project has a 180-mm (7-in.) asphalt layer and a 580 to 640-mm (23 to 25-in.) aggregate subbase layer.

2.4.1.1 Ruddock, Potter and McAvoy

In 1982, full-scale experiments reported by Ruddock, et al. (1982) showed that a woven multi-filament polyester geotextile had no effect on structural performance. A section with 160 mm (6.3 in.) of bituminous surfacing, and 300 mm (12 in.) of crushed granite base underlain by geotextile over a weak subgrade (CBR = 0.7) was loaded by a two-axle truck for 4600 repetitions. Then, the axle loading was increased to 133 kN (30k) for an additional 7700 passes. Instrumentation and measurements of surface deformations, dynamic stress and strain in the subgrade, permanent strain in the geotextile, and dynamic tensile strain in the bottom of the bituminous layer showed that there was no difference in structural performance between the reinforced and control sections.

2.4.1.2 Barksdale, Brown and Chan Studies

In a study conducted by Barksdale, et al. (1989), the location of geosynthetic in the base layer, pretensioning the geosynthetic, and prerutting both with and without a geosynthetic were varied to evaluate the performance of geosynthetics. Large-scale lab tests and analytical sensitivity studies were performed. The overall objective was to determine the potential structural and economic advantages of using geosynthetics as reinforcement in granular bases under flexible pavements from both a practical and theoretical standpoint. The sensitivity study attempted to design reinforced pavement sections and a strength equivalent to a nonreinforced section (Barksdale, et al., 1986). A

linear elastic finite element model having a cross-anisotropic aggregate base was used for the analytical study. The large-scale pavement tests consisted of a 25 to 38-mm (1.0 to 1.5-in.) thick asphalt surfacing placed over a 150 or 200-mm (6 or 8-in.) thick aggregate base. It was found that the effects of geosynthetic reinforcement on stress, strain, and deflection are all relatively small for pavements designed to carry more than about 200,000 equivalent 80-kN (18-kip) single axle loads (Barksdale, et al., 1989). Single equivalent axle loads are based on annual traffic and are used for the design of the road section. Important conclusions drawn from this study are that sections with an asphalt layer greater than 65 to 90 mm (2.5 to 3.5 in.) thick over subbase aggregate were not expected to show improvement with reinforcement geosynthetics, even if they were placed on weak subgrades. This is due to the fact that as the structural number increases as the asphalt layer thickness increases. Relatively little geosynthetic performance is seen with structural numbers greater than 2.5 to 3.0. In a sensitivity study, a section with 165 mm (6.5 in.) of asphaltic concrete surface was loaded. It induced very small radial stresses and it was concluded that "the change in stress resulting from the geosynthetic has a negligible effect on performance" (Barksdale, et al., 1986).

The best location of geosynthetic in thin pavement sections is dependent on the quality of base, strength of the subgrade, and thickness of the base. For thin pavement sections with low quality base it was recommended to place the reinforcement at mid-thickness. If the base was good quality but the subgrade was weak the reinforcement should go at the top of the subgrade. It was also found that 10 to 20% savings on base thickness could be seen using a high stiffness geotextile (700-1000 kN/m). Stiffness is

defined here as "the force in geosynthetic per unit length at 5% strain divided by the corresponding strain" (Barksdale, et al., 1986). Using the same strain criteria in the subgrade and the bottom of the asphalt surfacing, vertical permanent strain was redistributed due to the geosynthetic (Barksdale, et. al., 1986). When the reinforcement was placed at subgrade there was a decrease in permanent vertical strain at the top of the subgrade and an increase in permanent strain in the top of the base.

Prerutting and prestressing in thin pavements were found to significantly reduced permanent deformation. However, it was also found that prerutting "without reinforcement gave performance equal to that of prestressing and notably better performance compared to the use of stiff to very stiff, nonprestressed reinforcement" (Barksdale, et al., 1989). Investigation into the effect of geosynthetic slack showed that a 60% reduction of force in the geosynthetic occurs with a slack of only 0.1% which corresponds to 3.6 mm (0.14 in.) in a distance of 3.6 m (12 ft). A 90% reduction of force occurs with a slack of 0.4% (Barksdale, et al., 1989).

2.4.1.3 University of Waterloo

In an experimental program conducted at the University of Waterloo, Penner, et al. (1985) carried out a testing program that was divided into six series that studied geogrid reinforcement of granular bases. Each of the six series had four sections and varied in asphalt thickness, base thickness, reinforcement location in the granular layer and the subgrade CBR. Series 1, studied the location of the geogrid in a granular layer

over a subgrade with a CBR of 8. Series 2, studied the effect of granular base thickness over a weak subgrade (CBR = 4) and compared a thin reinforced granular base to a thicker unreinforced base. Series 3 studied a weaker subgrade whose strength was controlled by varying the moisture content with a thicker granular layer; and effect of grid location (Penner, et al., 1985). Series 4 studied the effect of granular base thickness in combination with a very weak subgrade (CBR =1). Series 5 studied pre-tensioning of geogrid over a very weak subgrade (CBR = 1). Series 6 evaluated weak subgrade and the effect of geogrid in both the subgrade and having two layers of geogrid located in the granular base (Penner, et al., 1985).

These tests were performed in a rectangular box, 4.5 m by 1.8 m by 0.9 m deep (15 ft by 6 ft by 3 ft deep) made with 19-mm (3/4 in.) plywood reinforced by a steel frame (see Figure 2.3). Each test section was loaded with a series of 40 kN (9,000 lb) dynamic loads (to simulate a set of dual wheels), at a frequency of 8 Hz. This was then followed by a single static load at predetermined cycle counts (Penner, et al., 1985). A 300 mm (12 in.) diameter loading plate was used.

The subgrade used for Series 1 through 3 was a very fine grained beach sand (99% passed the #40 sieve, 32% passing the #100 and 4% passing the #200). For Series 4 through 6 this soil was mixed with peat to obtain a CBR of 1. A well-graded aggregate was used for the base material. Hot mix asphalt was used for all test series. Series 1 had an asphalt thickness of 100 mm (4 in.), while Series 2 through 6 had an asphalt thickness

of 75 mm (3 in.). The reinforcement geogrid was Tensar SS1, a biaxially oriented polypropylene material.

Results from Series 1 showed that geogrid placed at the bottom of thin base layers (200 mm) showed improved performance in comparison with control sections with no reinforcement. After 10,000 cycles, the section with the reinforcement at the top of the aggregate layer and the unreinforced section began to deteriorate at a fast rate. The sections with the reinforcement at the subgrade and midway through the aggregate layer showed higher rutting only after 100,000 cycles.

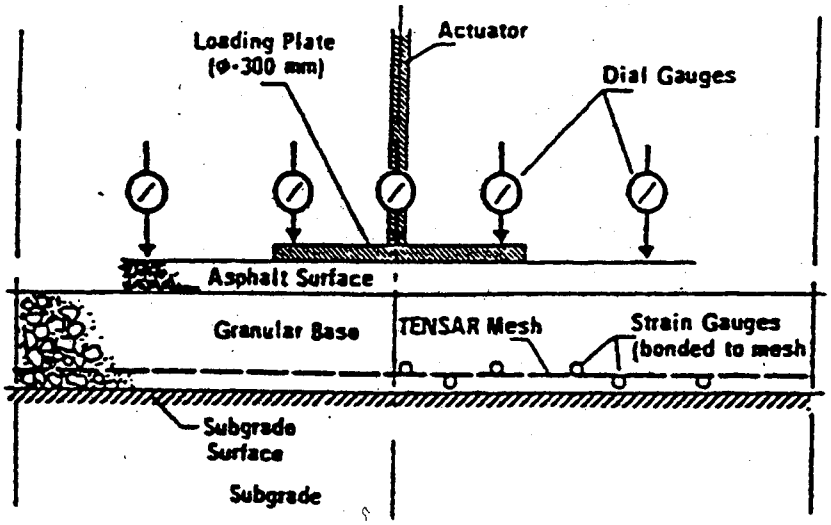

Figure 2.3. Testing apparatus, University of Waterloo (Penner et al., 1985).

Series 2 showed that sections with reinforcement at the subgrade and base thickness ranging from 100 to 200 mm (6 to 8 in.) carried three times the number of load cycles prior to failure compared to unreinforced sections. In Series 3, reinforced Sections 1 and 2 did not perform as well as Series 1 and 2. This was attributed to the increased

subgrade strength that occurred during Series 1 and 2 and the decreased asphalt thickness. Results from Series 4 showed that when the geogrid reinforcement was placed in the granular layer, the section could carry three times the number of load applications compared to the unreinforced section. It also showed a reinforced section with 25% less base thickness performed the same as the unreinforced section. The objective of Series 5 was to study the effects of pretensioning the reinforcement. It showed detrimental effects when the grid was placed at mid-thickness of the granular layer. Section 3, which had an increased granular layer, carried more load cycles than the equivalent unreinforced control section. Section 4 of Series 6, which had two layers of geogrid one at the mid-level and one at subgrade, carried the greatest number of load cycles and did not reach the failure criteria until 15,000 cycles (275% improvement over control). Sections with the grid placed in the subgrade and at the top of subgrade performed better than the control. Sections with geogrid placed within the subgrade took twice the number of cycles as sections with grid placed at the top of subgrade.

Haas, et al. (1988) concluded that geogrid reinforcement could be useful in low-deformation systems if designed properly. The most effective location for reinforcement is in the "zone of tensile stress during the first load application and remain in this tensile zone throughout its design life" (Haas, et al., 1988). Permanent strain in the geogrid was less than 1.5% for up to 700,000 load cycles. The strain is approximately zero at distances of 241 mm (9.5 in.) from the load center. At larger distances from the load center compressive strains in the geogrid were observed. When two layers of

reinforcement were used in a 305-mm (12-in.) thick base coarse the permanent deformation within the base was reduced.

This study concluded that for thin bases, 100 to 203 mm (4 to 8 in.) thick, the optimum position of the geogrid reinforcement is at the top of the subgrade. For thicker bases, 254 to 305 mm (10 to 12 in.) thick, it is more beneficial for the geogrid to be at mid-thickness of the base layer. A similar conclusion was made by Barksdale, et al. (1989). Like a beam, a road section has a zone of compression and a zone of tension, the benefits of geosynthetic reinforcement can only be observed in the zone of tension. It is noted that the pavement thickness in this study was 38 mm (1.5 in.) and the maximum subbase thickness was 203 mm (8 in.).

Cancelli, et al. (1996) tried to confirm the work done at the University of Waterloo (Beretta, et al., 1994). A test box with dimensions 1.8 m by 0.9 m by 0.9 m (6 ft by 3 ft by 3 ft) was divided into two sections, one with geosynthetic reinforcement and one unreinforced. The subgrade soil was a loose sandy soil, the base was a compacted crushed stone 300 mm (11.8 in.) thick, and the asphalt layer was 75 mm (3 in.) thick. The reinforcement was placed at the top of the subgrade and anchored by angling the material 90 degrees at the side of the box. A 40-kN (9,000-lb) load was applied to a 300-mm (11.8-in.) diameter plate. These loading cycles were performed at a frequency of either 5 or 10 Hz. Subgrade strengths varied from CBRs of 1 to 18 by varying the density. Five different kinds of geogrid and a slit film woven polypropylene geotextile were used.

Test results were analyzed and compared the following:

- Reinforced and unreinforced sections
- Reinforced sections with different CBR values
- Reinforced and unreinforced sections with different aggregate thickness
- Different geosynthetics

The results showed that there is little improvement due to reinforcement on strong subgrades. Improvement from geosynthetic reinforcement increases with weaker subgrades. Tensile forces are mobilized when the grid deforms, thus weaker subgrades that deform more than stronger subgrades will exhibit improved performance. Grids placed at the subgrade/aggregate interface are shown to increase service life. Using two layers of geogrid reinforcement, one placed at the interface and one at the mid-thickness, limit the rut depth at low CBR values. Two layers also distribute the load more uniformly and decrease settlement (Cancelli, et al., 1996). Other results showed that the geogrid layers "mobilize the stresses within the reinforced sections preventing local shear failure and deformation" (Cancelli, et al., 1996). Geogrid reinforced sections are the equivalent to a much thicker unreinforced section. A multi layer geogrid can also mobilize the bearing capacity at a much lower deformation. Reduction in rutting is more significant at lower CBR values. Lastly, depending on the subgrade strength the structural layer coefficient can be increased with geogrid reinforcement.

2.4.1.4 Virginia Polytechnic Institute Laboratory Studies

To simulate a typical secondary road in Virginia, four pavement sections were constructed to evaluate performance of pavements with and without geotextile/geogrid reinforcement. The tests were performed in a 3.1-m by 1.8-m by 2.1-m deep (10-ft by 6-ft by 7-ft deep) reinforced concrete testing pit. The four sections consisted of a control section, two sections reinforced with geotextiles and one section of geogrid reinforcement.

The loads applied to the sections consisted of a 40-kN (9,000-lb) load that represents a dual-tire loading of an 80-kN (18,000-lb) axle. The subgrade consisted of 1220 mm (48 in.) of compacted silty sand, a 150-mm (6-in.) base layer of well-graded gravel, and 70 mm (2.75 in.) of hot mix asphalt wearing surface.

The loads were applied by a 300-mm (12 in.) diameter steel plate, at a cyclic rate of 0.5 Hz. Loading was applied and continued until 25 mm (1 in.) of displacement had occurred on the pavement under the loading plate. After each test was completed the section was cut down the middle, the profile of layers was recorded and water contents were taken from each layer. Relationships between 1) the effect of loading cycles on displacement, 2) pavement displacement profile at 800 cycles, and 3) displacement beneath the center of the loading plate as a function of the applied number of cycles, were used to determine pavement performance. Permanent displacement profiles at 800 cycles show that reinforcement was definitely beneficial as shown in Figure 2.4. The geosynthetic-reinforced sections had less displacement under the load center. Both

geotextiles performed better than the geogrid. Major conclusions of this experiment were that geotextiles/geogrids can offer "substantial improvement to the performance of a pavement section constructed on a low CBR subgrade" (Al-Qadi, et al., 1994). However, it is noted that the base course was only 150 mm (6 in.) thick and the pavement was only 70 mm (2.75 in.) thick. The second conclusion was that geotextiles and geogrids have different reinforcing mechanism such as confinement and that geotextiles can serve as separators as well as reinforcement.

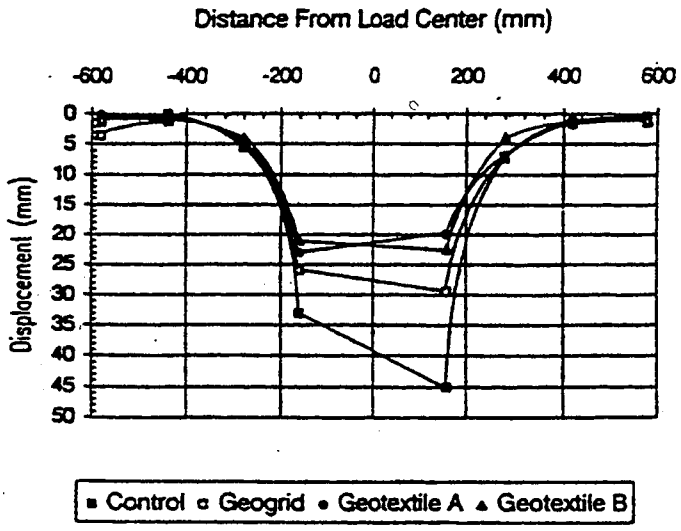

Figure 2.4. Permanent displacement profile at 800 cycles in VPI study (Al-Qadi, et al., 1994).

2.4.1.5 Montana State University

Montana State University (MSU) has done research on geosynthetic reinforced pavements with the support of the Montana Department of Transportation (Montana DOT). Montana DOT feels this research is very important since the quality and amount of gravel sources is very limited in the eastern portion of the state. The objectives of this study were to "verify previous work showing the positive benefit of using geosynthetics

for base course reinforcement, to quantify the stress strain response of laboratory scale reinforced pavement test sections such that mechanisms of reinforcement can be more clearly understood, and to develop a comprehensive methodology for the design of such pavements" (Perkins, et al., 1997). An extensive literature review was conducted and laboratory studies were performed to provide more information on potential benefits.

MSU had originally planned full-scale test sections constructed on a new or existing road, this was to include electronic instrumentation to measure the section performance. However, the pilot test section, proved "excessive uncertainty" with instrument survival and accuracy. Instead a test facility was constructed and used to study 15 sections. This facility is similar to those described previously. A reinforced concrete box 2-m by 2-m by 1.5-m (6.6-ft by 6.6-ft by 5.0-ft deep) was used and a load frame attached to the box. A 40-kN (9,000-lb) load was applied by a 305-mm (1-ft) diameter circular plate (Perkins, et al., 1997). The base coarse consisted of a well-graded gravel classified as A-1-a by AASHTO. The typical subgrade soil consisted of very silty fine sand with 40% fines, a liquid limit of 18, and plasticity index near zero resulting in a classification of A-4 by AASHTO or SM by ASTM. The subgrade was 1150 mm (45 in.) thick and was replaced after testing for Sections 1 and 2 but not for Sections 3 and 4. The subgrade CBR ranged from 18 to 23. The thickness of the base coarse aggregate was approximately 200 mm (8 in.) for all four sections. The reinforcement consisted of a biaxial geogrid (Sections 1 and 3) and a woven geotextile (Sections 2 and 4).

Stress, strain, temperature, and moisture content were monitored. The load was applied in two different ways. A "single load pulse at 25 different locations and a series of repeated loads in the center of the box" (Perkins, et al., 1997). Two test sections used a hot mix asphalt while the other two used a cold-mix asphalt. Both types were heated before being laid.

Instrumentation consisted of eight linear variable differential transformers (LVDTs) to measure pavement deflection, a loadcell to measure the applied cyclic load, and four strain gages to measure tensile strain in the bottom of the AC layer. Stress cells were placed in the base and subgrade to measure total stress. Strain gages were also attached to the geosynthetic to monitor strain at twelve locations.

The results of the instrumentation showed that the shear interaction between geosynthetics was greater for the geogrid due to its aggregate strike through and interlocking of the aggregate. When the reinforcement was placed at the interface of the subgrade and aggregate, strain in the geogrid and aggregate follow the same trend. The permanent radial strain deceased with increasing radial distance from the applied load. The maximum vertical strain of 0.48% occurred at the center of the load while the maximum radial strain of 0.03% occurred 400 mm (16 in.) from the load center. The base went into compressive strain approximately 175 mm (7 in.) from the applied load while the geogrid developed compressive strain 200 mm (8 in.) away from the load center. Tangential strain in both the aggregate and geogrid approaches zero with increasing distance (800 mm (31.5 in.) from the load center. An important observation

was that strain develops immediately with the first loading of the geosynthetic and before rutting develops. Also the amount of improvement depends on the level of strain and the tensile capacity development.

Conclusions of this experiment have shown that tensile strain does develop in geosynthetic reinforcement. The observed common trends between the aggregate and geosynthetic strain indicate a reduction of lateral and vertical aggregate movement due to development of shear interaction. Again it is noted that the base thickness was 200 mm (8 in.) and the pavement thickness was 70 to 75 mm (2.8 to 3.0 in.).

2.5 FIELD STUDIES

2.5.1 Ontario Field Study

In a study conducted by Anderson and Killeavy (1989), geogrid reinforcement was used in a flexible pavement design. The location was a trucking facility in southern Ontario. The road was designed for a 15-year design ESAL of 1.8 million. Several factors and constraints led engineers to design the roads with geosynthetics. The goals were to improve subgrade stability and uniformity. Three different sections were constructed: the access road that was used as the control section; the truck staging yard that was reinforced with geogrid; and the yard extension that used a separation geotextile. The control and reinforced sections had a 105-mm (4-in.) asphalt section. The control section had 450 mm (18 in.) of limestone base, while the reinforced section had a 200-mm (8-in.) granular base course with the Tensar SS1 geogrid at the subgrade. The truck staging yard expansion had a 90-mm (3.5-in.) asphalt layer, 150-mm (6-in.) limestone granular base, and 200-mm (8-in.) of limestone subbase, with the geotextile on subgrade.

Pavement performance was evaluated by dynamic deflection properties, and observing surface cracking and deformation (Anderson and Killeavy, 1989). Falling weight deflectometer (FWD) deflections were normalized to a load of 40 kN (9,000 lb) for comparative purposes between sections since the actual applied load varies with the pavement stiffness. Results of calculated granular layer moduli are shown in Table 2.2. The truck staging yard has the highest modulus, followed by truck yard expansion with only a geotextile and the unreinforced access road. The results of a FWD deflection basins and elastic layer analysis showed that after approximately 1100 ESAL's the reinforcement had reduced subgrade and asphalt strain. Pavement surface performance was observed for cracking, distortion, and rutting. Surface distortion as a percent of the total road area showed that the truck staging yard, which had the geogrid and geotextile, had less than 0.5% distortion of the total area. The access road and the yard extension had zero distortion. The truck staging area was "subjected to more severe and damaging truck turning movements than the access road" (Anderson and Killeavy, 1989). Visually there was no difference between the three sections. The locked–in stress was achieved after deformations in excess of 25 mm (1 in.) occurred in the granular base and subgrade as a result of high water contents during construction (Anderson and Killeavy, 1989).

Table 2.2 Summary of calculated granular layer moduli in MPa

Pavement Section	Mean	Standard Deviation	Range
Truck Staging Yard (Reinforced & Geotextile)	560	190	300 to 800
Access Road (not reinforced)	170	70	160 to 270
Truck Yard Expansion (geotextile only)	400	120	280 to 590

2.5.2 Virginia Polytechnic Institute Field Investigation

Full-scale pavement studies were constructed in 1996 on a secondary road in southwest Virginia. There are nine instrumented flexible pavement test sections 15 m (50 ft) long. The test sections study the effects of geogrid and geotextile stabilization (Brandon, et al., 1996). Three sections used geogrid reinforcement, three used geotextiles, and three were used as control sections. The asphalt was typically 89 mm (3.5 in.) thick and the base coarse ranged from 102 to 203 mm (4.0 to 8.0 in.) thick. The subgrade CBR was approximately 7. The road was instrumented with pressure cells, strain gages, thermocouples, soil moisture cells, and strain gages placed directly on the geogrid and geotextile (Brandon, et al., 1996). Eight months after construction survivability of the strain gages mounted on the geogrid was about 28%, while geotextile strain gages had a 6% survival.

2.6 Reinforcement Design Methods for Flexible Pavements

Few design procedures were found for geosynthetic reinforcement beneath flexible pavements. A design procedure developed by Penner, et al. (1985), uses a layer

coefficient ratio or equivalence factor that is applied to the reinforced layer to reflect the improved structural characteristics of the base. Using the AASHTO Interim Guide as a starting point, design relationships for geogrid reinforced base layers were developed. The AASHTO method allows comparison of the structural strengths of pavement sections. AASHTO defines the structural number as

$$SN = a_1d_1 + a_2d_2 + \ldots..a_nd_n \qquad \text{Equation 2.3}$$

If the structural number of the granular base layer (SN_{gr}) is

$$SN_{gr} = SN - a_1d_1 \qquad \text{Equation 2.4}$$

a_1 = layer coefficient for the asphalt concrete (assumed = 0.4)

d_1 = thickness of the asphalt concrete layer in the test section (inches)

The ratio that relates the reinforced to the unreinforced granular layer coefficients was determined through laboratory testing at the University of Waterloo (refer to Section 2.4.1.1) to be

$$A_r / A_u = (SN_{gr})_r \bullet d_u \; / \; (SN_{gr})_u \bullet d_r \qquad \text{Equation 2.5}$$

Where

$(SN_{gr})_r$ & $(SN_{gr})_u$ = structural number of reinforced and unreinforced granular layers, respectively

d_r and d_u = granular base thickness of reinforced and unreinforced sections

A_r / A_u = the effect of the geogrid on the structural capacity of the of the granular base layer

This ratio expresses the amount of improvement the geogrid can have on the structural capacity of the granular base layer. Comparing this ratio to the different test sections that the design was based on indicates that the thicker the base coarse the less improvement is seen with reinforcement. A variation of the A_r/A_u for all test series shown in Figure 2.6, indicates that the ratio becomes 1 approximately at a base thickness of 270 mm (11 in.). Although no tests were performed on sections greater than 300 mm (12 in.) it expected that no improvement would be observed for greater base thickness (Penner, et al., 1985).

2.7 SUMMARY

Investigation into geosynthetic performance for road applications began in the 1970's. Geosynthetics can serve many functions in temporary and flexible pavement roads including: separation, filtration, and reinforcement. There have been several laboratory, field, and computer studies performed to evaluate the effectiveness of geosynthetics in roadway design.

Studies show that geosynthetic reinforcement of unpaved roads is beneficial in reducing the amount of aggregate subbase required to maintain the road life (Robnett and Lai, 1982; Bender, et al., 1978; Thompson and Raad, 1981; Bathurst and Raymond, 1987). Unpaved roads typically are designed for a larger rut depth compared to low deformation paved roads. Larger rut depths increase the performance of the geosynthetic. Tensile forces are mobilized as the geosynthetic deforms, thus the more deformation the

more the geosynthetic provides tensile strength. Acceptable rut depths for temporary roads can range from 50 to 300 mm (2 to 12 in.) (Bender, et al., 1978). Geosynthetic reinforcement can allow designers to reduce the amount of aggregate needed to carry a certain capacity or, if the same aggregate thickness is used, geosynthetic reinforcement can increase the life of the road (Bender, et al., 1978; Thompson and Raad, 1981; Robnett and Lai, 1982). When used as a separating layer, a reinforcement geotextile can also reduce the amount of non-structural aggregate if properly designed (Christopher and Holtz, 1991). Non-structural aggregate is the aggregate that is not needed for load support, but more of a safety layer that compensates for contamination of the clean aggregate with fine material.

Geosynthetic reinforcement of paved roads has been shown to be beneficial if designed properly and if the base course is less than 300 mm (12 in.) thick. The performance of geosynthetic reinforcement in flexible pavements is dependent on properties of the road section. As the shear strength of the subgrade soil decreases the amount of improvement tends to increase. Depending on factors such as subbase thickness, location of the geosynthetic, and material properties of the geosynthetic, reinforcement in flexible pavements can be beneficial or of no benefit. Barksdale, et al. (1989) and Penner, et al. (1985), showed that geosynthetic reinforcement was ineffective for road sections that were either designed to carry more than 200,000 equivalent 80 kN (18-kip) single axle loads or had an aggregate base thicker than 300 mm (12 in.). Laboratory studies conducted on thinner aggregate reinforced sections showed an increase in the load cycles the system could carry or allowed for a reduction of the

aggregate thickness (Penner, et al., 1985; Haas, et al., 1988; Perkins, et al., 1997; Cancelli, et al., 1996). Other conclusions state that, under the proper circumstances, geosynthetic reinforcement can result in a more distributed rut pattern, reduce the rate of permanent deformation (rutting), and increase pavement life (Haas, et al., 1988). For thin bases, 100 to 203 mm (4 to 8 in.) thick, the reinforcement should be placed at the subgrade/subbase interface. The optimum location for thicker subbase sections, 254 to 305 mm (10 to 12 in.) thick, is the middle of the subbase aggregate. In Haas's work the force (strain) in the geogrid is developed by deformations caused by the applied load, there was no mention of a major increase in force when the overlying aggregate was placed and compacted as observed for the Frankfort-Winterport project. This will be discussed further in Chapter 5.

A full scale field study in Canada evaluated the use of geotextile and geogrid reinforcement in a paved road. Three roads were constructed, one with a geogrid and geotextile placed at subgrade, the second with only a geotextile at subgrade, and the last was a control. Base thickness ranged from 200 to 450 mm (8 to 18 in.) with asphalt layer of 105 mm (4 in.). The results of FWD and elastic layer analysis concluded that geosynthetic reinforcement was beneficial. However, visual observation showed essentially no difference in pavement performance in the three roads. A possible reason for the improvement predicted by the FWD and elastic layer analysis is that there was possibly added prestressing of the geosynthetic due to the adverse moisture conditions before the asphalt layer was placed.

Laboratory studies conducted at the University of Waterloo, Virginia Polytechnic Institute, and Montana State University evaluated the use of geosynthetics in flexible roadway design. There have been no studies of reinforcement with asphalt thicknesses greater than 100 mm (4 in.) or base thicknesses greater than 300 mm (12 in.) (Al-Qadi, et al., 1994; Penner, et al., 1985). Thus, there are no previous studies of geogrid or geotextile reinforcement with subbases 580 or 640 mm (23 or 25 in) thick or 180 mm (7 in.) pavement as used in the Frankfort-Winterport field trial performed for this study.

3. PROJECT DESCRIPTION

3.1 INTRODUCTION

Reconstruction of a 3.06-km (1.9-mile) Section of Route 1A in the towns of Winterport and Frankfort began in May, 1997. Construction continued until November, 1997, when work was stopped for the winter. Work resumed in April, 1998 and was completed in June, 1998. Construction began at the north end of the project at station 92+96 m (305+00) and proceeded generally southward to the southern end of the project at station 63+40 m (208+00).

This Section of Route 1A has very poor subgrade soils with AASHTO classifications of A-4, A-5, A-6, and A-7-5 (Hayden, 1996). The existing roadway was plagued with cracking, subgrade intrusions into the subbase, localized bearing failures, and aggregate movement. Laboratory CBR's on samples recompacted at the Modified Proctor optimum moisture content were less than 3 in some areas, making this site suitable for testing geosynthetics for different applications. The reconstructed Section of road is designed to carry 1.5 million equivalent 80-kN (18-kip) single axle loads. Reinforcement geogrid, reinforcement geotextile, separation geotextile, and high compressive strength geocomposite drainage net were used in this project to evaluate their reinforcement, separation, filtration, and drainage performance for Maine soil and climatic conditions.

Climatic conditions during construction were unusual. Maine experienced the second driest summer since records have been taken (Hayden, et al., 1998). Difficulties

in construction had been anticipated since the shear strength of the native soil was so low. The lack of rain in the summer of 1997 and resulting dry soils made construction move very rapidly with few problems, with the exception of the control Section, which was constructed early in the summer when the subgrade soils were still wet.

3.2 TEST SECTION LAYOUT

The project was divided into six sections with different geosynthetic applications. These sections were labeled A through F. Four of the test sections (A, B, C, and E) incorporated geotextile reinforcement, geogrid reinforcement, or geotextile separation. One section (D) used a drainage geocomposite to improve drainage and reduce frost heave. One section (F) was designated as a control section and used no geosynthetics. All test sections had 180 mm (7 in.) of asphaltic concrete pavement and 640 mm (25 in.) of aggregate subbase with the exception of Sections A and B-1 where a reduced aggregate subbase thickness of 580 mm (23 in.) was used. Reduced aggregate sections were used to determine if geosynthetic reinforcement could permit the use of less gravel. However, during construction a tolerance of 10 mm (0.34 in.) was allowed with grading. Given the construction tolerance, the 50-mm (2-in.) difference between the standard and reduced subgrade thickness may be insignificant. The six sections are shown in Figure 3.1. Most of the sections are divided into subsections that vary the location of geosynthetic in the subbase section or thickness of the subbase course. The layout of each section is discussed below.

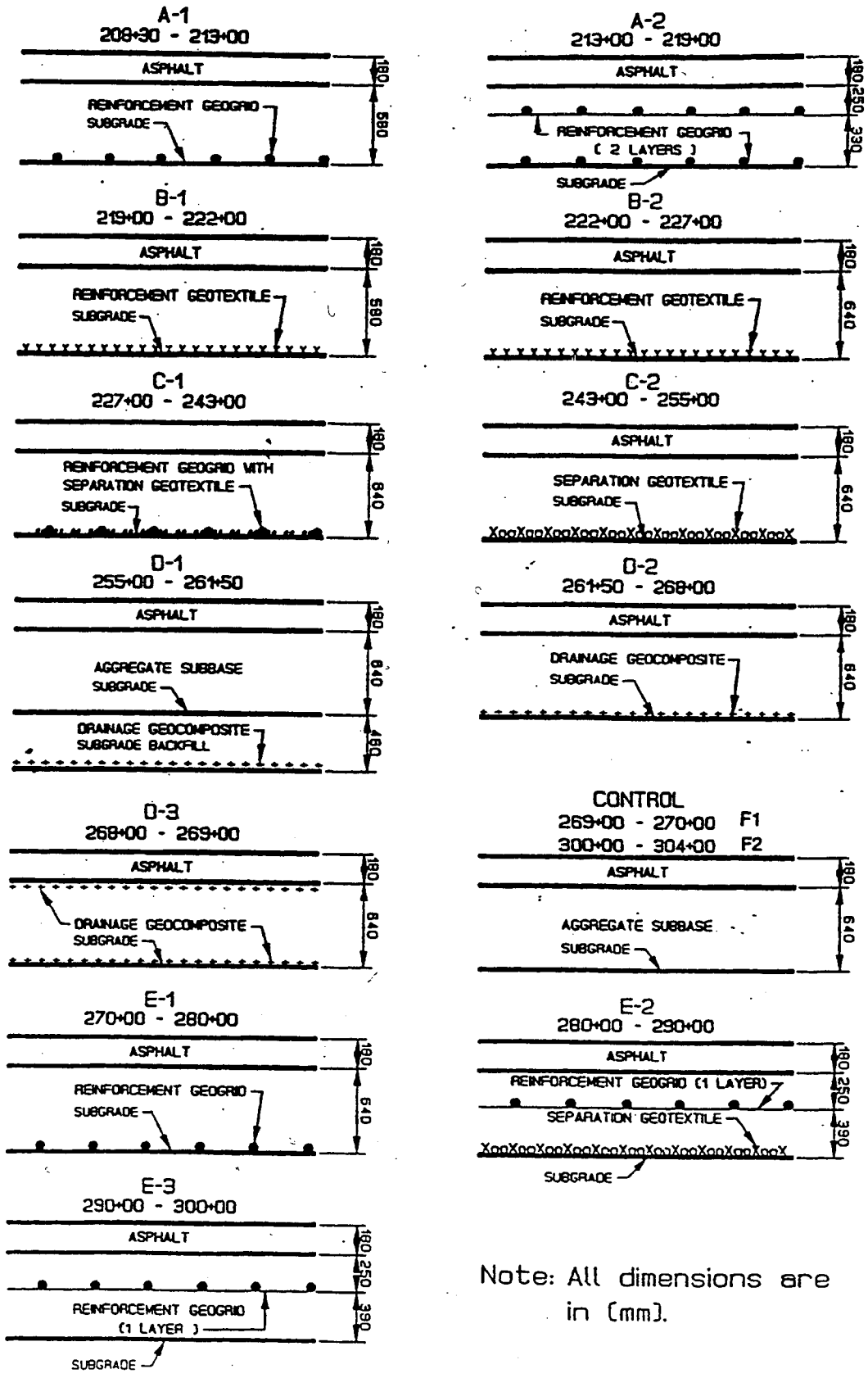

Figure 3.1 Test Section layout (Hayden et al., 1998).

3.2.1 Section A – Reinforcement/Reduced Structural Section

This section uses reinforcement geogrid and consists of subsections A-1 and A-2 as shown in Figure 3.1. The section has a reduced structural section with 580 mm (23 in.) of aggregate subbase and 180 mm (7 in.) of asphalt. Subsection A-1 has one layer of reinforcement geogrid placed on the subgrade at the bottom of the structural section. This subsection is instrumented at stations 64+12 m (210+38 ft) and 64+62 m (212+00 ft). Subsection A-2 has two layers of reinforcement geogrid placed within the aggregate subbase. The first geogrid layer is placed at the bottom of the 580-mm (23-in.) aggregate subbase and the second is placed 250 mm (10 in.) below the top of the aggregate subbase layer. The geogrid is instrumented at station 66+29 m (217+50 ft). Both layers of geogrid were instrumented, however all the instruments on the bottom layer failed during placement and compaction of the overlying aggregate. Station 64+12 m (210+38 ft) in subsection A-1 is located in a cut section, whereas stations 63+62 and 66+29 m (212+00 and 217+00 ft) in subsections A-1 and A-2 respectively are located in fill sections.

3.2.2 Section B – Reinforcement Section

This section uses reinforcement geotextile and consists of two subsections, B-1 and B-2, as shown in Figure 3.1. Both subsections have the reinforcement geotextile layer on the subgrade at the bottom of the structural section. However subsection B-1 was constructed with a reduced structural section of 580-mm (23-in.) of aggregate subbase, while subsection B-2 has the full structural section of 640 mm (25 in.) of subbase. Both instrumented stations in subsections B-1 and B-2 are located in cut sections. The reinforcement geotextile was tensioned by anchoring with an initial lift of aggregate, then traveling over the section with construction equipment to create rutting of

the subgrade. The geotextile is instrumented at stations 67+51 m (221+50 ft) and 67+82 m (222+50 ft).

3.2.3 Section C – Reinforcement / Separation Section

Subsection C-1 uses both separation geotextile and reinforcement geogrid at the bottom of the structural section while subsection C-2 uses only separation geotextile. A full structural section with 640 mm (25 in.) of aggregate subbase was used in both subsections. A set of three piezometers was installed in Section C-2 to monitor the pore water pressures at station 74+83 m (245+50 ft) which is located in a cut area. No other instrumentation was installed in this section.

3.2.4 Section D – Drainage Section

This section uses drainage geocomposite and consists of subsections D-1, D-2, and D-3, as shown in Figure 3.1. Geonet drainage geocomposite was placed across the entire roadway and was connected to a perforated collection pipe installed beneath each shoulder. Locations of the geonet drainage geocomposite are different in each subsection. Subsection D-1 has one layer of drainage geocomposite 460 mm (18 in.) below the bottom of the structural section. Subsection D-2 has one layer of drainage geocomposite on the subgrade at the bottom of the structural section. Subsection D-3 has two layers of drainage geocomposite, one placed at the bottom of the asphalt layer and the second on the subgrade at the bottom of the structural section. A set of three piezometers was placed in each subsection at stations 78+79, 81+53, and 81+84 m (258+50, 267+50, and 268+50 ft), to measure the pore water pressures. Instrumentation

in subsections D-1 and D-2 are located in cut areas, whereas subsection D-3 is located in a fill area.

3.2.5 Section E – Reinforcement Section

This section uses reinforcement geogrid. It was divided into subsections E-1, E-2 and E-3 as shown in Figure 3.1. A full structural section with 640 mm (25 in.) of subbase was used in all subsections. Subsection E-1 has one layer of reinforcement placed on the subgrade at the bottom of the structural section. Subsection E-2 has one layer of separation geotextile on the subgrade at the bottom of the structural section and one layer of reinforcement geogrid placed 250 mm (10 in.) below the top of subbase course. Subsection E-3 has one layer of reinforcement located 250 mm (10 in.) below the top of the subbase course. The geogrid is instrumented at stations 88+85 m (291+50 ft) and 88+54 m (290+50 ft) in subsection E-2. Both instrumented stations are in cut areas.

3.2.6 Section F – Control Section

There are two sections that have no geosynthetics. These two sections were used to compare the performance of sections with and without geosynthetics. Both control sections were intended to have a 180-mm (7-in.) asphalt layer and a 640-mm (25-in.) aggregate subbase. They were originally constructed with 640 mm (25 in.) of subbase aggregate, however, traffic loading on the exposed aggregate surface quickly caused the section to fail. The contractor had to re-excavate this section, undercutting an additional 610 mm (24 in.) into the weak subgrade soils. The contractor then placed a total of 1250 mm (49 in.) of subbase aggregate to bring the road back to its indented grade. This problem did not occur in any of the sections with geosynthetics even though the

contractor and resident engineer thought that undercutting was needed at several locations. This confirms that geosynthetics can be used to expedite construction of roads on soft subgrades.

3.3 GEOSYNTHETIC PROPERTIES

Four types of geosynthetics were used in this project: reinforcement geogrid, reinforcement geotextile, separation geotextile, and drainage geocomposite. The following paragraphs describe each type of geosynthetic.

3.3.1 Geogrid Properties

The reinforcement geogrid used in this project was Tenax MS330. This is a three-layered polyethylene, extruded geogrid with openings of approximately 60 mm by 40 mm (2.36 in. by 1.57 in.) and a rib thickness of about 2 mm (0.08 in.) that was custom made for this project. Its material properties along with the requirements of the project specifications are summarized in Table 3.1.

Table 3.1 Reinforcement geogrid mechanical properties.

Mechanical Property	Test Method	Minimum Value Permitted by Project Specifications	Properties Reported by Manufacturer*
Tensile Modulus @ 5% strain (TD)	ASTM D4595	350 kN/m (24,000 lb/ft)	350 kN/m (24,000 lb/ft)
Modulus @ 5% strain (MD)	ASTM D4595	175 kN/m (12,000 lb/ft)	175 kN/m (12,000 lb/ft)
Ultimate Tensile Strength	ASTM D4595	18 kN/m (both directions) 1200 lb/ft	18 kN/m (both directions) 1200 lb/ft
Percent Open Area		50%	50%

MD = Machine Direction (longitudinal to the roll)
TD = Transverse direction (across roll width)
*Tenax MS330 product information

3.3.2 Reinforcement Geotextile Properties

Mirafi 67809 was used as the reinforcement geotextile for this project. Its mechanical properties are given in Table 3.2.

Table 3.2 Reinforcement geotextile mechanical properties.

Mechanical Property	Test Method	Minimum Permissible Value Required by DOT	Properties Reported by Manufacturer*
Tensile Modulus @ 5% strain (TD)	ASTM D4595		700 kN/m (48,000 lb/ft)
Modulus @ 5% strain (MD)	ASTM D4595		350 kN/m (24,000 lb/ft)
Grab Tensile Strength (both directions)	ASTM D4632 or ASTM D5034 and ASTM D5035	1200 N (270 lb)	
Trapezoid Tear Strength	ASTM D4533 or ASTM D1117	334 N (75 lb)	334 N (75 lb)
Grab Elongation	ASTM D3786 or ASTM D5034 and ASTM D5035	15%	
Mullen Burst Strength	ASTM D3786 or ASTM D751	2960 kPa (430 psi)	2960 kPa (430 psi)
Puncture Strength	Modified ASTM D3787 or Modified ASTM D751	0.490 kN (110 lb)	0.490 kN (110 lb)

*Mirafi 67809 Data Sheet

3.3.3 Separation Geotextile Properties

Mirafi 180N, a heavy weight nonwoven geotextile, was used as a separator. The separation geotextile was required to have the properties specified for stabilization

geotextile in Section 722.01 of the MDOT Standard Specifications for Highways and Bridges (shown in Table 3.3) except for the following additions or exceptions.

- A 237-mL (8-oz.) non-woven, needle punched, polypropylene fabric shall be required.

Table 3.3 Separation geotextile mechanical properties.

Geotextile Mechanical Property	**Test Method**	**Minimum Permissible Value**	**Properties Reported by Manufacturer**
Grab Tensile Strength (both directions)	ASTM D4632 or ASTM D5034 and ASTM D5035	800 N (180 lb)	205/50
Grab Elongation	ASTM D4632 or ASTM D5034 and ASTM D5035	15 %	
Mullen Burst Strength	ASTM D3786 or ASTM D751	2000 kPa (290 psi)	2758 kPa (400 psi)
Puncture Strength	Modified ASTM D3787	330 N (75 lb)	578 N (130 lb)
Trapezoid Tear Strength	ASTM D4533 or ASTM D1117	220 N (50 lb)	356 N (80 lb)
Geotextile Hydraulic Property	**Test Method**	**Permissible Value**	
Apparent Opening Size (AOS)	CW-02215	Sieves Sizes between 850 μm and 150 μm [U.S. Std. Sieve number (s) between No. 20 and No. 100]	80000 μm (3.1 in.)
Permeability	ASTM D4491	0.01 mm/sec	

3.3.4 Drainage Geocomposite Requirements

The MDOT used Tenax Tendrain 100-2 as the drainage geocomposite because it was donated by the manufacturer. Its properties are given in Table 3.4. The

geocomposite has a tri-planar structure consisting of a thick supporting rib with diagonally placed top and bottom ribs. The ribs are extruded polyethylene. Two sheets of non-woven geotextile are thermally laminated on both sides to prevent intrusion of soil into the internal drainage structure.

Table 3.4 Drainage geocomposite mechanical properties (Tendrain 100-2).

Geocomposite Property	**Test Method**	**Typical Value**
Tensile Strength (MD)	ASTM D4595	35 kN/m (2380 lb/ft)
Thickness	ASTM D5199	8.9 mm (0.35 in.)
Flow Rate in soil @ 718 kn/m^2	ASTM D4716	
Hydraulic Gradient		
i = 0.10		14.5 liter/min/m (1.17 gal/min/ft)
Geonet Core Only		
Tensile Strength	ASTM D4595	13 kN/m (900 lb/ft)
Thickness	ASTM D5199	7.6 mm (0.3 in.)
Compression Behavior	ASTM D1621	65% @ 1197 kN/m^2 50% @ 1914 kN/m^2

3.4 SUBGRADE AND SUBBASE PROPERTIES

3.4.1 In-place Subgrade Properties

The soils in Winterport and Frankfort, Maine have a history of poor performance as subgrade soils. Route 1A in this area has been plagued with cracking, rutting, and potholes. The rutting was so severe and subsurface drainage so poor in some sections that water was observed coming up through the cracks (Hayden, 1996).

A subsurface investigation (Hayden, 1996) reported poor subgrade soil conditions along the entire length of the project. Moist clay soils were the dominant soil type encountered in each subsurface exploration. These soils were glacial marine clay known as the Presumpscot Formation. The soil was laid down between 11,000 and 14,000 years ago during the Wisconsinan glaciation (Schnitker and Borns, 1987). The Presumpscot Formation consists of fine material that was discharged from the retreating glacier that had covered the state of Maine (Schnitker and Borns, 1987). These soils are plastic and moist with water contents greater than 20% in some areas of the project (Hayden, 1996). Water seepage was encountered above the proposed subgrade elevation at several locations. Samples of this soil are typically classified as AASHTO A-6 with liquid limits as high as 37 and plasticity indexes of 17. These soils have poor load bearing characteristics. Three laboratory CBR tests were conducted on representative samples at recompacted at Modified Proctor optimum moisture contents. These tests produced values of 2.6, 3.2, and 3.6.

3.4.2 Common Borrow Properties

Common borrow was used in the fill sections below the subgrade elevation. The common borrow was generally weathered Presumpscot marine clay with a lower water content than the underlying clay. The common borrow was from cut sections. In some cases the clay was mixed with aggregate subbase excavated from old highway alignment. The common borrow generally had a lower moisture content than the in-place subgrade soils. Thus, the subgrade soils in fill sections was generally stronger and stiffer than subgrade soils in cut sections. When evaluating the performance the performance of a particular section of road, it is important to consider whether it is in a cut or fill section.

3.4.3 Subbase Properties

The subbase used in the Winterport/Frankfort project was uniformly graded sandy gravel. Figure 3.2 shows typical grain size curves of the subbase aggregate. The subbase has very little fines and approximately 50% of the soil is between 12 mm and 75 mm (0.47 and 3.0 in.). It is classified as an AASHTO A-1-a soil.

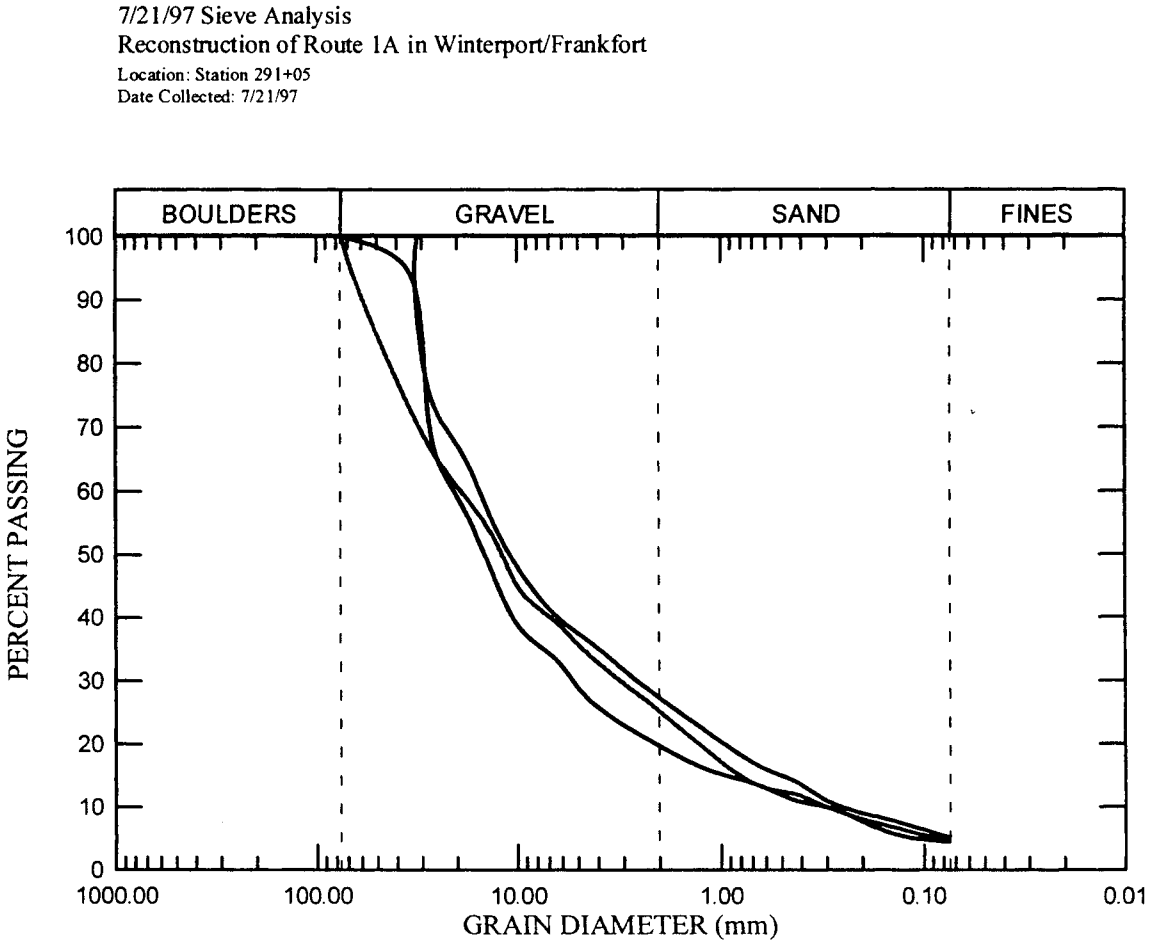

Figure 3.2 Sieve analysis of subbase aggregate.

3.5 CONSTRUCTION PROCEDURES

The construction procedures for the placement of the geogrid, reinforcement and separation geotextile, and the drainage geocomposite are outlined in the following sections.

3.5.1 Geogrid Placement

The following construction procedures for geogrid placement were adopted for this project. They were based on recommendations made by Dr. Barry Christopher, a geotechnical consultant in the geosynthetics industry.

1. Geogrid was laid at the proper elevation and alignment as shown on the construction drawings.
2. The geogrid was oriented such that the roll length ran parallel to the centerline.
3. Adjacent rolls of geogrid were overlapped a minimum of 30 mm (12 in.)
4. The geogrid was overlapped so that placement of granular material would not uplift the material.
5. All seams along the geogrid were tied together with plastic ties spaced 1500 to 3000 mm (60 to 120 in.) apart.
6. Granular fill material was back dumped from trucks riding on top of the reinforced fill and bladed onto the geogrid in such a manner that the fill rolled onto the grid ahead of the blade (e.g. by gradually raising a dozer blade while moving forward).

7. Construction equipment was not allowed to travel over the geogrid without a minimum of 200 mm (8 in.) of aggregate covering the geogrid.
8. Compaction was done with a dozer initially and then with a smooth-drum vibratory roller to obtain a minimum compacted density of 95% of Modified Proctor (AASHTO T180).
9. In areas where the reinforcement geogrid was placed within the aggregate subbase, the layer of underlying aggregate was first graded to a tolerance of plus or minus 25 mm (1 in.) of the desired elevation, then the geogrid was placed followed by the overlying aggregate.
10. In areas where rutting greater than 75 mm (3 in.) deep developed within the initial granular lift, the contractor was required to increase the thickness of the initial granular lift. This occurred at the north end of the project.
11. Ruts that formed during construction were filled with additional aggregate rather than by blading in aggregate from high areas between the ruts. This procedure is needed to prevent damage to the geogrid in the high areas between the ruts.

3.5.2 Reinforcement Geotextile Placement

The construction requirements for placement of reinforcement geotextiles is described in Section 620.00 of the MDOT Standard Specifications for Highways and Bridges (MDOT, 1997). Section 620.00 of the MDOT Standards specifies the following procedures of furnishing and installing geotextile fabric.

- Seams along the geotextiles were sewn (J seam with a double row 401 stitch) except for the centerline seam between the north bound and south bound lanes

where a 460-mm (18-in.) overlap was used. Overlapping the centerline seam was considered acceptable since this area would not receive significant traffic loading.

- Construction equipment was not allowed to travel over the reinforcement geotextile without a minimum of 200 mm (8 in.) of aggregate covering the geotextile.
- The initial lift of granular base could not exceed 200 mm (8 in.) due to the 130-mm (5-in.) rutting criteria. The use of loaded construction equipment passing over the initial lift was used to produce the desired rutting. Actual rutting depths varied from zero to 200 mm (8 in.) in Section B.
- All rutting formed during construction was filled with new subbase material. In no case was rutting filled by leveling the soil off with the dozer.

The reinforcement geotextile was tensioned in Sections B-1 and B-2. To create this tension the fabric was anchored and the subgrade directly beneath the geotextile fabric was rutted 130 mm (5 in.). This process was accomplished in steps and the construction of this test segment was conducted one lane at a time. Because of this the following construction procedures were developed to insure proper installation of the reinforcement geotextile. The following procedure describe the construction of only one travel lane.

1. The geotextile was placed along subgrade extending from approximately centerline to 2130 mm (84 in.) beyond the shoulder break.

2. 203 mm (8 in.) of subbase aggregate was placed on the geotextile extending from approximately centerline (leaving enough uncovered geotextile for overlapping and sewing at centerline. The outer edge (610 mm (24 in.)) of the uncovered geotextile

beyond the shoulder break was folded back over the aggregate and buried for anchoring.

3. The inside edge of the geotextile was marked in the vicinity of centerline. This location was monitored while the subgrade was rutted to ensure the inside edge of the geotextile remained stationary. Loaded construction equipment was driven across the 203 mm (8 in.) of subbase aggregate to tension the fabric by rutting the subgrade. Construction equipment used for rutting was confined between an offset between 3050 mm (120 in.) from centerline and the shoulder break. The uncovered inside edge of the geotextile did not show any signs of movement during the rutting process.

4. When the desired rut depth of 150 mm (6 in.) was reached, the contractor placed and compacted additional subbase aggregate to bring the road cross section to the final grade.

3.5.3 Separation Geotextile Placement

The construction requirements for the use of stabilization geotextiles (separation application) is described in Section 620.00 of the MDOT Standard Specifications for Highways and Bridges (MDOT, 1997). Before placing the geotextile, the site was leveled and made free from obstructions and depressions that could tear or puncture the fabric. The fabric was then laid out with 457-mm (18-in.) overlaps and a minimum of 200 mm (8 in.) of cover material was placed over the geotextile. At no time was

construction equipment allowed on the fabric when less than 200 mm (8 in.) of aggregate material was covering the geotextile.

3.5.4 Drainage Geocomposite Construction Procedure

A special construction procedure was adopted to install the drainage geocomposite in Section D.

1. The geocomposite was oriented such that the roll length ran perpendicular to the roadway alignment.
2. Joints were overlapped 75 mm (3 in.) in Sections D-1, and D-2, as well as the bottom layer of the drainage geocomposite in Section D-3. Butt joints were used for the upper drainage geocomposite in Section D-3 (see Figure 3.3).
3. Adjacent geocomposite were joined by tying the geonet cores together with plastic fasteners. These ties were spaced every 900 mm (36 in.) along the roll length and every 300 mm (12 in.) across the roll width.
4. Geocomposite rolls joined by butt joints were tied at the edge and spaced at 300-mm (12-in.) intervals.
5. The overlapped geotextile layer was secured by stitching using a flat or prayer seam. This differs from a J-seam in that the geotextile is not folded back on itself prior to stitching. The geotextiles were layered in a down slope manner consistent with the direction of the fill placement.
6. Construction equipment was not allowed to travel over the geocomposite without a minimum compacted fill thickness of 200 mm (8 in.) covering the geocomposite.

7. Compaction of the first lift above the geocomposite was done with a dozer initially and then with a smooth-drum roller with the vibrator turned off.

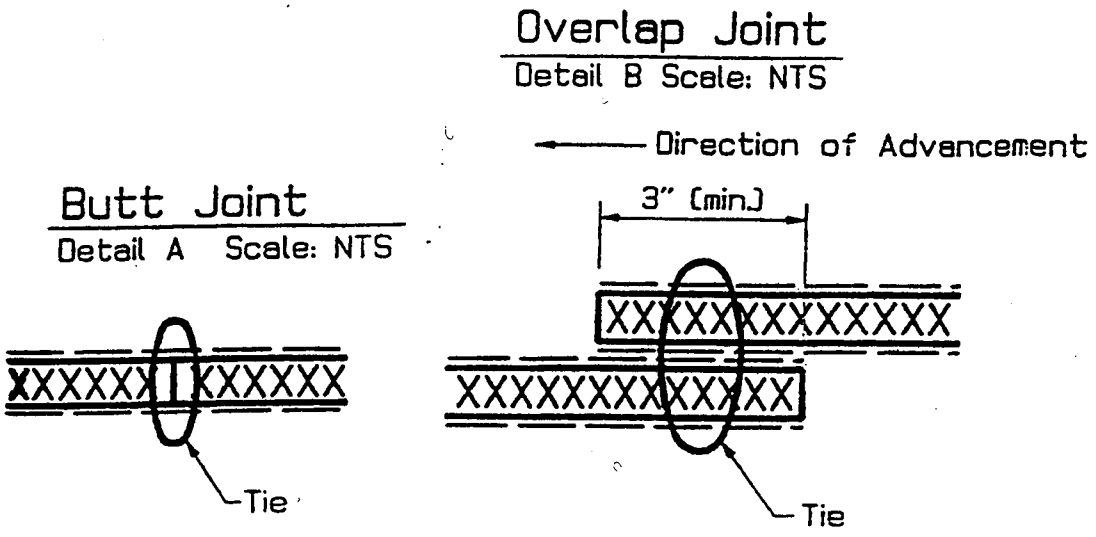

Figure 3.3 Geocomposite overlaps and joint schematics

3.6 SUMMARY

The reconstruction of 3.06 km (1.9 mi.) of Route 1A in the towns of Winterport/Frankfort, Maine presented an opportunity to evaluate use of four types of geosynthetics on weak subgrade soils. The subsurface soils on this road section were generally moist clays classified as A-6 and had CBR values of about 3.0. Historically the road has been plagued with cracking, localized bearing failures, and poor drainage.

Road sections in this project consist of a 180-mm (7-in.) layer of asphalt, and a 640-mm (25-in.) layer of aggregate subbase. Two Sections had subsections with a reduced aggregate subbase Section of 580 mm (23 in.). The original design of the road required an additional 150 mm (6 in.) of underlying granular soil to act as a stabilization

platform. However, with the incorporation of geosynthetics the proposed 150-mm (6-in.) stabilization lift was eliminated.

Reinforcement geogrid, reinforcement geotextile, separation geotextile and drainage geocomposite geonet were used in this project to evaluate their reinforcement, separation, filtration, and drainage performance for Maine soil and climatic conditions. This was done by comparing instrument measurements to previous literature of laboratory and field studies.

Construction occurred from May, 1997 to November, 1997, when work stopped for the winter. Work resumed in April, 1998 and was completed by June, 1998. Maine encountered its second driest summer since records have been taken (Hayden, 1996), making construction much easier than anticipated due to increased shear strength of the clay subgrade soil. The project was divided into six sections labeled A through F, with different geosynthetic applications. Four sections were designed using several combinations of reinforcement geogrid, reinforcement geotextile, and separation geotextile. One Section used a drainage geocomposite to improve drainage and reduce frost heave. These sections differ in placement of the geosynthetic and thickness of the subbase layer. These materials have different mechanical properties and installation techniques as described in this chapter.

This the first time that the State of Maine has used a three-layered geogrid, a high strength geotextile used for reinforcement, or a drainage geocomposite. The reinforcement geogrid, Tenax MS 330, was a three-layered polyethylene, extruded

geogrid with openings of approximately 60 mm by 40 mm (2.36 in. by 1.57 in.) and a rib thickness of about 2 mm (0.08 in.). The high modulus woven geotextile used in a reinforcement application was Mirafi 67809. A high strength drainage geocomposite was used in the drainage section (Tendrain 100-2) to maintain a high in-plane flow. The separation geotextile was Mirafi 180N, a heavy weight nonwoven geotextile.

Procedures for placing the geosynthetics were developed by Maine DOT with the assistance of Dr. Barry Christopher, a geotechnical consultant in the geosynthetics industry. The geogrid and high strength geotextile were laid at the proper elevation and alignment, so that the roll length ran parallel to the centerline. The geogrid was overlapped and tied with plastic ties and the geotextile was sewn with a J-stitch. The granular material was back dumped from trucks riding on top of the reinforced fill and bladed onto the geogrid so that the fill rolled onto the material ahead of the dozer. A minimum of 200 mm (8 in.) of material was required before construction equipment could travel on it. Compaction was done with the dozer, then followed by a smooth drum vibratory roller to achieve a minimum compacted density of 95% of the Modified Procter density (AASHTO T180). The reinforcement geotextile was rutted to mobilize tensile stresses. This was done by running loaded trucks over the geotextile after 203 mm (8 in.) of overlying subbase aggregate was placed. The drainage geocomposite was oriented with the roll length perpendicular to the roadway alignment. Joints were overlapped in Sections D-1 and D-2, butt joints were used for the upper layer of geocomposite in Section D-3. Construction equipment was not allowed to travel over the geocomposite without a minimum compacted fill thickness of 200 mm (8 in.) covering the geocomposite.

4. INSTRUMENTATION AND FIELD MEASUREMENTS

4.1 INTRODUCTION

Instrumentation was installed to monitor the performance of the test sections. The reinforcement geogrid was instrumented with loadcells, the reinforcement geotextile was instrumented with strain gages, frost penetration was measured with thermocouples, and piezometers were used to measure pore water pressures. In addition, falling weight deflectometer (FWD) measurements were taken at several locations in each test section to monitor pavement performance.

4.2 GEOGRID INSTRUMENTATION

The reinforced geogrid was Tenax MS330. This material proved to be very difficult to instrument. The thin ribs (2-mm (0.08-in.) thickness) prevented strain gages from being mounted directly on the ribs and it would have been necessary to mount strain gages on each of the three separate layers.

A special process of instrumentation was adopted that required use of an additional material to mount the strain gages on. A geomembrane with a stiffness similar to the geogrid was used to replace selected geogrid ribs. Strain gages were mounted on the geomembrane and wired in a Wheatstone configuration to form a loadcell to measure force in the geogrid.

4.2.1 Loadcell Design

To measure the force in all three layers, it was necessary to develop a relationship between the forces in the substitute material and the geogrid. An equation that relates the force in each material was derived to determine the dimensions of the substitute material that would have similar stiffness properties to the geogrid.

$$A_m = \frac{E_g \cdot L_m \cdot W_g}{L_g \cdot E_m} \qquad \text{(Equation 4.1)}$$

$$A_m = W_m \cdot t_m \qquad \text{(Equation 4.2)}$$

where:

A_m = cross sectional area of substitute material

W_m = width of the substitute material

W_g = width of geogrid space the material would replace

E_g = modulus of elasticity of the geogrid

L_m = length of the substitute material

L_g = length of the geogrid the substitute material would replace

E_m = modulus of elasticity of the substitute material

t_m = thickness of substitute material

The length of the substitute material was chosen to be 114 mm (4.5 in.) and equation 4.1 was solved by trial and error to determine the width of substitute material. The length of the grid replaced by the loadcell L_g was 152 mm (6 in.), and the width of grid replaced W_g was 124 mm (4.88 in.). The length of the material (L_m) does not equal

the length of geogrid replaced (L_g) because of the clamps used to attach the loadcell to the geogrid. A light reflective high density polyethylene geomembrane (Gundle model GSE HD) with a thickness t_m of 2.5 mm (100 mils) and modulus of elasticity of 552 MPa (80 ksi) was selected as the substituted material. The geomembrane was donated by the manufacturer. The material properties of this geomembrane can be found in Table 4.1. The width of the substitute material was calculated to be 27 mm (1.06 in.). To form a load-cell, this material was cut into a dog bone shape as specified by ASTM D638 (ASTM, 1994) and four strain gages were attached in a Wheatstone Bridge configuration as shown in Figure 4.1. A Wheatstone Bridge is capable of measuring minute resistance changes and converts the change in resistance to a change in voltage.

Table 4.1 Properties of Grundle GSE HD light reflective HDPE CX 2.5 mm (100 mils) geomembrane.

Yield Strength	**Break Strength**	**Tear Resistance ASTM D1004**	**Shear Strength ASTM D4437**
37.8 kN/m	70.0 kN/m	0.58 Kn.	35.5 kN/m

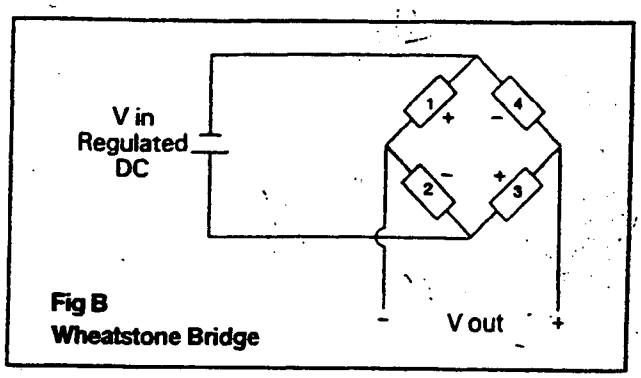

Figure 4.1 Wheatstone Bridge (OMEGA Engineering, 1988)

4.2.2 Loadcell Fabrication

The loadcells on the geogrid were fabricated from four strain gages that were attached to geomembrane and wired together. The strain gages were MicroMeasurement type EP-08-250BG-120. These gages are made from a special grade of fully annealed constantan with maximum ductility for use in the measurement of post-yield or plastic strains. MicroMeasurement terminals were also used to attach the lead wires to the strain gage wires. The following procedure, as recommended by Measurements Group tech note TN-5-5-4, was used to attach the strain gages to the geomembrane. First the geomembrane was cut into a dog-bone shape as shown in Figure 4.2. Then, 80 grit followed by 220 grit sandpaper was used to create a cross-hatching pattern of abrasion to provide a better epoxy bond. The surface was then marked with a light lead drafting pencil to position the strain gages, cleaned with phosphoric acid, and then neutralized with ammonia water. Terminals from MicroMeasurements were used to attach the strain gage wires to the lead wires. This was done to simplify the wiring scheme since the lead wires were large and difficult to attach to the small strain gage terminal. The gages and terminals were then placed on a clean surface and cellophane tape was applied. The cellophane tape was used so that it could be easily transferred to the geomembrane.

Armstrong adhesive epoxy (MM A-12 adhesive) was then applied to the gage and the gage was placed on the geomembrane with the tape. Two gages were attached on one side at one time. Neoprene rubber pads were placed over the gages and C-clamps were used to apply pressure for a period of 24 hours. The procedure was then repeated for the other side. Gages were attached to both sides of the geomembrane as shown in Figure 4.2. The four gages were attached by 34-gage single conductor copper wire. A schematic of the wiring can be seen in Figure 4.1.

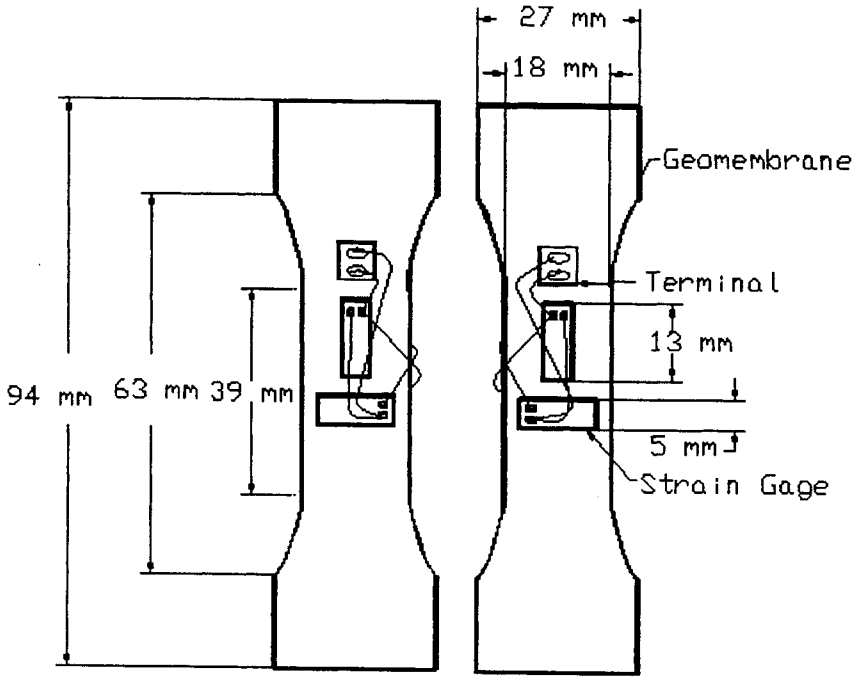

Due to the non-uniform opening spacing in the three-layered geogrid, the 94-mm dimension is approximate.

Figure 4.2 Schematic of loadcell

4.2.3 Loadcell attachment to geogrid

Ribs were removed from the geogrid in the areas where the loadcells were attached so that the loadcell would be carrying the tensile force. The loadcells were attached to the geogrid with aluminum bar, bolts and epoxy as shown in Figure 4.3. The procedure that was used to attach the loadcells to the geogrid is given below.

1. In the laboratory sawhorses were used to suspend a 3.8 by 15 m (12.5 by 50 ft) section of geogrid about 1.15 m (3.75 ft) off the floor.
2. Plywood sheets were laid on the topside of the grid to serve as platforms for workers to kneel on while attaching the instruments.
3. The loadcell locations were laid out on the geogrid. For stations with a single travel lane, two load cells were attached perpendicular to the centerline at each of the following offsets: 2.4, 2.7, and 3.0 m (8, 9, and 10 ft) from the centerline. One gage was placed parallel to the centerline at a 2.7-m (9-ft) offset. In Section A-2, which has a climbing lane, six loadcells were attached perpendicular to the centerline at each of the following offsets: 6.1, 6.4, and 6.7 m (20, 21, and 22 ft) from the centerline. One loadcell was attached parallel to the centerline at an offset of 6.4 m (21 ft).
4. Two rows of four ribs (three for gages parallel to the road centerline) that run parallel to the loadcell were removed as shown in Figure 4.3.
5. Two-aluminum bars with dimensions of 160 mm by 38 mm by 6 mm (6.30 in. by 1.50 in. by 0.25 in.) covered with West Epoxy 105 resin and 206 hardener mixed in a ratio of four parts resin to one part hardener were used to clamp the loadcell to the geogrid. The aluminum bars were bolted together with the loadcell and the geogrid sandwiched between them.

6. The aluminum bars were attached with six 10-32 round head steel machine screws (4.8 mm diameter by 25.4 mm long), washers, and nuts. Thus, the loadcell was connected to the geogrid by a combination of bolts and epoxy.
7. For field installation a watertight seal was used around the cells. Teflon coating was placed on the gages and the leads. Then MicroMeasurements M-coat F, which is a butyl rubber, was put around the gages and the geomembrane. This was then covered by neoprene rubber.
8. Silicone caulking was used to seal the interface between the neoprene rubber and geomembrane. This protective coating served to waterproof the loadcells and to protect the gages from the impact of the subbase aggregate.

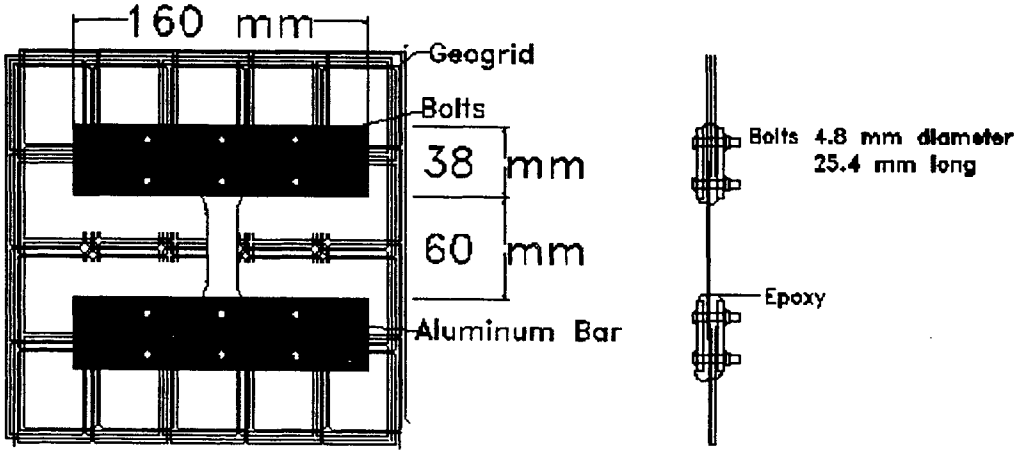

Figure 4.3 Loadcell on geogrid.

Seven loadcells were attached to a 15.0-m by 3.8-m (50.0 ft by 12.5 ft) sheet of reinforcement geogrid. These loadcells were staggered in the outside wheelpath of the right lane of traffic. In Sections A-1, E-2, and E-3, where there is no climbing lane, the parallel loadcell was placed 2.7 m (9 ft) from the centerline of the road. Two loadcells

were attached perpendicular to the centerline at offsets of 2.4, 2.7, and 3.0 m (8, 9, and 10 ft) from the centerline as shown in Figure 4.4 and Table 4.2. For Section A-2, where there is a climbing lane, the loadcells are placed in the outside wheelpath of the climbing lane, offset from the right side of the inner lane, as shown in Figure 4.5 and Table 4.3.

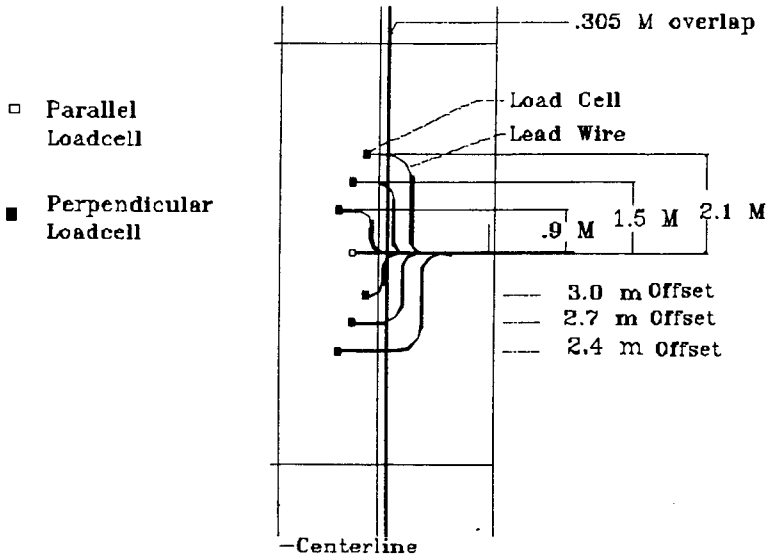

Figure 4.4 Loadcell layout for Sections A-1, E-2 and E-3.

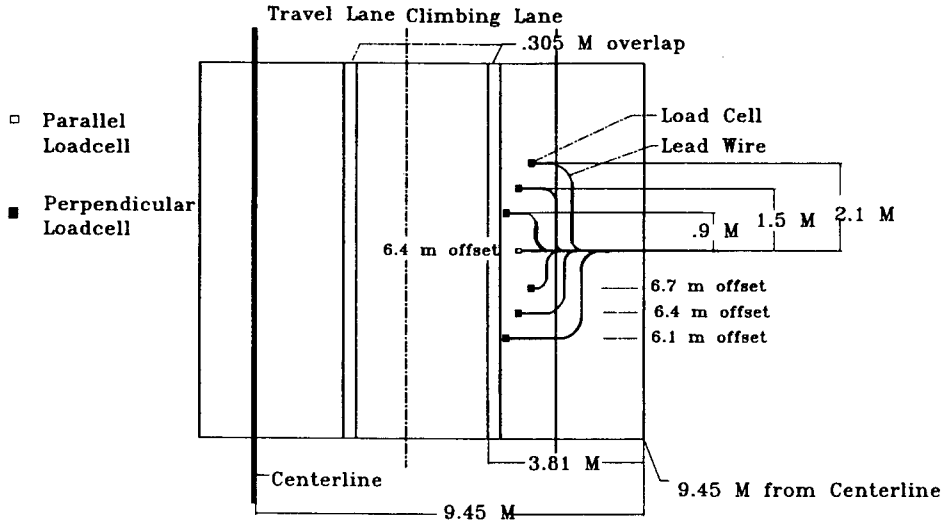

Figure 4.5 Loadcell layout for Section A-2.

Table 4.2 Load cell locations for Sections A-1, E-2, and E-3.

Loadcell position	Loadcell orientation	Station relative to loadcell D (m)	Offset from C/L (m)
A	Perpendicular	-2.1	2.4
B	Perpendicular	-1.5	2.7
C	Perpendicular	-0.9	3.0
D	Parallel	0.0	2.7
E	Perpendicular	+0.9	2.4
F	Perpendicular	+1.5	2.7
G	Perpendicular	+2.1	3.0

Table 4.3 Load cell locations for Section A-2.

Loadcell position	Loadcell orientation	Station relative to loadcell D (m)	Offset from C/L (m)
A	Perpendicular	-2.1	6.1
B	Perpendicular	-1.5	6.4
C	Perpendicular	-0.9	6.7
D	Parallel	0.0	6.4
E	Perpendicular	+0.9	6.1
F	Perpendicular	+1.5	6.4
G	Perpendicular	+2.1	6.7

4.2.4 Field Installation

The geogrids were rolled up and transported to Winterport/Frankfort by pickup truck. Then the instrumented geogrid was centered on the station so that the center parallel gage was at the desired location. The center parallel gage was positioned to be 2.7 m (9 ft) from the centerline in sections without a climbing lane (see Figure 4.4), and 6.4 m (21 ft) from the centerline in sections with a climbing lane as shown in Figure 4.5.

Lead wires from two or three loadcells were then snaked through 19-mm (¾ in.) flexible ENT conduit. The three pieces of conduit needed for one section were then brought to the edge of the geogrid, tied together and placed in a 300-mm (12-in.) deep trench. The trench was dug to a 152-mm (6-in.) diameter vertical PVC pipe where the

wires are kept protected from the environment (see Figure 4.10). Initially fine sand was placed over the loadcells to protect them from placement and compaction of the overlying subbase. After a few stations had been installed an additional procedure of placing halved pieces of PVC pipe that fit over the loadcell was adopted. This was an attempt to better protect the loadcells but it was not effective in reducing loadcell failure. Installation dates of instrumented sections are listed in Table 4.4.

Table 4.4 Dates instrumented geogrid stations were installed.

Station	Installation Date	Comments
88+85 m (291+50 ft)	7/23/97	Loadcells and thermocouples were installed. Seven functioning cells were installed, five functioning after compaction.
88+54 m (290+50 ft)	7/28/97	Six loadcells were functioning at the time of installation. When checked after the first lift of overlying aggregate was spread, only four were functioning; when checked after the aggregate was compacted, the number of functioning gages had increased to five.
64+12 m (210+38 ft)	9/5/97	Six functioning loadcells were installed on geogrid. Five survived the first lift; five were still functioning after compaction.
64+62 m (212+00 ft)	9/9/97	Loadcells and thermocouples were installed. Five cells were functioning at the time of installation and these five cells were still functioning after the first lift of overlying aggregate was spread. However, only four cells were functioning after the aggregate was compacted.
66+29 m (217+50 ft)	9/15/97	Loadcells and thermocouples were installed on subgrade. Only two cells were functioning at the time of installation, however, zero survived compaction.
	9/18/97	Geogrid installed 250 mm below the bottom of asphalt. Six functioning cells were installed; five were still functioning after compaction.

4.2.5 Loadcell calibration

A series of calibration tests were performed on the geogrid loadcells to obtain calibration factors to correlate the loadcell output to the force present in the geogrid. Since there are loadcells both perpendicular and parallel to the centerline of the road, two

sets of tests were performed. A set of six tests was performed in the transverse direction (perpendicular to centerline) and a second set of six tests in the machine direction (parallel to centerline).

Loadcells attached to geogrid specimens, as described above, were calibrated in a wide strip tensile test. The tests were performed in general accordance with ASTM D4695 (ASTM, 1994). The specimen size was 1520 mm wide by 300 mm (60 in. by 12 in.) between the grips. The loadcell was attached to the center of the grid. The two long sides of the specimen were clamped between a pair of steel C-channels 51 mm by 25 mm by 5 mm (2 in. by 1 in. by 0.2 in.) with nine 9.5 mm diameter by 38 mm long (0.37 in. diameter by 1.50 in. long) bolts as shown in Figure 4.6. The grid was anchored in the channels by applying West System 105 epoxy resin and 206 slow epoxy hardener mixed in a 4:1 ratio. The epoxy was applied to the ends of the geogrid, which extended approximately 50 mm (2 in.), beyond the C-channels. A lead wire was attached to the loadcell. The strains were read by a MicroMeasurements P3500 digital strain indicator. The specimen was tested in an Instron tension/compression machine. Three load/unload cycles were applied. Load was applied at a rate of 0.25 mm per minute (0.01 in./min) and loaded to approximately 4 kN/m (274 lb/ft). Field measurements were less than this value. The load/unload cycles and strain measurements exhibited an open hyterisis shape. The first loading cycle was chosen for the calibration factor because in the field the geogrid would not be unloaded from the initial loading (see Figure 2, in Appendix). An average of the first loading cycle from the six tests was used as the calibration factor for the perpendicular geogrid, as shown in Figure 4.7. The parallel calibration tests showed a curve that was fit by two functions, a power curve and a linear curve.

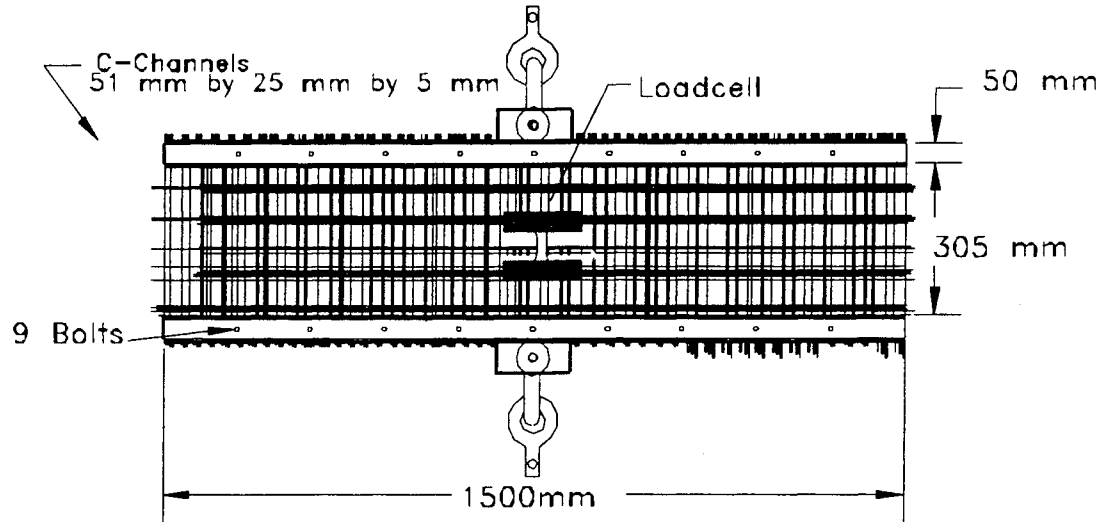

Figure 4.6 Geogrid loadcell calibration setup

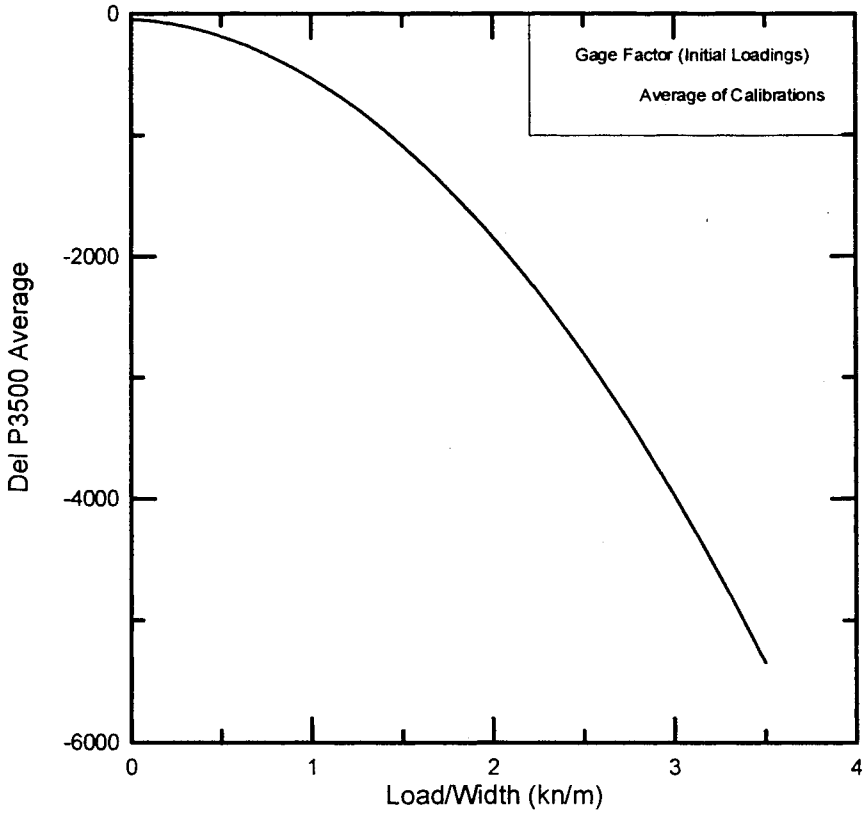

Figure 4.7 Average of first loading from six perpendicular geogrid calibration tests

4.3 REINFORCEMENT GEOTEXTILE INSTRUMENTATION

The reinforcement geotextile was Mirafi 67809, a woven polypropylene material. The geotextile was much easier to instrument than the reinforcement geogrid. Strain gages were used to monitor the force in the geotextile.

4.3.1 Strain Gage Characteristics

The strain gages were Texas Measurements model YL-60 with presoldered lead wires. These gages are used to measure strains up to 10 to 20% elongation without creeping or cracking. The YL-60 strain gage is 60 mm by 1 mm (2.36 in. by 0.04 in.). A sheet of geotextile 3.8 m wide by 15.0 m long (12.5 ft by 50 ft) was instrumented with seventeen strain gages. Approximately nine gages were placed on the bottom side and eight gages were attached to the topside of the geotextile. In general one gage was attached on top and bottom at the same location, and the values were averaged at each location to eliminate the effects of bending.

4.3.2 Strain Gage Attachment to Geotextile

Strain gages were attached to the geotextile in the laboratory. The strain gages were attached to the geotextile in the same pattern as the geogrid loadcells (see Figure 4.8 and Table 4.3). To attach the strain gages to the geotextile, the surface was thoroughly cleaned with soapy water, and then a poly-primer, Texas Measurements surface preparation agent B, was applied to assure a good bond. Cyanoacrylate CN adhesive was then applied to the gage and the gage was attached to the geotextile. Pressure was

applied to the gage for one minute while the adhesive cured. The gages were protected using two different methods. The first used nitrile rubber and neoprene with silicon caulking to seal the sides. The other method just used silicon caulking to form a protective coating over the gage. One side of the geotextile was instrumented and waterproofed at a time and then it was flipped over to instrument the other side. The presoldered lead wires were collected on the topside of the geotextile by making small holes in the geotextile to feed the wires through. Then longer lead wires were attached so that all of the lead wires were on the topside of the geotextile.

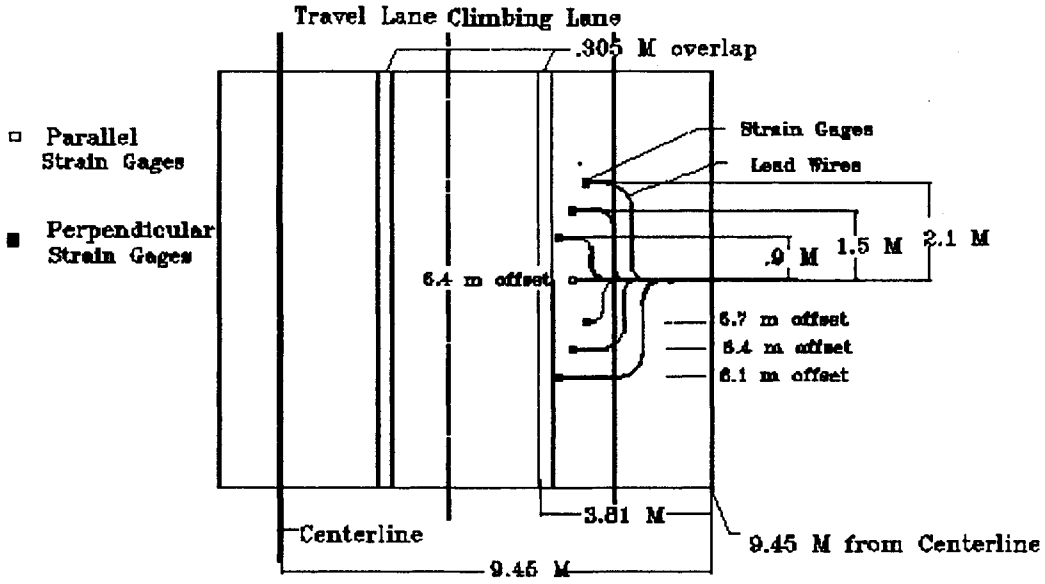

Figure 4.8 Reinforcement geotextile layout.

4.3.3 Strain Gage Calibration

The geotextile was tested in the same set of clamps as the geogrid. However, a different anchoring method was used. To prevent slippage in the clamps, the fabric was wrapped around a 60.3-mm (2-3/8 in.) outer diameter steel pipe and then looped back

into the channel section. Then the channels were bolted together (see Figure 4.9). The inside edges of the C-channel and geotextile were sprayed with orange paint. This served as a check to make sure there was no slippage in the geotextile and grips. No splipage was observed. Epoxy was not needed to anchor the specimens.

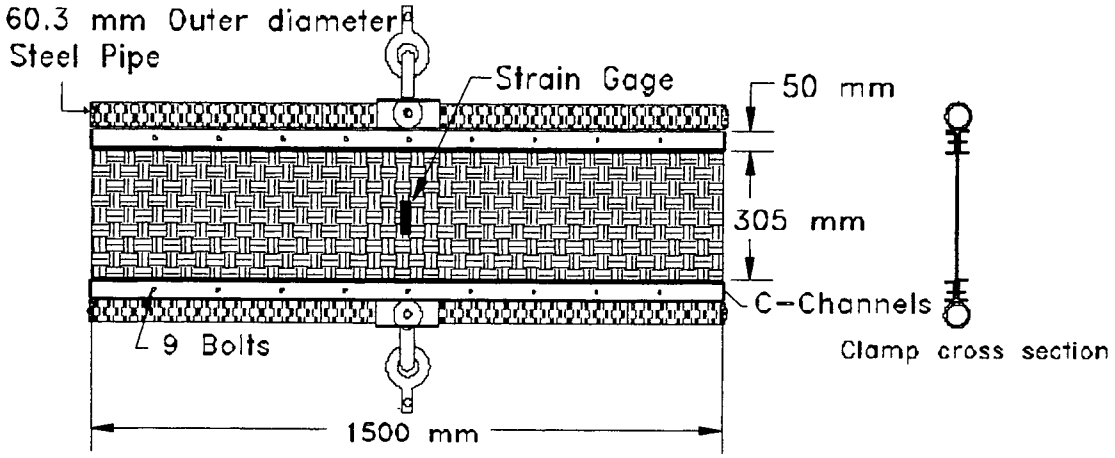

Figure 4.9 Geotextile strain gage calibration setup.

Eleven calibration tests were done on the geotextile, six with the strain gage in the perpendicular direction (TD) and five with the strain gages parallel to the centerline of the road. The tests were performed in the same manner as the geogrid. The geotextile was loaded into the Instron Machine and then subjected to three cycles of loading and unloading. The geotextile was brought up to a stress of approximately 6 kN/m, which was greater than the maximum force from the field. For the gages perpendicular to the centerline there was a linear relationship between the strain gage readings and the applied stress. However, the gages parallel to the centerline followed a nonlinear relationship and were fitted with a power curve. The best fit equations and test results can be found in Appendix A.

4.3.4 Field Installation

The instrumented geotextile was placed in the field with the gage that was parallel to the centerline at the desired station. Two lead wires were then snaked through one 19 mm (¾ in.) flexible ENT conduit. The nine conduit tubes required for one station were then brought together at the edge of the geogrid and placed in a 300-mm (12-in.) deep by 300-mm (12-in.) wide trench. The trench was dug to a 152-mm (6-in.) diameter PVC pipe that was set vertically in the ground, which kept the wires protected from the environment as shown in Figure 4.10. The installation timetable for the geotextile is given in Table 4.5.

Table 4.5 Dates of installed instrumented Sections

Station	Installation Date	Comments
67+51 m (221+50 ft)	9/18/97	Instrumented geotextile installed. Seventeen gages were installed, seventeen survived first lift and compaction. Rutting was done so that the wheels of dump truck straddled the strain gages.
67+82 m (222+50 ft)	9/19/97	Instrumented geotextile and thermocouples installed. Seventeen were installed, sixteen were functioning after compaction and rutting. Rutting was done on the left side of the gages.

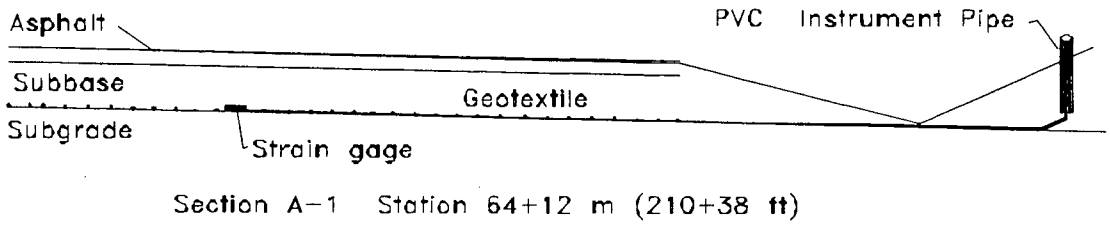

Figure 4.10 Cross section of instrumentation and collection pipe.

4.4 FROST PENETRATION MEASUREMENT

Thermocouples were used to monitor frost penetration. The University of Maine installed thermocouples at four stations. Additional thermocouples were installed by the U.S. Army Cold Regions Research and Engineering Lab and are not discussed in this report.

4.4.1 Thermocouple Characteristics

The thermocouples used in this project are 20-gage copper constantan (Type T). A bi-metal reaction occurs at the joined ends of the wires and measurement of the resulting electrical potential allows the temperature to be determined. The initial calibration tolerances for the thermocouples was +/- 1.1°C (2 °F) for standard limits. The thermocouples were attached to 25-mm (1-in.) diameter wooden dowels. Eleven sensors were placed vertically every 150-mm (6 in.), from top to the bottom of the dowel, the twelfth sensor was a flyer, that was not attached to the dowel and was placed in the soil 150 mm (6 in.) above the top of the dowel.

4.4.2 Thermocouple Locations

A string of thermocouples was installed in each of the following sections: A-1, A-2, B-2, and E-3. They were installed just prior to placement of the geosynthetic. Split spoon samples were taken at each section when the thermocouples were installed. The water contents of these samples are shown in Table 4.6. The depths of the thermocouples are given in Table 4.7. A layout of Section A-1 is shown in Figure 4.11. This is typical of the other three sections. In Section E-3, the top of the dowel is even with the

reinforcement geogrid placed 430 mm (17 in.) below the top of pavement. Thus, in Sections A-1, A-2, and B-2 the top of the dowel is even with the subgrade.

Table 4.6 Water contents at thermocouple stations.

Section and Station	**A-1; 64+62 m (212+00)**		**A-2; 66+29 m (217+50)**		**B-2; 67+82 m (222+50)**		**E-3; 88+85 m (291+50)**	
Installation Date	**9/9/97**		**9/15/97**		**9/19/97**		**7/23/97**	
	Depth (mm)	Water Content	Depth (mm)	Water Content	Depth (mm)	Water Content	Depth (mm)	Water Content
	1370	10.8%	1370	10.1%	1430	9.00%	1040	7.5%
	1980	16.2%	1980	10.4%	2040	10.52%	1650	7.7%
	2590	14.2%	2590	13.2%	2650	11.19%	2260	7.0%

(1) Note: Depth measured from the top of pavement

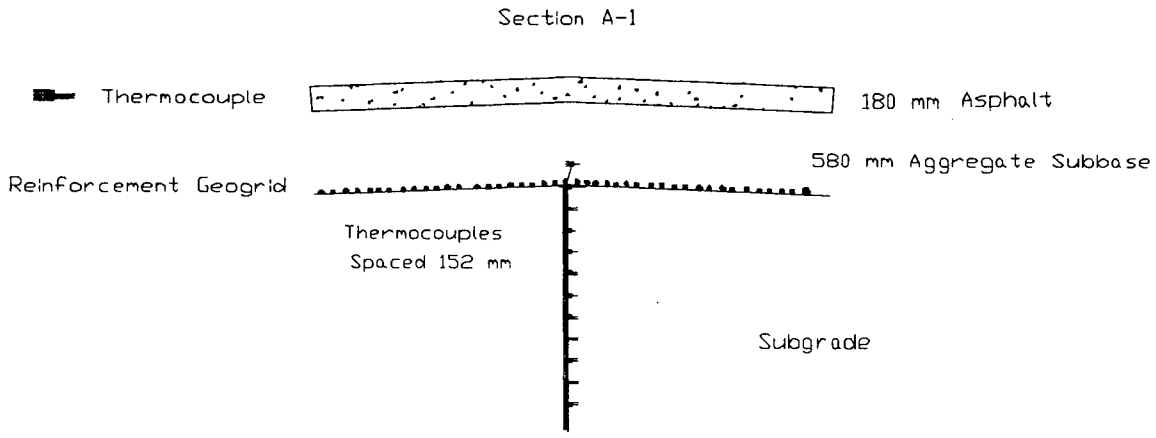

Figure 4.11 Section A-1, thermocouple layout.

Table 4.7 Thermocouple depths.

Station				
Section	**E-3**	**B-2**	**A-2**	**A-1**
T-Sensor	**291+50 (mm)**	**222+50 (mm)**	**217+50 (mm)**	**212+50**
1	430	820	760	760
2	582	972	912	912
3	734	1124	1064	1064
4	886	1276	1216	1216
5	1038	1428	1368	1368
6	1190	1580	1520	1520
7	1342	1732	1672	1672
8	1494	1884	1824	1824
9	1646	2036	1976	1976
10	1798	2188	2128	2128
11	1950	2340	2280	2280
12	2102	2492	2432	2432

(1) Note: measurements taken from top of pavement (mm)

4.4.3 Field Installation

Thermocouples were installed near the highway centerline just prior to placement of the instrumented geosynthetic. A Maine DOT drill rig augured a 102-mm (4-in.) diameter hole to approximately 2.0 m (6.5 ft) below subgrade. Split spoon samples were taken at depths of approximately 0.61 m, 1.22 m, and 1.83 m (2 ft, 4 ft, 6 ft) below subgrade. For sections with geogrid, the wire was fed through the grid and the cable was bundled on top of the geogrid with the ENT conduit, and placed in the trench to the vertical PVC pipe. For sections with geotextile, the thermocouple cable was placed in a 25-mm (1-in.) deep trench under the geotextile and then bundled with the ENT conduit

starting at the edge of the geotextile. The conduit and cable were then laid in a trench to the 152-mm (6 in.) diameter vertical PVC protective pipe (see Figure 4.10).

Manual readings were taken using a hand-held electronic thermometer (Omega Type 450 ATT) approximately once a week during the winter. The accuracy of the readings can be improved by keeping the electronic thermometer at a constant temperature. This was done by keeping the electronic thermometer inside a heated vehicle. Since the lead wires from the thermocouples were too short to reach the vehicle, an extension cord was made from thermocouple wires with couplings that attached to the thermocouple leads.

4.5 PIEZOMETERS AND TILT BUCKETS

Piezometers were used to monitor pore water pressures in Sections C, D, E, and in the control section. They were used to evaluate the efficiency of the drainage geocomposite in reducing the pore water pressure in the subbase course and subgrade. The piezometers were installed beneath the right breakdown lane.

Six tilt buckets attached to outlet pipes were installed in Sections D-1, D-2, and D-3 to monitor the amount of water removed from each section (see Figure 4.13). A micro switch was positioned on the tilt buckets and was actuated every other time the tilt bucket dumped (Hayden, et al., 1998). Data was collected with a traffic counter 24 hours a day and downloaded over phone lines to the Maine Department of Transportation offices (Hayden, et al., 1998).

4.5.1 Piezometer Characteristics

RocTest PWS vibrating wire piezometers were used for this project. They have a low air entry sintered ceramic porous stone and a 34 kPa (5 psi) range of measurement. Measurements are taken with a RocTest MB-6T unit. A low air entry porous stone was chosen because the surrounding soil would be partially saturated for at least a portion of the year and the low air entry stone would help to maintain saturation of the inner cavity of the piezometer body. To increase the functioning life of the piezometers in a freezing environment the porous stone (filter) and inner portion of the piezometer body was saturated with 95% ethyl alcohol using the following procedure. The filters were removed piezometer body. The filters were placed in a vacuum, then alcohol was added to the vacuum. The vacuum was released. The piezometer body with the filter removed was immersed in an alcohol bath. With the diaphragm end pointing upwards and submerged, the filter was placed back into the piezometer body. The piezometers were kept submerged in the alcohol until they were installed.

4.5.2 Piezometer Location

Fifteen piezometers were installed for this project. Three were placed in the same hole at five different stations (see Figure 4.12 for dimensions). Due to time constraints the piezometers were not placed at centerline which was the original design. Instead they were placed beneath the break down lane, 3.7 m (12 ft) right of centerline, after the first lift of asphalt had been laid. In Sections C-2, D-2, and D-3, a hole was dug to the top of the geosynthetic, a small hole was punched through it with a metal rod and the bottom piezometer was placed about 150 mm (6 in.) below the geosynthetic. The middle

piezometer was placed just above the geosynthetic and the top one was placed at mid-thickness of the subbase aggregate. In Section D-1, the undercut section, the bottom piezometer was placed 153 mm (6 in.) below the drainage geocomposite, the middle piezometer was placed at the interface between the subgrade backfill and subbase. The top piezometer was placed in the aggregate subbase layer. In the control section, the bottom piezometer was placed 216 mm (8.5 in.) below subgrade, the middle instrument was placed just above the top of subgrade, and the third piezometer was placed at mid-

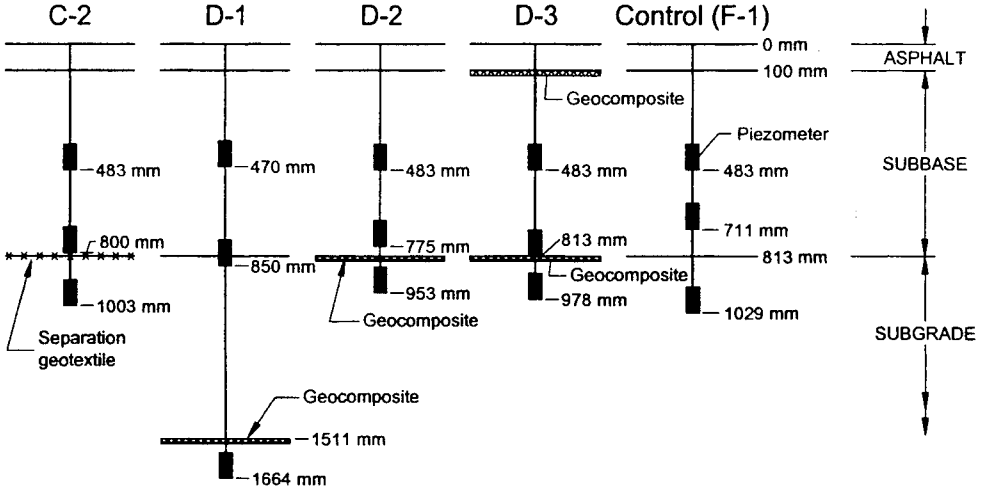

Notes: 1. Depths are measured from top of pavement.
2. Piezometers were installed beneath the right shoulder. In the shoulder, the pavement thickness is 100 mm (4 in.) and the subbase thickness is 713 mm (28 in.).

thickness of the aggregate subbase.

Figure 4.12 Piezometer layout.

4.5.3 Field Installation

To install the piezometers, MDOT drilled a hole with a 100 mm (4 in.) solid auger to the approximate depth of the drainage geocomposite. A rebar with approximately the same diameter as the piezometer was punched through the

geocomposite and advanced approximately 150 mm (6 in.) below the geocomposite. The bottom piezometer was installed at the bottom of the hole made by the rebar. The soil excavated from the hole was packed down to the depth of the second piezometer. The second piezometer was placed and more soil or subbase aggregate was placed in the hole to the depth of the top piezometer. The last piezometer was placed and the wires were gathered at the surface. A pavement cutter was used to cut a groove in the pavement for the wires to lay in. Then a crack sealer was used to seal the groove with the three wires in it. The wires were then placed in a 150-mm (6-in.) deep trench on the side of the road. The ends of the wires were fed into a vertical PVC pipe to protect them from the environment.

4.5.4 Tilt Bucket Location and Description

A tilt bucket is a device to measure water flow. A metal bucket with a known volume is used to collect water from the end of an outlet pipe. When the bucket is full, it automatically dumps and triggers a counter that records the number of bucket dumps (see Figure 4.13). Tilt buckets were installed at six different stations in three sections as described in Table 4.8.

Table 4.8 Monitored outlet locations and details (Hayden et al., 1998).

Outlet Locations	Test Section Designation	Drainage Pipe Location and Length	Geocomposite Location
Outlet A 79+67 m right	D-1	77+72 – 79+25 m right 152 m run	Geocomposite is located 460-mm below subgrade and is placed along the low side of a super-elevated turn.
Outlet B 79+67 m left	D-1	79+25 – 79+71 m left 46 m run	Geocomposite located 460-mm below subgrade in a section with standard cross slope.
Outlet C 79+67 m right	D-1	79+25 – 79+71 m right 46 m run	Geocomposite located 460-mm below subgrade in a section with standard cross slope.
Outlet D 81+69 m left	D-2	79+71 – 81+69 m left 200 m run	Geocomposite is located at subgrade along the low side of a super-elevated turn.
Outlet E 81+69 m left	D-3	81+69 – 81+99 m 30 m run	Geocomposite is located at subgrade in a section with standard cross slope.
Outlet F 81+69 m left	D-3	81+69 – 81+99 m 30 m run	Geocomposite is located directly beneath the pavement in a section with standard cross slope.

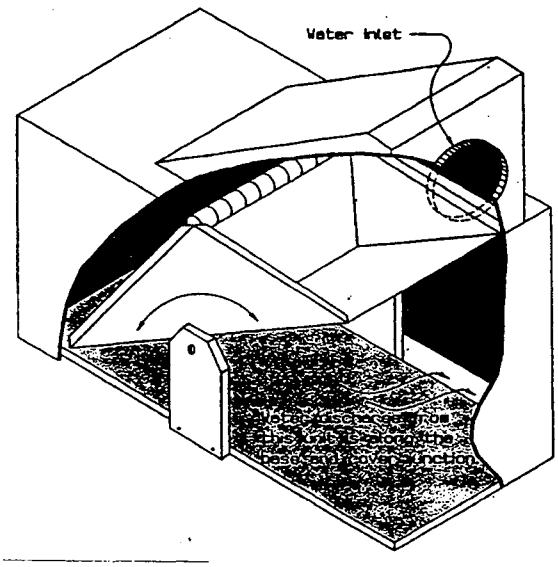

Figure 4.13 Tilt bucket schematic

4.6 FALLING WEIGHT DEFLECTOMETER MEASUREMENTS

Falling weight deflectometer (FWD) tests were used to measure the pavement performance and determine the impulse stiffness modulus. The purpose of these measurements was to determine if the impulse stiffness modulus was improved by the geosynthetics.

4.6.1 FWD Test Procedure

The Falling Weight Deflectometer (FWD) is an impact load device that applies a single-impulse transient load of approximately 25 to 30 millisecond duration. A dynamic force is applied to the pavement surface by dropping a weight onto a set of rubber cushions, which results in an impulse loading on an underlying 305-mm (12-in.) diameter plate in contact with the pavement. The impulse force is controlled by dropping a 27-kN, 40-kN, and 53-kN (6, 9, and 12-kip) weight. Accelerometer readings are taken by sensors located at predetermined distances from the load location. The trailer is outfitted with sensors that record the amount of downward vertical movement of the pavement as the weight strikes the pavement. For the set of tests taken prior to reconstruction, the approximate sensor spacing relative to the center of the plate were as follows: 0 (at the center of the plate), 203, 305, 457, 610, 914, and 1524 mm (0, 8, 12, 18, 24, 36, and 60 in.). For tests taken after reconstruction, MDOT changed the spacing to 0 (at the center of the plate), 305, 457, 610, 914, 1219, and 1524 mm (0, 12, 18, 24, 36, 48, and 60 in.) from the center of the plate. This change in spacing does not affect the resulting data.

4.6.2 Test Locations for Pre and Post-Construction Measurements

Falling Weight Deflectometer (FWD) measurements were taken at several stations, in each section, before construction began and then again in April, 1998. Only the average values have been reported.

4.7 SUMMARY

Several types of instruments were installed during reconstruction of Route 1A in Winterport and Frankfort, Maine to monitor performance of geosynthetic reinforcement, separation and drainage layers. Reinforcement geogrid and geotextile was instrumented with load cells and strain gages, respectively, to measure the axial force in the material. Frost penetration was monitored with thermocouples. Piezometers were installed to measure the pore water pressure in sections with drainage geocomposite and adjacent control sections. Falling weight deflectometer (FWD) measurements were taken before and after construction to determine the structural coefficient of the pavement in each section. These instruments provide useful information to monitor the performance of the geosynthetics that were used in this roadbed.

Loadcells were custom made to measure forces in the reinforcement geogrid. Calibration tests were performed on both the load cells and strain gages that were attached to the reinforcement geogrid and geotextile, respectively, to correlate the field measurements to force per unit width in the geosynthetic. Instrumentation was installed by October, 1997, and readings were taken at least monthly through August, 1998.

5. RESULTS

5.1 INTRODUCTION

The University of Maine installed instruments to evaluate the use of geosynthetics in Route 1A in Winterport and Frankfort, Maine. Loadcells were used to measure tensile forces in the geogrid. Likewise, strain gages were attached to the geotextile to measure tensile forces. Piezometers were installed in Sections C-2, D-1, D-2, D-3, and in the control section to measure the pore water pressure above and below the geosynthetic. Thermocouples were installed at stations 64+62, 66+29, 67+82, and 88+85 m (212+00, 217+50, 222+50, and 291+50 ft) to monitor frost penetration. Details of instrumentation characteristics and installation procedures are given in Chapter 4. Falling weight deflectometer (FWD) readings were taken before and after construction to determine the structural coefficients of the asphalt and subbase. Loadcell, strain gage, piezometer, and thermocouple readings were taken from installation through August, 1998. This chapter will present the results from these instruments.

5.2 GEOGRID LOADCELL RESULTS

Seven loadcells were attached to the geogrid in Sections A-1, A-2, and E-3. The survival of these loadcells ranged from zero to 57% as summarized in Table 5.1. Loadcells were custom made for Tenax 330 three-layered geogrid as described in Chapter 4. The majority of the loadcell failures occurred during placement and compaction of the overlying subbase aggregate. After the first geogrid installation at station 88+85 m

(291+50 ft), halved PVC pipes were placed over the loadcells to better protect the instrument. This did not significantly improve loadcell survivability. Loadcell failures could have been caused by impact from the overlying aggregate, severe bending, debonding of a strain gage from the loadcell, excessive elongation of one or more of the strain gages that make up the loadcell, water intrusion, or disconnection of a branch of the electrical circuit.

Table 5.1 Geogrid loadcell survivability

GEOGRID LOADCELLS									
Station (meters)	**1**	**2**	**3**	**4**	**5**	**6**	**7**	**Survival at end of Const.**	**Long Term Survival**
88+85 (E-3)	F(C)	F(A)	F(C)	W	F(C)	F(C)	F(C)	29%	14%
88+54 (E-3)	F(A)	F(C)	W	F(A)	W	F(C)	W	71%	57%
64+12 (A-1)	F(C)	W	F(C)	W	W	F(A)	F(C)	57%	43%
64+62 (A-1)	W	F(C)	F(C)	F(C)	F(C)	F(A)	F(C)	29%	14%
66+29 (A-2) Top Geogrid	F(C)	F(C)	F(C)	F(A)	F(A)	W	F(A)	57%	14%
66+29 (A-2) Bottom Geogrid	F(C)	F(C)	F(C)	F(C)	F(C)	F(C)	F(C)	0%	0%

W = Working
F(C) = Failed during construction
F(A) = Failed after construction

5.2.1 Loadcells Perpendicular to Centerline

The instrumented reinforcement geogrid was installed with six loadcells positioned perpendicular to the centerline. These loadcells were placed at different offsets from the centerline to read the force in the outside wheel path of the right hand lane (see Figure 4.4). Most of the force developed during construction as discussed in the following section.

5.2.1.1 Construction Force

The majority of the forces developed during placement and compaction of the first layer of overlying soil. After compaction of the soil above the loadcells, additional increases in force were small. Section A is a reduced subbase section with 580 mm (23 in.) of subbase aggregate. Section A-1, which had one layer of geogrid placed at top of subgrade, and Section A-2, which had two layers of geogrid (one at top of subgrade, the second 250-mm (10 in.) below asphalt), exhibited similar behavior as shown in Figure 5.1. Both layers of geogrid were instrumented in Section A-2, however all the instruments in the bottom layer failed so the only functioning loadcells are on the layer that is 250 mm (10 in.) below the asphalt. Section E-3 had one layer of reinforcement geogrid placed 250-mm (10 in.) below the asphalt. There are two instrumented stations in this section (88+54 and 88+85 m; 290+50 and 291+50 ft). The short-term stresses at these two stations are very similar to Section A as shown in Figure 5.2. The results for Section A-2 are shown in both Figures 5.1 and 5.2 to illustrate the similar behavior of the geogrid in Sections A-1, A-2, and E-3.

The forces in Sections A-1, A-2, and E-3, after placement of overlying aggregate are similar. Eleven of the loadcells show tensile forces between 0.40 and 1.0 kN/m (27 and 69 lb/ft). Thus, the majority of the loadcells are showing forces in the geogrid that are only a small fraction of the ultimate tensile strength of the geogrid which is 17.5 kN/m (Hayden et al., 1998). In Section E-3 at Station 88+54 m (290+50 ft), 3.05 m (10 ft) offset, the loadcell is a reading compressive force. A possible explanation is that the wave of geogrid that typically advanced ahead of the aggregate placement could have

trapped a loadcell in a geogrid wrinkle. This raises the possibility that the geogrid may have developed very localized areas of compression. The loadcell in Section E-3 at station 88+85 m (291+50 ft) offset 2.74 m (9 ft) from the centerline, developed the highest initial stress reaching approximately 5 kN/m (343 lb/ft). This is about 30% of the ultimate tensile strength of the geogrid. The water content of the subgrade soils at this station was about 7% versus 10% to 16% in Sections A-1 and A-2. This suggests that the higher force was not due to weaker subgrade soils in Section E-3.

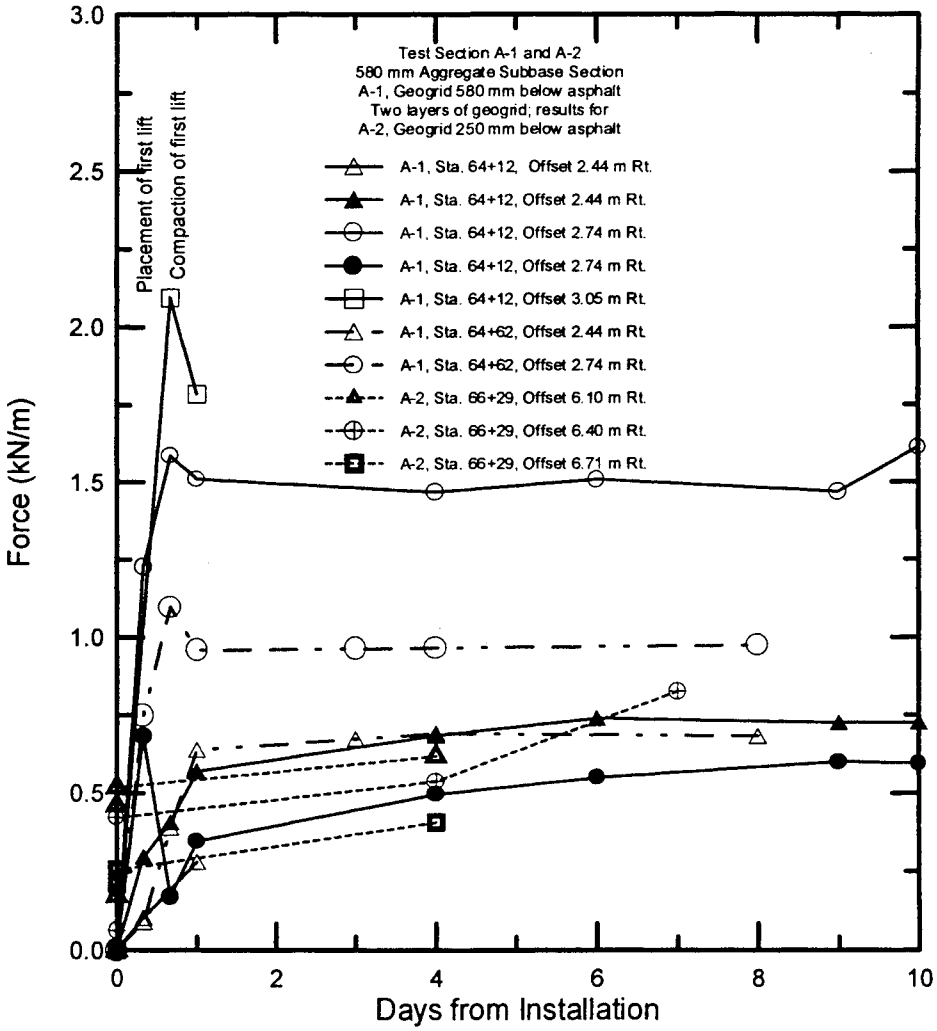

Figure 5.1 Construction force in Sections A-1 and A-2.

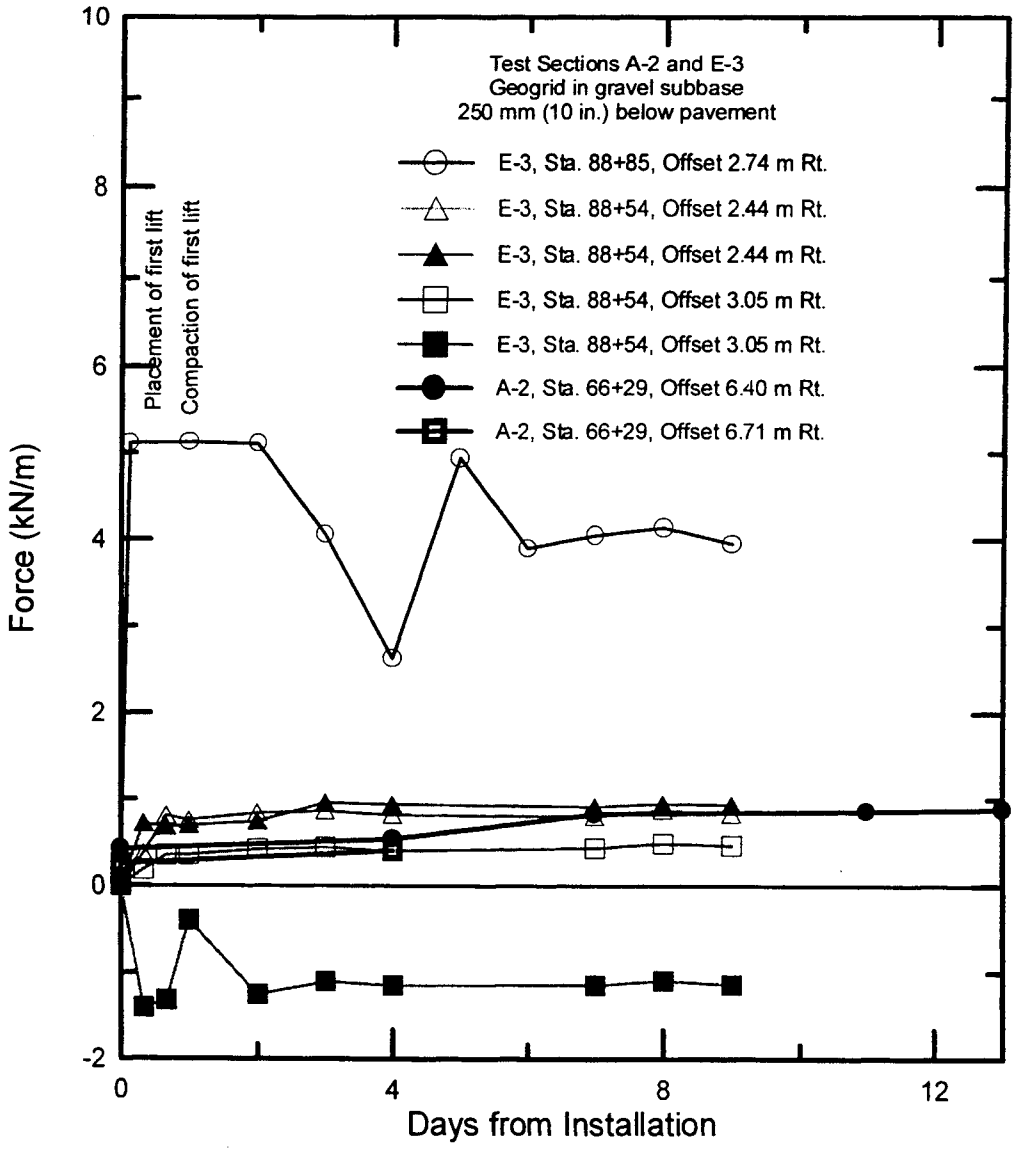

Figure 5.2 Construction force, Sections A-2 and E-3.

5.2.1.2 Long Term Force

Forces measured in the geogrid after construction show little change. Of the gages that were functioning beyond the end of construction, the highest measured stress was less than 2 kN/m (137 lb/ft) as shown in Figures 5.3 and 5.4. Five out of the eight

loadcells carry tensile stresses between about 0.75 and 1.0 kN/m (51 and 69 lb/ft). This is approximately 5% of the ultimate tensile strength of the geogrid. One gage (Sta. 64+12 m (210+38), offset 2.74 m (9 ft) Rt.) measured a higher force of 1.75 kN/m (120 lb/ft), while another gage (Sta. 64+62 m (212+00 ft), offset 2.44 m (8 ft) Rt) measured a lower force of approximately 0.5 kN/m (34 lb/ft). Nearly all the force developed when the overlying subbase aggregate was placed and only a small change in force was observed with time. Section A-2, which had two layers of geogrid in a reduced thickness subbase layer, only had one loadcell on the top layer that was functioning after construction. This loadcell behaved very similarly to the loadcells in Section A-1 and E-3. In section E-3, Sta. 88+54 m (290+50 ft) the loadcell offset 3.05 m (10 ft) exhibited unexpected behavior. The loadcell sometimes reads about 2.25 kN/m (154 lb/ft) in compression, compared to about 1 kN/m (69 lb/ft) in compression for the remainder of the readings. It was assumed that the latter readings were correct.

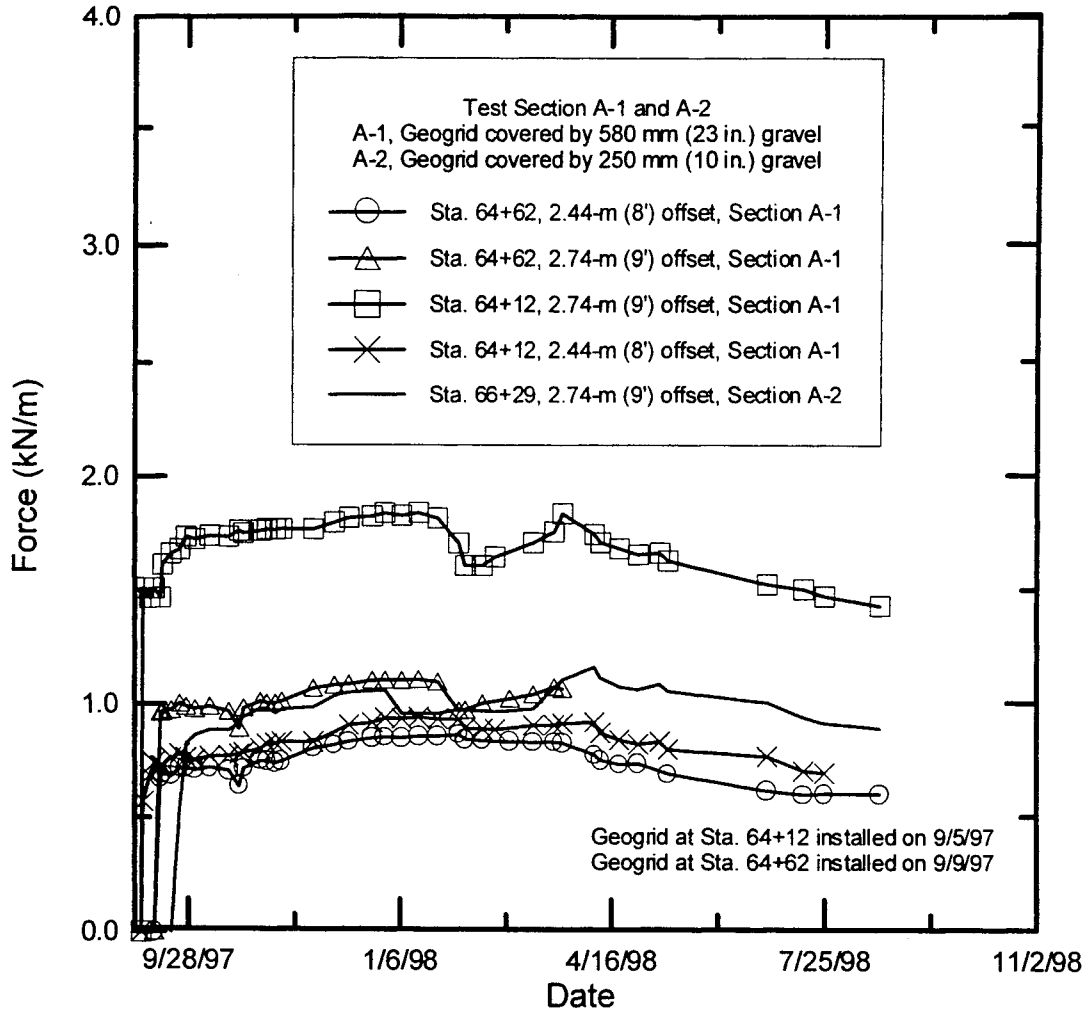

Figure 5.3 Long term force in Sections A-2 and E-2.

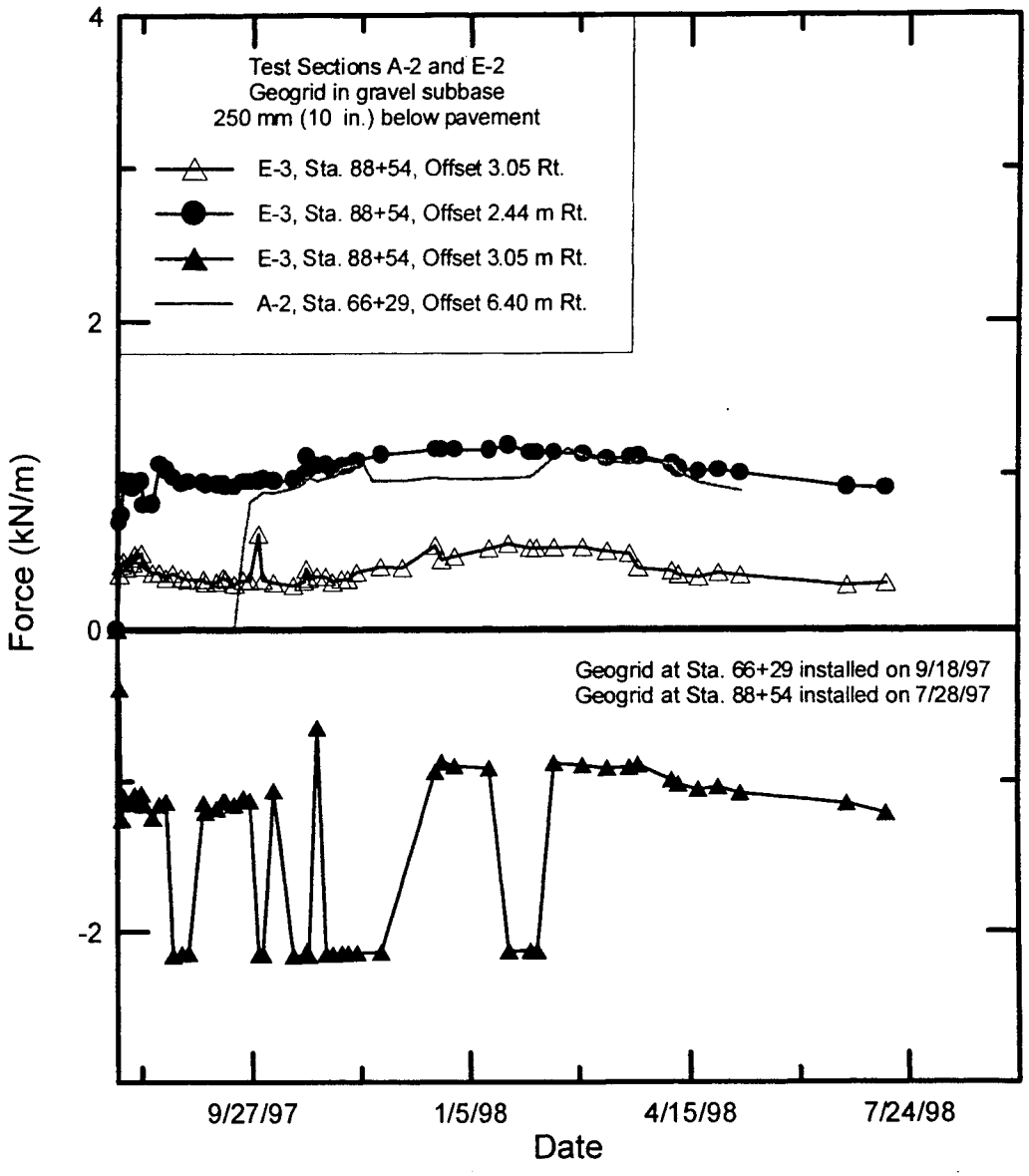

Figure 5.4 Long term force in Sections A-1 and A-2.

5.2.2 Loadcells Parallel to Centerline

Every station with an instrumented layer of reinforcement geogrid had one load-cell that was parallel to the centerline. These loadcells measured the force in the geogrid parallel to the centerline. The loadcell was attached at a 3.05-m (9-ft) offset from the

centerline in Sections A-1 and E-3. In Section A-2 the loadcell was located in the climbing lane at a 6.4-m (21-ft) offset from the centerline. Three loadcells continued to work after placement and compaction of overlying subbase aggregate. Two loadcells continued to measure forces through September 1998.

5.2.2.1 Construction Force

The majority of the force gain in the loadcells that were positioned parallel to the centerline occurred during construction (see Figure 5.5). The parallel gage at station 88+85 m (291+50 ft), sometimes fails and gives a reading of zero, these readings were removed so that the overall trend can be seen more clearly. The maximum forces in these loadcells ranged from 1.2 to 2.9 kN/m (82 to 199 lb/ft). The trend was for the force to dramatically increase with placement and compaction of the first lift.

5.2.2.2 Long Term Force in Geogrid, Parallel to Centerline

One loadcell was positioned parallel to the centerline at each station of instrumented geogrid. As of August 1998 only two loadcells were functioning. It is difficult to see a trend in the long-term stress of these parallel loadcells (see Figure 5.6). There is an initial increase in force followed by a sharp decrease, the forces then seem to increase again. The increase in force in Section A-1 seems to coincide with the latter part of the spring thaw. Section E-3 is showing higher tensile force reaching 3 kN/m (206 lb/ft) in comparison to Section A-1 where there is a maximum force of 1 kN/m (69 lb/ft).

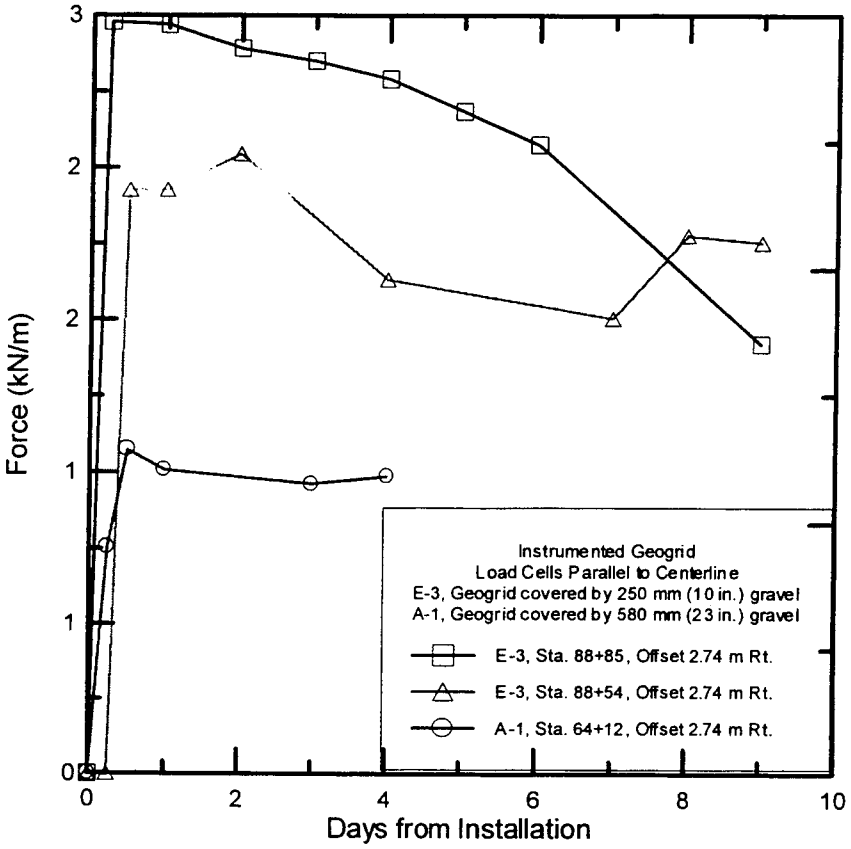

Figure 5.5 Loadcells parallel to centerline (construction force).

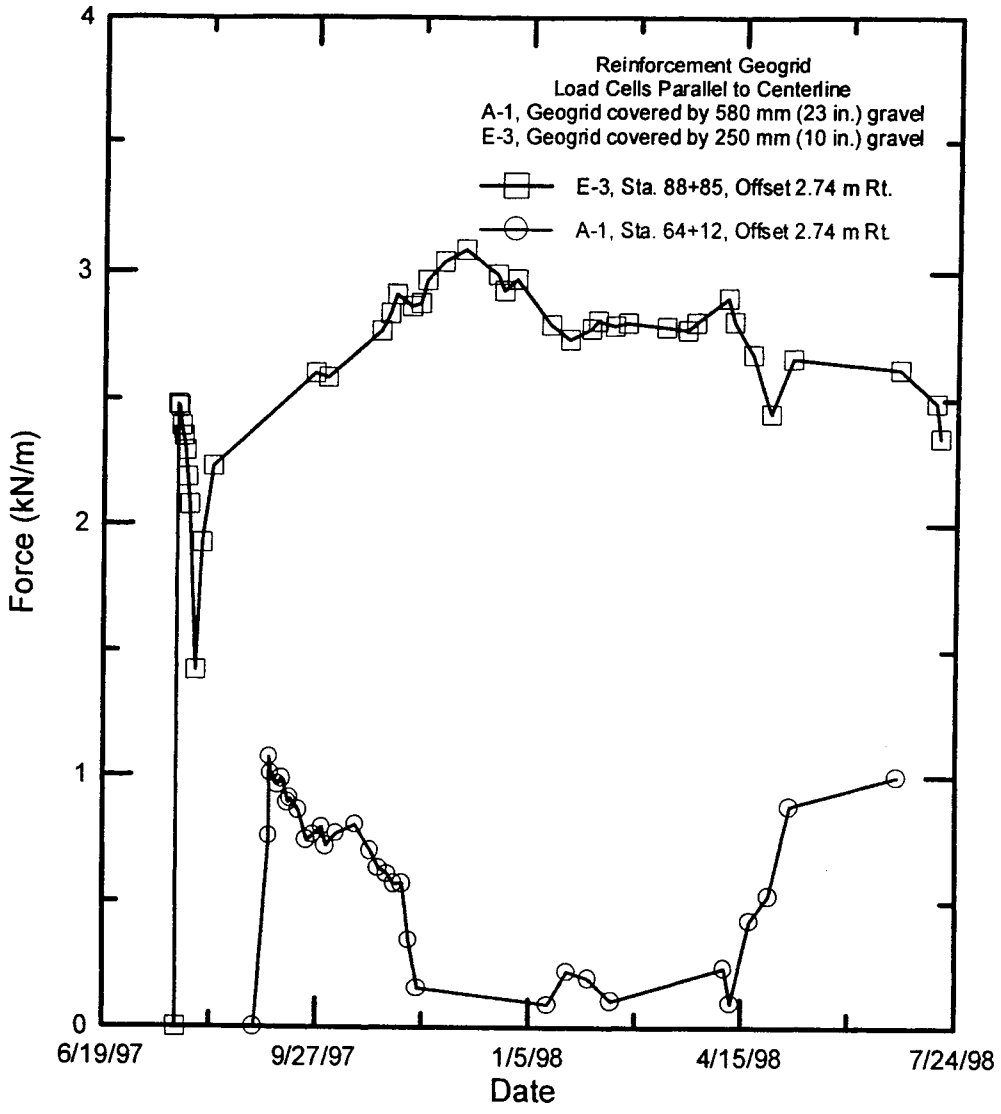

Figure 5.6 Long term force in geogrid, parallel loadcells.

5.3 GEOTEXTILE STRAIN GAGE RESULTS

Strain gages were attached to the reinforcement geotextile at one station each in Sections B-1 and B-2. Each station was instrumented 17 strain gages (see Figure 4.6). Gages were generally placed as pairs, one on each side of the geotextile to eliminate the effects of bending. They were offset from the centerline 6.10, 6.40, and 6.71m (8, 9, and

10 ft). The forces from pairs of gages on top and bottom were generally similar and the average was taken to represent the force in the geotextile (see Appendix A for full data set). Three extra gages were attached on each sheet, so that some offsets actually had two gages on the bottom side and one on the top. The two bottom gages were averaged and then the result was averaged with the top gage. For each section a 3.8 by 15.0 m (12.5 by 50 ft) sheet of geotextile was instrumented with two sets of gages at different offsets as shown in Figure 4.6. Strain gages were attached both perpendicular and parallel to the centerline. There was a high survival of the geotextile strain gages in comparison to the reinforcement geogrid loadcells as shown in Table 5.2.

The two sections were rutted by construction equipment after placement of the first lift of overlying soil to induce tension in the geotextile. Section B-1 was rutted so that the wheels of the dump truck straddled the strain gages. In Section B-2 the trucks were offset to the left side of the strain gages when rutting the geotextile. In the following sections, first the construction force per unit width will be examined followed by long term force per unit width.

5.3.1 Strain Gages Perpendicular to Centerline

Sections B-1 and B-2, both have instrumented sheets of reinforcement geotextile in the roadbed. Section B-1 has a reduced subbase layer with the one layer of geotextile at top of subgrade (580-mm (23 in.) below the bottom of the asphalt layer). Section B-2, has a full subbase layer with one layer of geotextile at top of subgrade (640-mm (25 in.) below the bottom of the asphalt layer).

Table 5.2 Reinforcement geotextile strain gages

Section B-1 67+51 m (221+50)		**Section B-2 67+82 m (222+50)**	
Strain Gage/Offset	**67+51 m (221+50)**	**Strain Gage/Offset**	**67+82 m (222+50)**
1 / 6.7 m (22 ft)	W	1 / 6.7 m (22 ft)	F(A)
2 / 6.1 m (20 ft)	W	2 P / 6.4 m (21 ft)	W
3 / 6.7 m (22 ft)	W	10 / 6.7 m (22 ft)	F(A)
7 / 6.1 m (20 ft)	W	11 / 6.7 m (22 ft)	W
9 / 6.4 m (21 ft)	W	12 / 6.4 m (21 ft)	W
11 / 6.7 m (22 ft)	W	13 / 6.4 m (21 ft)	W
13P / 6.4 m (21 ft)	W	14 / 6.1 m (20 ft)	W
15 / 6.1 m (20 ft)	W	15 / 6.1 m (20 ft)	W
17 / 6.4 m (21 ft)	W	16 P / 6.4 m (21 ft)	W
19 / 6.7 m (22 ft)	F(A)	17 P / 6.4 m (21 ft)	W
30 / 6.1 m (20 ft)	F(A)	18 / 6.7 m (22 ft)	W
32 / 6.4 m (21 ft)	W	19 / 6.7 m (22 ft)	F(A)
34 / 6.7 m (22 ft)	W	20 / 6.4 m (21 ft)	W
36 P / 6.4 m (21 ft)	F(A)	21 / 6.4 m (21 ft)	W
38 / 6.1 m (20 ft)	W	22 / 6.1 m (20 ft)	W
40 / 6.4 m (21 ft)	F(A)	23 / 6.1 m (20 ft)	F(C)
42 / 6.7 m (22 ft)	W	25 / 6.1 m (20 ft)	W
% Survival	76%	% Survival	76%

W = Working
F(C) = Failed during construction
F(A) = Failed after construction

5.3.1.1 Construction Force Perpendicular to Centerline

The geotextile was rutted after the first 200 mm (8 in.) of compacted gravel was placed. Section B-1, station 67+51 m (221+50 ft) was rutted so that the strain gages were straddled. Section B-2, station 67+82 m (222+50 ft) was rutted so that the rutting was offset to the left side of the instruments. Possibly more force could have been induced if rutting was directly over the gages.

The force after placement and compaction was less than 0.3 kN/m (21 lb/ft) at most of strain gage locations. Moreover, at some gage locations the force appeared to be negative. This may be due to the gages being trapped in a compression zone caused by a wrinkle in the geotextile. However, at two gages (Sta. 67+50 m, 6.7-m offset and Sta. 67+53 m, 6.1-m offset), the force was between 1.2 and 1.5 kN/m (82 and 103 lb/ft) in tension.

Rutting increased the force in most of the gages. After rutting, the force in five of the twelve functioning gages was between 0.8 and 1.7 kN/m (55 and 116 lb/ft) and another gage had a higher force of 3.7 kN/m (253 lb/ft). Rutting caused the force at some gages to increase from a small compressive value to tension. Nonetheless, the force in six gages was small, ranging between 0.3 and –0.5 kN/m (21 and –34 lb/ft). Thus, the force in the geotextile after rutting was nonuniform and, at about half of the gage locations, the force was near zero.

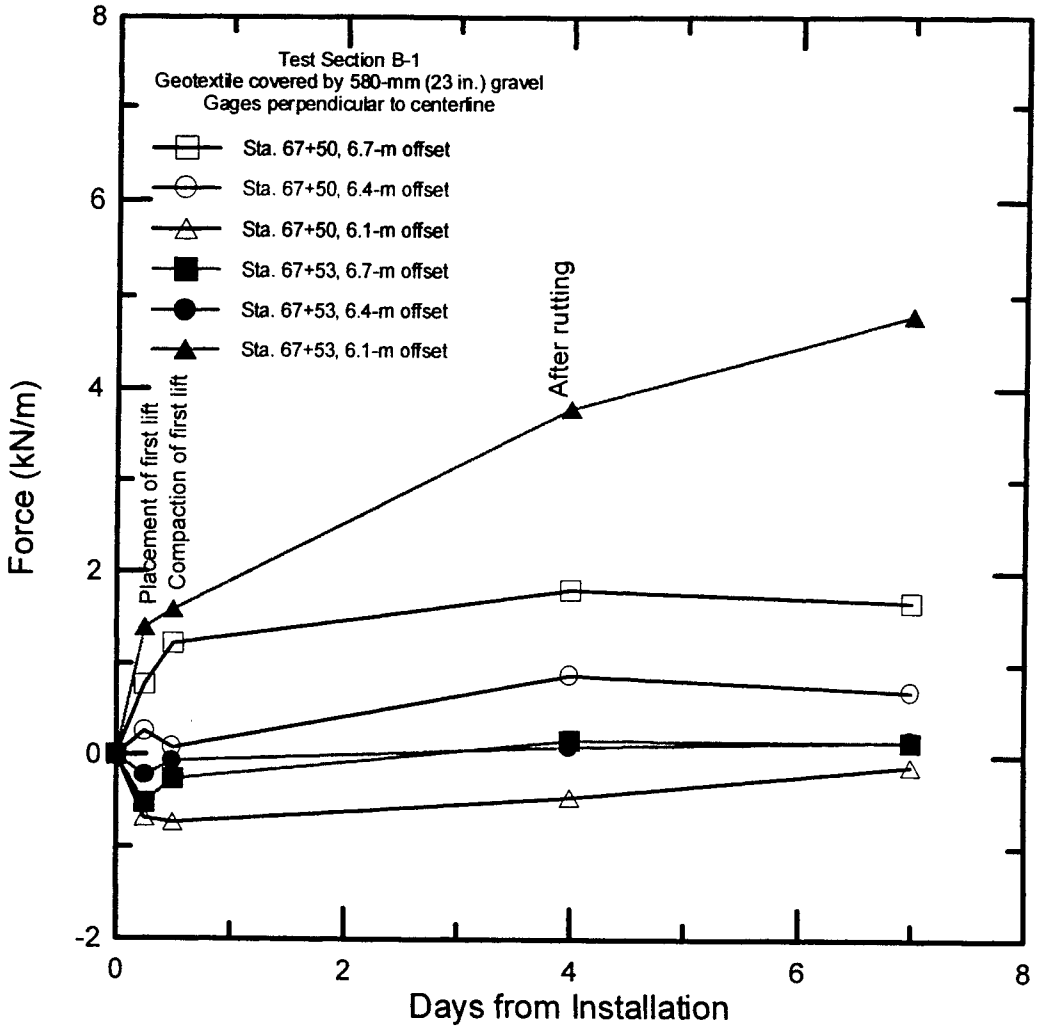

Figure 5.7 Construction force in Section B-1.

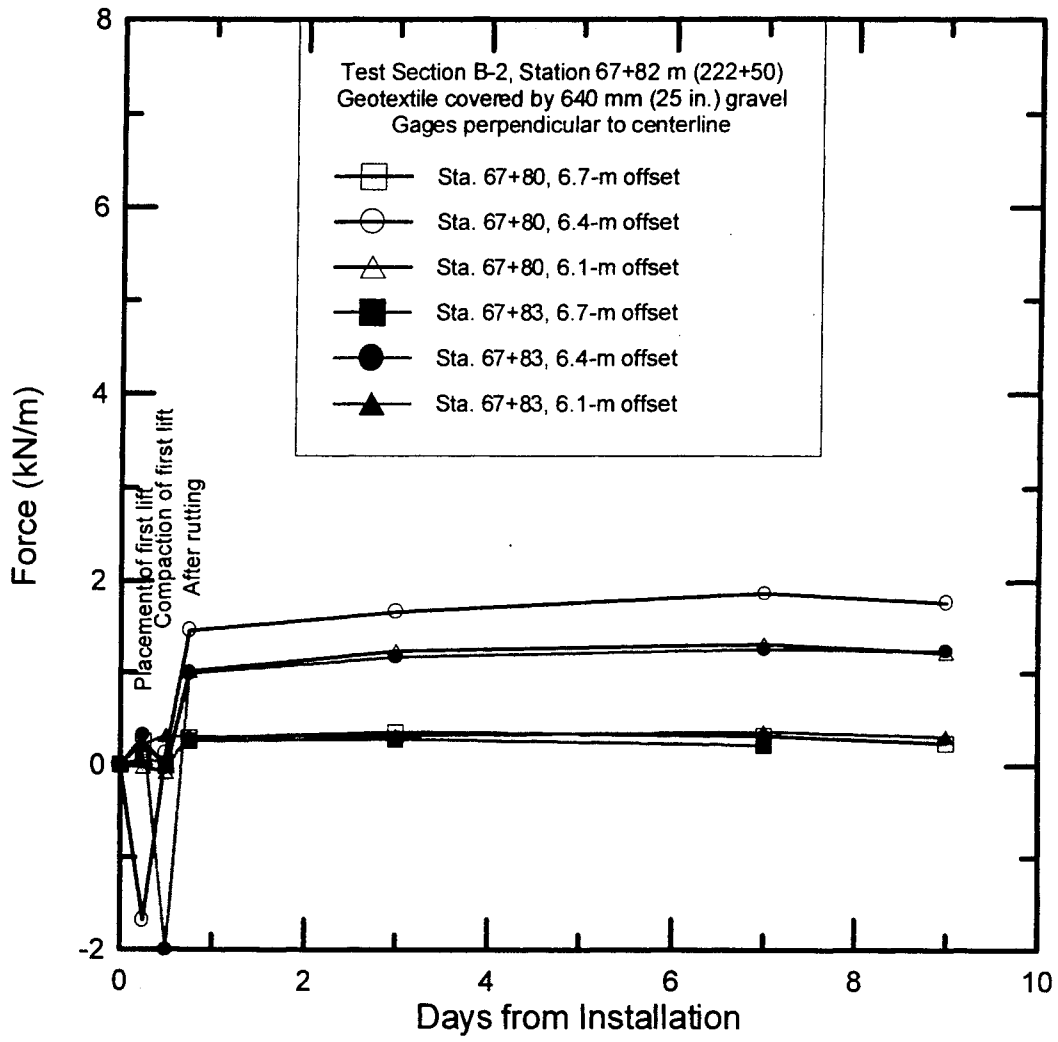

Figure 5.8 Construction force in Section B-2.

5.3.1.2 Long-term Force Perpendicular to Centerline

The long-term forces in the reinforcement geotextile are shown in Figures 5.9 and 5.10. The top and bottom gages at the same offsets were averaged to negate the effects of bending. After completion of construction, the forces measured by the gages ranged from about zero to 6 kN/m (0 to 411 lb/ft). This indicates that the force that developed in

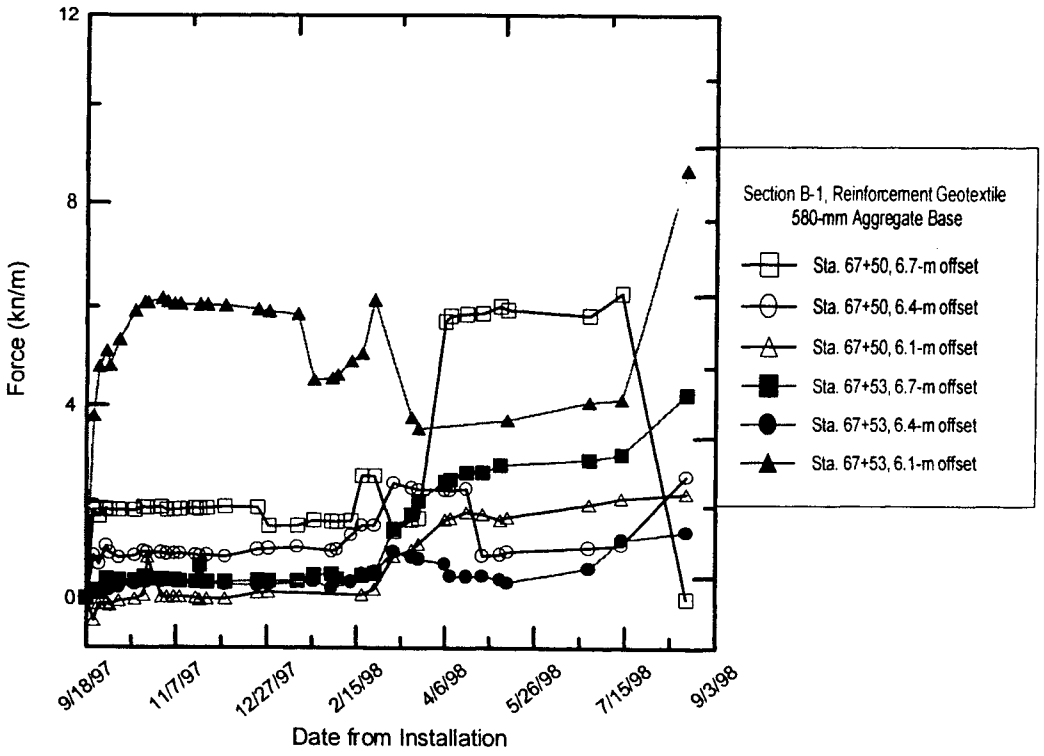

Figure 5.9 Long term force in Section B-1.

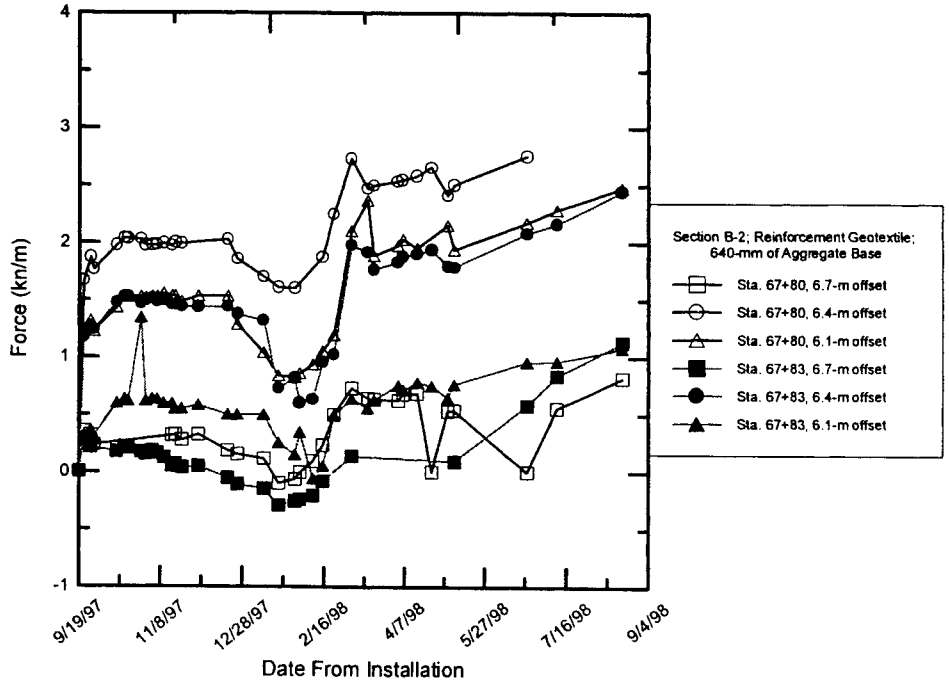

Figure 5.10 Long term forces in Section B-2.

the geotextile was influenced by local conditions such as the initial slack in the geotextile, the strength of the underlying subgrade, and the degree of tensioning that occurred due to the rutting by construction vehicles.

In Section B-1, the force determined from five out of the six gages (all but Sta. 67+53, 6.1-m offset (221+54 ft, 20 ft offset)) remained relatively constant for the period from completion of construction in September, 1997, through mid to late February, 1998 as shown in Figure 5.9. Starting in late February, 1998, the gages experienced an apparent increase in stress that roughly coincided with spring thaw. For three of the gages (Sta. 67+50, 6.7-m offset (221+47, 22 ft); Sta. 67+53 6.7-m offset (221+54, 22 ft); and Sta. 67+50, 6.1-m (221+47, 20 ft)), the increase in stress was permanent. In fact, the gage at Sta. 67+50, 6.7-m offset (221+47, 22 ft) increased in force to 6 kN/m (422 lb/ft) and this force was still present at the end of the monitoring period. In contrast, by the beginning of May, 1998, the forces in two of the gages (Sta. 67+50, 6.4-m offset (221+47, 21 ft); and Sta.67+53, 6.4-m (221+54, 21 ft)) returned to roughly their pre-February, 1998 values. The long term force was termed "apparent force" since the force in the geotextile was determined indirectly using the strain gages mounted on the geotextile. This opens the door to factors that could have changed the strain gage reading but not the force in the geotextile. Thus, it was necessary to examine other possible factors. It is possible that the gages were affected by temperature, however, the stable readings during penetration of the freezing front in December, 1997, and January, 1998, suggests that this is not the case. The geotextile could also undergo creep, which is strain of the geotextile under constant force. This would cause an increase in strain, but the

force could remain constant or even decrease. However, creep appears unlikely to have caused an increase in strain since the force in some of the gages before mid to late February, 1998 was near zero. This is much less than 60% of the geotextile's ultimate tensile strength, which is reported in the literature as the minimum force needed before the onset of significant creep (Shrestha and Bell, 1982). Thus, it appears that the geotextile did experience an increase in force during the spring melt and that the increase was permanent at some of the gage locations although other possible causes cannot be completely discounted.

The gages in Section B-2 follow a trend similar to Section B-1. The force calculated in all six gages remained relatively constant for the time period from completion of construction in September, 1997, through January, 1998 as shown in Figure 5.10. All gages in Section B-2 exhibit a decrease in force for the month of January. Three gages, Sta. 67+83, 6.1-m (20 ft) offset, Sta. 67+80, 6.7-m (22 ft) offset, and Sta. 67+83, 6.7-m (22 ft) offset initially showed small compressive forces. Starting in February, 1998, the gages experienced an apparent increase in force that coincided with spring thaw. For five out of the six gages, the increase in stress was permanent. The remaining gage (Sta. 67+80, 6.7 m offset (222+44, 22 ft offset)) returned to approximately its pre-January 1998 reading. Based on the discussion for Section B-1, the apparent force carried by the geotextile increased during spring melt and the increase was permanent at most gage locations. The effects of temperature and creep were examined as possible explanations. Readings did go down in Section B-2 during frost penetration but forces are higher in the Summer, 1998 than in Fall, 1997 when the temperature was

about the same. Thus, temperature did not appear to have a significant effect on the readings. Moreover, the force is much less than 60% of the geotextile's ultimate tensile strength, which is reported in the literature as the minimum force needed before the onset of significant creep (Shrestha and Bell, 1982). This suggests that temperature and creep are not contributing to the increase in force during the spring melt. Readings should be continued to better determine the long-term changes in the force in the geotextile.

5.3.2 Strain Gages Parallel to Centerline

In each section of instrumented geotextile, strain gages were attached parallel to the centerline. Section B-1 was instrumented with two parallel gages, one on each side at the same offset. The measurements were averaged to account for the effects of bending. Section B-2 was instrumented with three parallel gages, two on the bottom and one on the top located at the same offset. The two bottom readings were averaged and the result was then averaged with the top gage. These gages measure the longitudinal force in the geotextile. Construction and long term force will be discussed separately.

5.3.2.1 Construction Force

The results from the gages attached in the longitudinal direction on the geotextile at station 67+51 m (221+50 ft) (Section B-1) exhibit an increase in force during the first ten days as shown in Figure 5.11. This could be due to weak subgrade or rutting caused by the construction equipment. In contrast, the results from Section B-2 show very little force increase in the first few days after construction.

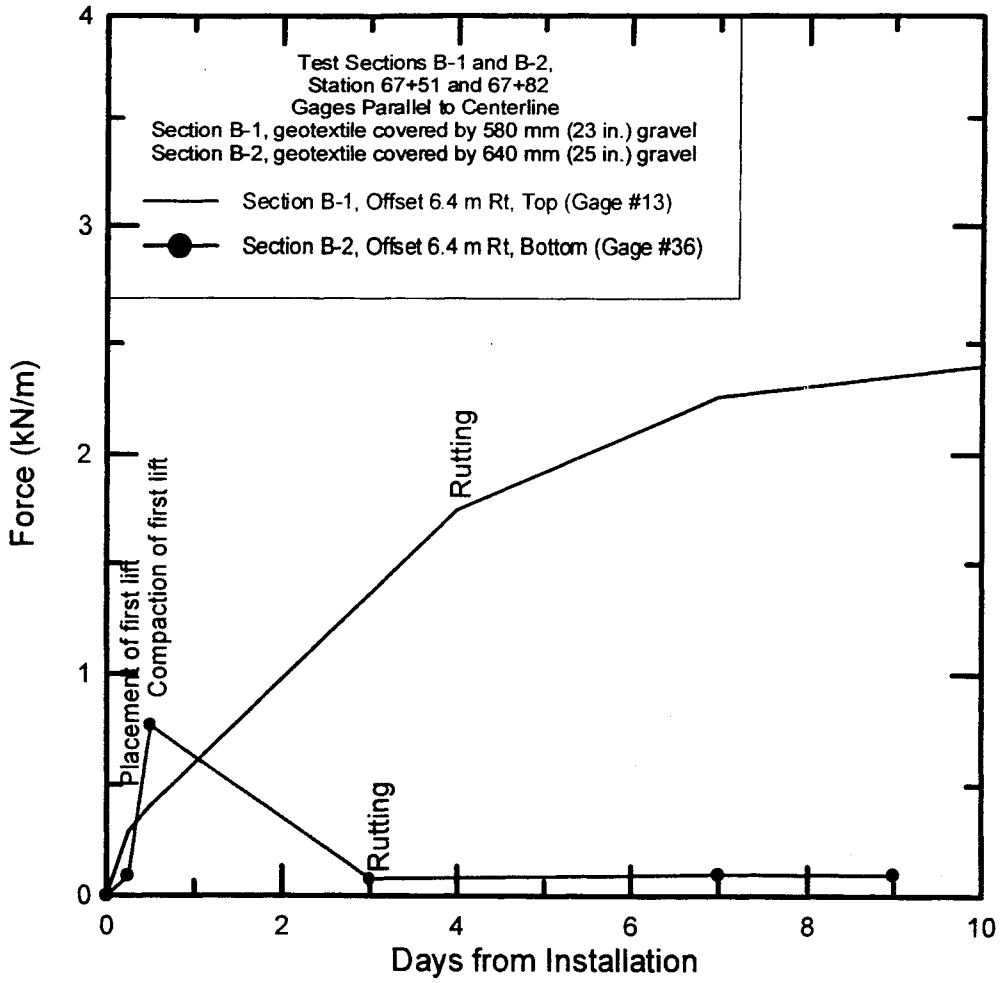

Figure 5.11 Section B-1, construction forces in parallel strain gages

5.3.2.2 Long Term Force

Long-term stress measurements of the strain gages mounted in the longitudinal direction are shown in Figures 5.12. Both Sections B-1 and B-2, show increasing force with time. Section B-2 shows a much higher force compared to Section B-1. In Section B-1 the force values never increased past 0.4 kN/m (27 lb/ft), while in Section B-2 the force reached a maximum value of 3.0 kN/m (206 lb/ft) by August, 1998. The difference

in force could be due to differences in the strength of the subgrade, wrinkles in the geotextile at time of placement, or the effectiveness of rutting procedures.

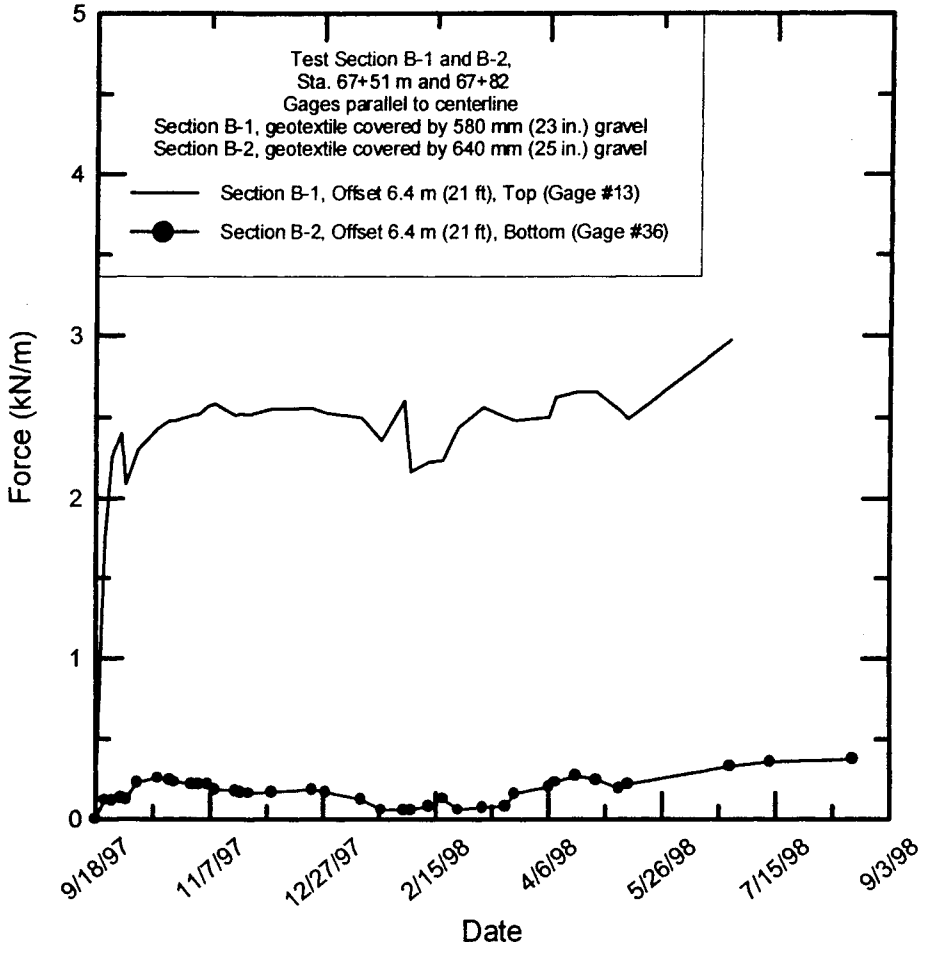

Figure 5.12 Section B-1, long term force in parallel gages

5.4 SEPARATION GEOTEXTILE RESULTS

No instruments were installed to monitor the performance in the sections that used separation geotextile. However, Falling Weight Deflectometer (FWD) readings were taken prior to construction and then again in April, 1998. Results of the FWD testing will be discussed in Section 5.7.

5.5 DRAINAGE GEOCOMPOSITE RESULTS

Tilt buckets were installed at six outlet pipes to measure water flow in the drainage sections. The tilt buckets were connected to a traffic counter that recorded every other time the bucket dumped the water. Data was collected 24 hours a day for three test sections as shown in Table 4.6 (Hayden, et al., 1998).

Results of data collected from March to June, indicate that Section D-1 has the greatest amount of flow as shown in Table 5.3. Since the outlets drain different lengths of road, the data in Table 5.3 is shown as flow per unit length of drain. Data was not collected for Outlet A until late June. The greatest monthly flows occurred in March during the spring thaw. The volume of discharge in the month of March accounted for 58% of the total four-month discharge volume (Hayden, et al., 1998). Discharges from April through June corresponded to precipitation events. The greatest outflow occurred in Section D-1, where the geocomposite is placed 460 mm (18 in.) below subgrade and drains a 46-m (150-ft) length of road. The second greatest outflow occurred in Outlet D in section D-2, where a geocomposite is placed at the subgrade/subbase interface and drains a 200-m (650-ft) length of road. Section D-3 was located in a fill section. Outlet E, which drained the geocomposite placed on subgrade, had less flow than in Sections D-1 and D-2. This is probably because there was less water present in a fill section than in a cut section. Outlet F, which drained the geocomposite located directly under the pavement, had no flow. This indicates that, as expected, the new pavement did not allow ingress of water or that any water that penetrated the pavement was drained away by the subbase course.

Table 5.3 Discharge volumes (L) from monitoring outlets (Hayden, et al., 1998).

	Outlet A D-1 Cut Section (L/m)	**Outlet B D-1 Cut Section (L/m)**	**Outlet C D-1 Cut Section (L/m)**	**Outlet D D-2 Cut Section (L/m)**	**Outlet E D-3 Fill Section (L/m)**	**Outlet F D-3 Fill Section (L/m)**
March	-	77	1094	118	0.17	0
April	-	0.12	0	91	0.00	0
May	-	0.00	0.02	94	0.00	0
June	0.25	3.50	63	73	5.50	0
Totals	0.25	80	1156	377	6	0

(1) Note: Units are liters/meters of installed drainage pipe. Refer to Section 4.6, for details on tilt bucket location and layout.

Piezometers were installed in Sections C-2, D-1, D-2, D-3, and in the control section (see Figure 4.12 for layout). These instruments were used to evalate if the geocomposite dissipated pore water pressures. Unfortunately few readings were taken at the critical time of spring thaw. The RocTest MB-6T vibrating wire readout used to record the measurements was not working properly through the mid-winter to spring months. Even though the readout box was returned to the manufacturer for repair, they could not discover the problem. Moreover, during the winter months few readings were taken, due to the frozen PVC pipe that encased the piezometer wires. The best way to use the available data was to average piezometer values for two time periods: October through November, 1997, and June through August, 1998. The results are shown in Table 5.4. Bar graphs of individual readings can be found in Appendix A. The depth of each piezometer was shown in Figure 4.12.

Table 5.4 Average values of piezometers

Average piezometric values for dates	10/22/97 to 11/25/97			
		Piezometric Head (mm)		
	Section	Top	Middle	Bottom
Separation Geotextile at 820 mm	C-2	137.5	95.2	210.4
Geocomposite 460 mm below subgrade	D-1	29.4	359.1	3.1
Geocomposite at 820 mm	D-2	10.0	57.8	-15.4
Geocomposite at 180 and 820 mm	D-3	117.7	22.8	73.6
Control - No Geosynthetic	Control	414.0	348.5	148.8

Average piezometric values for dates	6/27/98 to 8/19/98			
		Piezometric Head (mm)		
	Section	Top	Middle	Bottom
Separation Geotextile at 820 mm	C-2	-137.5	-154.50	-224.4
Geocomposite 460 mm below subgrade	D-1	-81.9	-88.2	57.7
Geocomposite at 820 mm	D-2	-501.0	-110.2	-84.0
Geocomposite at 180 and 820 mm	D-3	-158.1	-154.6	-151.0
Control - No Geosynthetic	Control	236.6	246.7	-377.6

Piezometer readings from October through November, 1997 show that Sections D-2 and D-3 have lower pressure readings than the control section suggesting that geocomposite material placed at the subgrade interface removed water from the pavement system. Section D-1, has lower pressure in the subbase aggregate and the subgrade below the geocomposite, but is higher in the clayey backfill over the geocomposite when compared to the control section and Section C-2. Section C-2, with separation geotextile has lower pressure in the subbase aggregate than the control section. This could be due to local conditions such as the subgrade soil and elevation.

Piezometer readings for June, 1998 through August, 1998 are difficult to interpret and do not show a clear trend. Many of the readings were negative. This could mean the instruments were damaged by freezing in the winter.

5.6 FROST DEPTH RESULTS

Subsurface temperatures were monitored in four sections (A-1, A-2, B-2, and E-3) from December, 1997 to February, 1998. The frost depth in each section was calculated by linear interpolation for the 0° C (32° F) temperature using the temperature recorded by the thermocouples. The results are shown in Figure 5.13. Field measurements indicate that Section E-3 did not have any frost penetration so is not included in Figure 5.13. In Section A-1, frost penetration reached a maximum depth of 465 mm (18 in.) below the top of subgrade. Section A-2 reached a maximum frost depth of 605 mm (24 in.) below the top of subgrade, while in Section B-2 frost reached a maximum depth of 760 mm (30 in.) below the top of subgrade. Temperatures in E-3 were as low as 0° C (32° F) in a thermocouple located at a depth of 430 mm (17 in.). This suggests that soils close to the surface were below freezing. Section E-3 is in a more residential area with less shade, which could be a possible reason for the lack of frost at depths greater than 430 mm (17 in.).

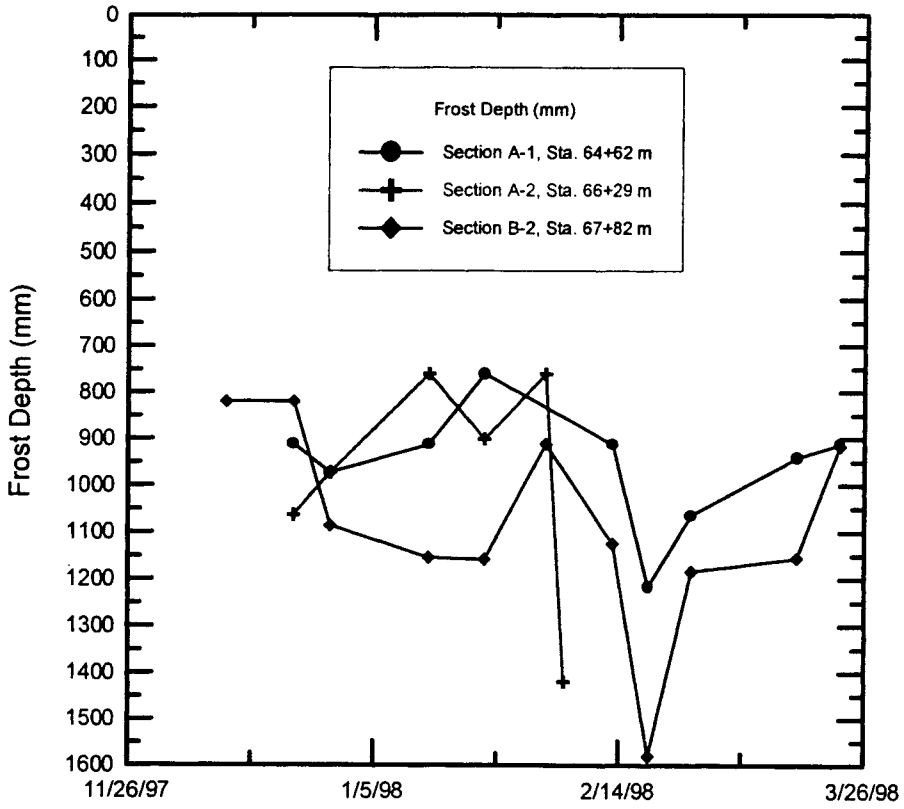

(1) Note: E-3 did not having freezing temperatures and is not included in this figure

Figure 5.13 Depth of frost penetration vs. date, Sections A-1, A-2 and B-2.

5.7 FALLING WEIGHT DEFLECTOMETER RESULTS

Falling weight deflectometer (FWD) measurements were taken prior to reconstruction and after reconstruction in April 1998, soon after the end of the spring thaw. Before construction began in the spring of 1997 the road typically had between 127 to 254 mm (5 to 10 in.) of pavement, but in some deeply rutted areas there was up to 610 mm (24 in.) of pavement. When the readings were taken in April 1998 the pavement thickness was 146 mm (5.75 in.) (Hayden, et al., 1998). Readings from April 1998 were taken in cut sections. The FWD results were input into the Darwin Pavement Design and

Analysis System and the pavement structural numbers (SN) were back calculated. The results are shown in Figure 5.16. The results of the FWD tests are misleading in some cases. The highest SN values came from control section (F-1 and F-2) with no geosynthetics. However, during construction an additional 600 mm (24 in.) of subbase aggregate was placed in the control section due to poor subgrade conditions. Section D-1, the undercut section with the drainage geocomposite had the second highest structural number. This could be due to the compacted subgrade fill placed on the geocomposite being stiffer than the in-place material. Subgrade water contents taken during construction were lower in Sections E-3 than in Sections A-1, A-2 and B-2. This suggests that the subgrade in Section E-3 is stronger than in Sections A-1, A-2, and B-2, and could be the reason for the higher SN in Section E-3 in April, 1998.

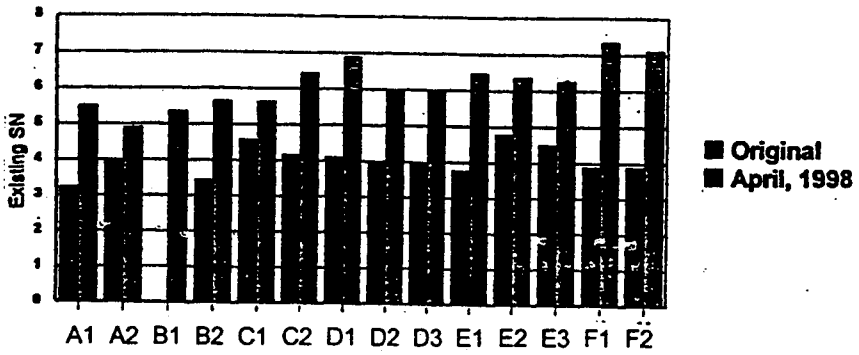

Figure 5.16 Original and April structural numbers (Hayden et al., 1998)

Due to the undercutting of the original control section by 610 mm (2 ft) another section was used as a basis for comparison. In evaluating the effectiveness of the geosynthetics used in this project, section C-2 which has only a separation geotextile placed at subgrade was taken as the basis for comparison. Table 5.5 illustrates that the structural number in each section of reinforcement geosynthetic is lower than Section C-

2. Moreover, Section A-1, which had one layer of reinforcement geogrid, had a higher SN than Section A-2, which had two layers of geogrid. This indicates that the reinforcement was not effective in increasing the SN as backcalculated from FWD tests. The highest SN from the April, 1998, readings was in section D-1, which was the undercut section with drainage geocomposite. However, this SN was only slightly higher than in C-2. It is possible that the FWD was incapable of detecting the beneficial effects of the geosynthetics.

It was stated earlier that before reconstruction, some sections of road had up to 610 mm (24 in.) of asphalt, this is important to realize when comparing original readings to the April readings.

Table 5.5 Structural numbers of C-2 compared to other sections with geosynthetics.

Section	April Structural Number	(April Structural Number / C-2 Structural Number)
A-1	5.50	0.85
A-2	4.80	0.74
B-1	5.40	0.84
B-2	5.60	0.87
C-1	5.60	0.87
D-1	6.90	1.07
D-2	6.00	0.93
D-3	6.00	0.93
E-1	6.50	1.01
E-2	6.40	0.99
E-3	6.20	0.96
F-1	7.20	1.17
F-2	7.10	1.10
C-2	6.45	1.00

5.8 SUMMARY

Instruments were installed to monitor the performance of the geosynthetics. Loadcells were attached to reinforcement geogrid to measure induced forces. Strain gages were attached to reinforcement geotextile to measure the force in the geotextile. Thermocouples were installed to measure frost penetration. Piezometers and tilt buckets were installed in the drainage section to monitor the performance of the drainage geocomposite. Falling weight deflectometer (FWD) readings were taken before and after construction. Instrument readings have been taken since installation to evaluate geosynthetic performance.

Seven loadcells were attached to reinforcement geogrid in Sections A-1, A-2, and E-3. Loadcell survivability ranged from zero to 57%. The majority of failures occurred during construction. Sections A-1, A-2, and E-3 showed a force between about 0.75 and 1.0 kN/m (51 to 69 lb/ft), except that one loadcell showed a higher force of 1.75 kN/m (120 lb/ft), while another showed a force of 0.5 kN/m (34 lb/ft). One loadcell suggests that there may be localized areas of compression in the geogrid. The majority of force in the reinforcement developed during initial placement and compaction of the overlying aggregate. There has been little change in force since completion of installation.

Reinforcement geotextile strain gage survivability was much higher than the geogrid, with 76% of installed strain gages still functioning in August, 1998. Seventeen strain gages were attached to the geotextile. They were positioned in the right wheel path of the climbing lane. Results indicate that the forces ranged from about zero to 5 kN/m

(343 lb/ft). This suggests that the forces that developed in the geotextile were influenced by local conditions such as the strength of the underlying subgrade, degree of wrinkling of the geotextile at the time of placement, and the degree of tensioning that occurred with rutting by construction vehicles. The majority of force in the geotextile was induced during construction. However, there was an additional force increase during March and April of 1998. Some gages showed a slow increase in force from April through August, 1998, which was the last set of readings taken for this report.

In some sections, the drainage geocomposite removed a substantial amount of water from the pavement system from March to June 1998. Section D-1, with a geocomposite placed 460 mm (18 in.) below the subgrade removed the most water followed by Section D-2 with a geocomposite placed at subgrade. There was little water removed from the two outlets (Outlets E and F) located in Section D-3, which was located in a fill section. This suggests that there is less water in the fill section. Outlet F, which drained the geocomposite located directly under the pavement, had no flow. This indicates, as expected, that the new pavement prevented water penetration to the underlying subbase aggregate or that the subbase was able to drain away any infiltration. Piezometers were installed in Sections C-1, D-1, D-2, D-3 and the control section. Due to a malfunction with the instrument reading unit, pore pressures could not be obtained during the critical spring thaw period. However, readings from Oct. through Nov. of 1997 generally show that the pore pressures are lower than the sections with drainage geocomposite.

Falling Weight Deflectometer (FWD) measurements were taken before reconstruction and after reconstruction in April 1998. The FWD results were processed with the Darwin Pavement Design and Analysis System and sections are compared with the backcalculated structural number (SN). In April, 1998, the control sections (F-1 and F-2) had the highest SN. However, the control sections failed during construction due to a weak subgrade and were undercut an additional 610 mm (2 ft). Section A-1, which had one layer of geogrid, had a higher SN value compared to Section A-2, which had two layers of reinforcement geogrid. This suggests that the reinforcement was not effective in increasing SN values backcalculated from FWD tests. It could be that FWD tests cannot detect the benefit provided by the reinforcement.

6. SUMMARY, CONCLUSIONS, AND RECOMMENDATIONS

6.1 SUMMARY

The Maine Department of Transportation is evaluating the reinforcing, separation and filtration potential of geosynthetics in a 3.0 km (1.9 mile) portion of U.S. Route 1A in the towns of Frankfort and Winterport. Previous studies of geosynthetic reinforcement in flexible pavement systems have examined subbase thickness ranging from 50 to 305 mm (2 to 12 in.). This project goes beyond previous work by evaluating the effectiveness of geosynthetics as reinforcement, separation, and drainage layers in paved roadway sections with subbases ranging from 580 to 640 mm thick (23 to 25 in.).

The objective of this study was to evaluate the effectiveness of geosynthetics in terms of reinforcement, separation, and drainage for roadways constructed in cold regions where the aggregate base course is thicker than investigated in previous studies. Primary emphasis was given to the reinforcement application. To perform this evaluation the following tasks were accomplished:

1. A literature review was conducted of laboratory tests, field work, and computer analyses of geosynthetics used beneath unpaved and paved roads.

2. A 3.0 km (1.9 mile) portion of U.S. Route 1A was instrumented with strain gages, loadcells, piezometers, and thermocouples to evaluate the reinforcing and drainage effectiveness of the geosynthetics.

3. The roadway was monitored from construction during summer and fall, 1997 through August, 1998. The stress in the geogrid and geotextile, pore water pressures in the drainage section, and the frost depth in several the sections were investigated.

4. Pavement performance was measured before and after construction with a falling weight deflectometer (FWD). Structural numbers were then obtained by processing the FWD results in the Darwin Pavement Design and Analysis System. The performance of each section was evaluated by comparing the improvement of the before and after structural numbers as well as direct comparison of the after structural numbers obtained from the sections.

The literature review included studies on unpaved temporary or haul roads, and flexible pavements with reinforcing geosynthetics in the substructure. Possible reinforcement mechanisms included: providing confinement for aggregates in the subbase course, confinement of the subgrade layer, increases in the effective shear strength, and improved load distribution. The geosynthetic must be deformed to mobilize the tensile force needed to obtain a reinforcing benefit. This presents a problem for paved roads, since the pavement cannot tolerate large deformations.

There have been few studies evaluating the use of geosynthetics in flexible pavement systems. Laboratory studies that related load cycles to rut depth and pavement performance were conducted at the University of Waterloo, Montana State University, Georgia Institute of Technology, and Virginia Polytechnic Institute. Many of these

studies quantify the benefits of geosynthetics by measuring the increased load applications and/or reduced aggregate thickness made possible by the geosynthetics. The laboratory studies applied loads to a circular plate. This could overestimate the potential benefits of the geosynthetic since the applied force will be in all directions (axisymmetric), in comparison to an actual roadbed, which is plane strain loading, where there is negligible strain in the direction parallel to the centerline. Observed improvement was dependent on sectional properties such as subgrade strength, aggregate thickness, geosynthetic location and geosynthetic stiffness. Results reported by Perkins, et al. (1997); Haas, et al. (1988); Cancelli, et al. (1996); Barksdale, et al. (1989); Penner, et al. (1985); Kennepohl, et al. (1985); Al-Qadi, et al. (1994); and Montanelli, et al. (1997), have shown some benefits of geogrid/geotextile reinforcement in flexible pavements. However, the maximum subbase thickness in these studies was 300 mm (12 in.) and the maximum pavement thickness was 160 mm (6.3 in.) thick. In general the reinforcing benefit decreased as the aggregate subbase thickness, pavement thickness, and subgrade strength increased. No literature was found that studied the effects of geosynthetic reinforcement in cold region areas with the subbase and asphalt layers that are as thick as used in Maine.

A computer analysis conducted by Barksdale, et al. (1989) showed that sections with an asphalt layer greater than 65 to 90 mm (2.5 to 3.5 in.) thick were not expected to show improvement with reinforcement geosynthetics, even if they were placed on weak subgrades. Barksdale, et al. (1989), also showed that the effect of geosynthetics beneath flexible pavements in terms of stress, strain and deflection are relatively small for

geosynthetic reinforced sections designed to carry more than about 200,000 equivalent 80-kN (18-kip) single axle loads. The reconstructed section of Route 1A is designed to carry 1.5 million equivalent 80-kN (18-kip) single axle loads.

A design procedure was proposed for geosynthetic reinforcement in flexible pavements by Penner, et al. (1985). It uses a layer coefficient ratio or equivalence factor that is applied to the reinforced layer to reflect the improved structural characteristics of the base. This analysis procedure predicts that geosynthetic reinforcement would provide no benefit for subbase aggregate layers greater than 300 mm (12 in.).

A full-scale field trial evaluating the use of reinforcement geogrid and geotextile, separation geotextile, and drainage geocomposite in the reconstruction of US Route 1A in the towns of Winterport and Frankfort was begun in May 1997 and completed in June 1998. Historically, this area has had poor pavement performance. The subsurface exploration revealed weak subgrade soil with an AASHTO classification of A-6 and an average laboratory CBR value of 3. The project was divided into five test sections. Each section was divided into two or three subsections each with a different position of the geosynthetic.

The project was divided into six sections (A-F) and evaluated four different geosynthetics. Tenax M330 reinforcement geogrid and Mirafi 67809 high strength geotextile were used in different sections (A-1, A-2, E-3, B-1, and B-2) for reinforcement. Mirafi 180N, a heavy weight nonwoven geotextile, was used for separation in Sections C-2 and E-2. Tenax Tendrain 100-2 drainage geocomposite was used in Sections D-1, D-2, and D-3 as a drainage layer. The road section consisted of a

580 to 640-mm (23 to 25-in.) layer of subbase aggregate overlain by a 180 mm (7 in.) asphalt layer. The reinforcement geogrid was placed at different depths in Sections A-1, A-2, and E-3. In Section A-1, the geogrid was placed at the bottom of a 580-mm (23-in.) subbase aggregate layer. Section A-2 had two layers of geogrid, one place at the bottom of a 640-mm (25-in.) subbase aggregate layer and the other at mid-thickness of that layer. In Section E-3, the geogrid was placed 250 mm (10 in.) below the asphalt layer. Reinforcement geotextile was placed at the bottom of a 580-mm (23-in.) subbase aggregate layer in Section B-1, and at the bottom of a 640-mm (25-in.) subbase aggregate layer in Section B-2. The drainage geocomposite was placed 460 mm (18 in.) below the subgrade layer in Section D-1, at the bottom of a 640 mm (25 in.) subbase aggregate layer in Section D-2, and at the top and bottom of a 640 mm (25 in.) subbase layer in Section D-3.

A control section was also included. It was originally constructed with 640 mm (25 in.) of subbase aggregate, however, traffic loading on the exposed aggregate surface quickly caused the section to fail. The contractor had to re-excavate this section, undercutting an additional 610 mm (24 in.) into the weak subgrade soils. The contractor then placed a total of 1250 mm (49 in.) of subbase aggregate to bring the road back to its indented grade. This problem did not occur in any of the sections with geosynthetics even though the contractor and resident engineer thought that undercutting was needed at several locations. This confirms that geosynthetics can be used to expedite construction of roads on soft subgrades.

The University of Maine instrumented sections of this project to monitor the performance of the geosynthetics. Custom-made loadcells were attached to the geogrid

at five different stations. Strain gages were attached to the geotextile to monitor the tensile forces in two sections. The loadcells or strain gages were attached at offsets that positioned the instruments in the outside wheel path of the right (northbound) lane. Three piezometers were placed at each of five stations to monitor pore water pressures in sections with drainage geocomposite as well as adjacent sections for comparison. Frost penetration was measured at four stations with thermocouples. Instrument measurements were taken from installation until August 1998.

Seven loadcells were attached to geogrid in each instrumented section. In a given section, the loadcells mounted on the geogrid had a survival rate that ranged from zero to 57%. Fortunately, sufficient loadcells remained to allow evaluation of geogrid performance. Results indicate that little force was induced in the geogrid with the majority gained during placement and compaction of the first lift of overlying subbase aggregate. There was little subsequent change in force. In Sections A-1 and A-2 the geogrid is covered by 580 mm (23 in.) and 250 mm (10 in.) of gravel, respectively. In these sections the loadcells showed a force between about 0.75 and 1.0 kN/m (50 and 70 lb/ft). Two loadcells showed higher forces of up to 1.7 kN/m (116 lb/ft) which is only 5% of the ultimate tensile strength of the geogrid. One loadcell was in compression suggesting that there are localized areas of compression. This could have been created by a wave of geogrid that generally advanced ahead of aggregate placement being locally trapped beneath the aggregate.

Strain gages were mounted on the reinforcement geotextile in subsections B-1 and B-2 to measure the tensile stress during and after construction. Gages were placed in pairs, one on each side of the geotextile, to eliminate the effects of bending by averaging

the reading from each pair. These gages were reliable and had 76% survival. Forces ranged from zero to 5 kN/m. For most gages, the majority of force was induced during construction. In addition, there was an apparent increase in force in most strain gages that coincided with spring thaw. Some strain gages also showed continued slow increase in the apparent force after spring thaw. Temperature change and creep were examined as possible reasons for the apparent increase in force, but stable readings during frost penetration and the force being only a small fraction of the ultimate tensile strength, tend to discount these factors. Thus, it is likely that the geotextile did experience an increase in force during the spring thaw.

Piezometers were installed in Sections C-2, D-1, D-2, D-3, and in the control section. These instruments were used to determine if the drainage geocomposite aided in dissipating pore water pressures. Pressures were averaged for the months of October through November, 1997 and June through August, 1998. Due to a malfunctioning readout box, readings were not taken at the critical period of spring melt. The Fall, 1997 readings in the subbase layer of drainage sections (D-1, D-2 and D-3) ranged from 10 to 118 mm (0.4 to 4.6 in.) of water head, while the control section had 414 mm (16 in.) of head and Section C-2 had 138 mm (5.4 in) of head. Theses readings also showed that the amount of head in the subgrade soil of the drainage sections had lower levels (-15.4 to 74 mm (0.6 to 3.0 in)) in comparison to the control section (149 mm (6.0 in.)) and Section C-2 (210 mm (8.0 in.). Readings taken in summer, 1998 show negative head in many piezometers. This could be due to damage to the piezometers during the winter.

A substantial amount of water has come out of outlet pipes. The flow rate was highest during the spring thaw (March). After March, periods of increased flow

coincided with precipitation events. Section D-1, which had a geocomposite placed 460 mm (18 in.) below the subgrade, removed the most water followed by Section D-2 with a geocomposite placed at subgrade. Section D-3 was located in a fill section. Outlet E in this section, which drained the geocomposite placed on subgrade, had less flow than in Sections D-1 and D-2. Outlet F in Section D-3, which drained a geocomposite located directly under the pavement, had no flow. This suggests that the new pavement did not allow ingress of water or that any water that penetrated the pavement was drained away by the subbase course.

Pavement performance has been measured with a falling weight deflectometer (FWD). Readings were taken prior to reconstruction and after reconstruction in April of 1998. The FWD readings were processed with the DARWin Pavement Design and Analysis System (version 3.0). The pavement thickness prior to reconstruction ranged from 127 to 254 mm (5 to 10 in.), making comparison of data from before reconstruction to after reconstruction difficult and possibly misleading. The highest structural number (SN) was obtained in the control sections that had to be under cut 610 mm (24 in.) due to poor subgrade conditions encountered during construction. Since the control section could not be used it for its intended purpose, Section C-2, which only had a separation geotextile placed 640 mm (25 in.) below the asphalt layer, was used as the basis for comparison with the other sections. The April 1998 structural numbers of Section C-2 were higher than the geotextile and geogrid reinforced sections. It is possible that the FWD was incapable of detecting the beneficial effects of the geosynthetics. Subgrade water contents taken during construction were lower in Section E-3 than in Sections A-1, A-2, and B-2. This suggests that the subgrade in Section E-3 was stronger than Sections

A-1, A-2, and B-2. This could be the reason that Section E-3 had a higher SN value in April, 1998. Section A-1, which had one layer of geogrid, had a slightly higher SN value compared to Section A-2, which had two layers of geogrid. The amount of improvement from the original FWD testing and post construction readings show that the greatest improvement is in the undercut section with drainage geocomposite (Section D-1).

6.2 CONCLUSIONS

1. Previous literature indicates little improvement in performance of flexible pavements reinforced with geogrid if the subbase course is thicker than 300 mm (12 in.) and if the pavement is designed to carry more than about 200,000 equivalent 80 kN (18-kip) single axle loads.

2. Forces in the geogrid were induced during placement and compaction of the first lift of overlying aggregate. The forces remained essentially constant during subsequent construction operations and after completion of construction.

3. The force in the geogrid was essentially the same when placed at depths of 250, 580, and 640 mm (10, 23, and 25 in.) in a flexible road section with a 180 mm (7 in.) asphalt layer.

4. Long term forces in the geogrid ranged from –1.5 kN/m to 1.7 kN/m (-103 to 116 lb/ft) for loadcells perpendicular to the centerline. It is less than 5% of

the ultimate strength of the geogrid. This is expected to give only a small reinforcement benefit.

5. Field measurements of force in the geotextile ranged from 0.05 to 5.0 kN/m (3 to 343 lb/ft). This range could be due to factors such as differences in subgrade strength, wrinkles in the fabric during application of the first lift of overlying aggregate, and the degree and location of rutting by construction vehicles.

6. The structural number (SN) in sections with reinforcement geogrid and geotextile ranged from 74 to 101% of the value obtained in a section with only separation geotextile. Thus, reinforcement did not increase the SN as backcalculated from Falling Weight Deflectometer tests.

7. Such a small magnitude of induced force in the geogrid and geotextile and little improvement in structural number suggest little reinforcing benefits for the thick subbase course used in this study.

8. The structural number (SN) in the Section D-1 with drainage geocomposite placed 460 mm (18 in.) below subgrade was 7% higher than the SN in a section with only separation geotextile. However, the SN of sections with drainage geocomposite on subgrade was 7% lower than the section with only the separation geotextile. This suggests that the drainage geocomposite may slightly improve the SN when placed below the subgrade.

9. The geocomposite drainage layers aided in removing water from the road system, especially in the months of spring thaw. Section D-1, with a drainage geocomposite 460 mm (18 in.) below the subgrade had the largest amount of water discharge. In contrast, Section D-3, with drainage geocomposite at subgrade and at the bottom of the asphalt, which is located in a fill section, had negligible discharge of water. This suggests that drainage geocomposites are more beneficial in cut sections and should be located as far below the pavement as possible.

6.3 RECOMMENDATIONS FOR FURTHER RESEARCH

The 3.0-km (1.9-mile) section of U.S. Route 1A in the towns of Frankfort and Winterport should be monitored for at least the next 5 years. After the first 5 years of monitoring, the type of monitoring that is needed for the next 5-year increment should be determined. During the first 5 years, instrument readings should be taken five times per year for loadcells, strain gages, thermocouples and piezometers. Additional weekly piezometer readings should be taken during spring melt. Falling weight deflectometer readings should be taken during the summer and weekly during the spring melt. Visual observations of rutting patterns and depths, and cracking should be conducted annually.

The next research objective should be to monitor use of geogrid and geotextile reinforcement, and geocomposite drainage on pavement sections with thinner subbase courses. A proposal focused on this objective has been submitted to the New England Transportation Consortium.

BIBLIOGRAPHY

Al-Qadi, I., Brandon, T., Valentine, R., Lacina, B., and Smith, T. (1994), "Laboratory Evaluation of Geosynthetic-Reinforced Pavement Sections," Transportation Research Record No. 1439, Transportation Research Board, Washington, D.C., pp. 25-31.

Anderson, P. and Killeavy, M. (1989), "Geotextiles and Geogrids: "Cost Effective Alternate Materials for Pavement Design and Construction", Proceedings of Geosynthetics '89, San Diego, Ca., pp. 353-364.

Barksdale, R. D., and Brown, S. F. (1987), "Geosynthetic Reinforcement of Aggregate Bases of Surfaced Pavements." Paper presented at the 66th Annual TRB Meeting, Washington, D.C. pp. 1-32.

Barksdale, R. D., Brown, S. F., and Chan, F. (1989) "Potential Benefits of Geosynthetics in Flexible Pavement Systems." National Cooperative Highway Research Program Report 315, Transportation Research Board, Washington, D.C.

Bathurst, R. J., and Raymond, G. (1987), "Geogrid Reinforcement of Ballasted Track," Transportation Research Record No. 1153, Transportation Research Board, Washington, D.C., pp. 8-14.

Bender, D. A., and Barenberg, E. J. (1978), "Design and Behavior of Soil-Fabric-Aggregate Systems" Transportation Research Record No. 671, Transportation Research Board, Washington, D.C., pp. 64-73.

Brandon, T. L., Al-Qadi, I. L., Lacina, B. A., and Bhutta, S. A., (1996), "Construction and Instrumentation of Geosynthetically Stabilized Secondary Road Test Sections" Transportation Research Record No. 1534, Transportation Research Board, Washington, D.C., pp. 50-57

Cancelli, A., Montanelli, F., Rimoldi, P., and Zhao, A., (1996) "Full Scale Laboratory Testing on Geosynthetics Reinforced Paved Roads" Proceedings of The International Symposium on Earth Reinforcement, Vol. I. pp. 573-578.

Christopher, B. R., and Holtz, R. D. (1991), "Geotextiles For Subgrade Stabilization in Permanent Roads and Highways" Proceedings of Geosynthetics '91, Atlanta, Georgia, pp. 701-713.

Christopher, B. R. (1998), "Geotextiles in Filtration Applications", Christopher Consultants, Roswell, Georgia, pp. 1-17.

Collin, J. G., Kinney, T. C., and Fu, X. (1996), "Full Scale Highway Load Test Of Flexible Pavement Systems With Geogrid Reinforced Base Courses," Proceedings of Geosynthetics International, Vol. 3, No.4 pp. 537-549.

Farrag, K., Oglesby, J., and Griffin, P. (1994), "Large Strain Measurements in Geogrid Reinforcement," Transportation Research Record No. 1439, Transportation Research Board, Washington D.C. pp. 41-45.

Giroud, J. P. (1985), "Design of Unpaved Roads and Trafficked Areas With Geogrids," PolymerGrid Reinforcement, Thomas Telford Limited, London, pp. 116-127.

Glynn, D. T. and Cochrane, S. R. (1987), "The Behavior of Geotextiles as Separating Membranes on Glacial Till Subgrade," Proceedings of Geosynthetic '87 New Orleans, LA, pp. 26-36.

Haas, R., Walls, J., and Carroll, R. G. (1988) "Geogrid Reinforcement of Granular Bases in Flexible Pavements," Transportation Research Record No. 1188, Transportation Research Board, Washington D.C., pp. 19-27.

Halim, A., Haas, R., and Phang, W. A. (1983) "Geogrid Reinforcement of Asphalt Pavements and Verification of Elastic Theory," Transportation Research Record No. 949, Transportation Research Board, Washington D. C., pp. 55-65.

Halliday, A. R., and Potter, J. F., (1984) "The Performance of a Flexible Pavement Constructed on a Strong Fabric," Transport and Road Research Laboratory, Report LR1123.

Hayden, S.A., and Dunn, P.A., Jr. (1996) "The Use of Geosynthetics with Reinforcement, Separation, and Drainage Applications for Highway Construction Along a 3.0 km (1.9-mile) Portion of Route 1A in the Towns of Frankfort and Winterport (Final Proposal)," State of Maine Department of Transportation, Bangor, Maine.

Hayden, S.A., Christopher, B. R., Humphrey, D. N., Dunn, P. A., and Fetten, C. P. (1998) "Instrumentation of Reinforcement, Separation and Drainage Geosynthetic Test Sections used in the Reconstruction of a Highway in Maine" Proceedings of the Conference on Cold Regions Impact on Civil Works, ASCE, New York, pp. 420-433.

Henry, K. S. (1996), "Geotextiles to Mitigate Frost Effects in Soils: A Critical Review," Transportation Research Record No. 1534, Transportation Research Board, Washington D. C., pp. 5-11.

Henry, K. S. (1991), "Effect of Geotextiles on Water Migration in Freezing Soils and The Influence of Freezing on Performance," Proceedings of Geosynthetics '91, Atlanta, Georgia, pp. 469-483.

Jewell, R. A. (1985), "Interaction between Soil and Geogrids" Polymer Grid Reinforcement, Thomas Telford Limited, London. pp. 18-30.

Jarrett, P. M. (1985), "Evaluation of Geogrids for Construction of Roadways Over Muskeg," Polymer Grid Reinforcement, Thomas Telford Limited, London. pp. 149-153.

Kennepohl, G., Kamel, N., Walls, J., and Haas, R. C. (1985), "Geogrid Reinforcement of Flexible Pavements Design Basis and Field Trials," Asphalt Paving Technology, Association of Asphalt Paving Technologists, Vol. 54, San Antonio, Texas, pp. 45-76.

Kinney, T., and Barenberg, E., (1982), "The Strengthening Effect of Geotextiles on Soil Geotextile-Aggregate Systems", Proceedings of The Second International Conference on Geotextiles, Las Vegas, NV, pp. 347-352.

Kinney, T. C., and Savage, B. M. (1989), "Using Geosynthetics to Control Lateral Spreading Of Pavements in Alaska-Preliminary Results," Proceedings of Geosynthetics '89, San Diego, CA, pp. 324- 333.

Milligan, G. W. E., Love, J. P. (1985), "Model Testing of Geogrids Under An Aggregate Layer on Soft Ground," Polymer Grid Reinforcement, Thomas Telford Limited, London. pp. 128-138.

Penner, R., Haas, R., and Walls, J., (1985), "Geogrid Reinforcement of Granular Bases," Presented to Roads and Transportation Association of Canada Annual Conference, Vancouver. pp. 263-292.

Perkins, S. W., Ismeik, M., Fogelson, M.L., Wang, Y., and Cuelho, E. V. (1998), "Geosynthetic-Reinforced Pavements: Overview and Preliminary Results." Proceedings of Sixth International Conference on Geosynthetics, Atlanta, GA, pp. 1-8.

Perkins, S. W., Ismeik, M., and Fogelsong, M. (1998) "Mechanical Response of a Geosynthetic-Reinforced Pavement System to Cyclic Loading," Fifth International Conference on the Bearing Capacity of Roads and Airfields, Trondheim, Norway, Vol. 3, pp. 1503-1512.

Perkins, S. W., and Ismeik, M. (1997), "A Summary of Geosynthetic Reinforced Flexible Pavements," Proceedings of the 32nd Symposium on Engineering Geology and Geotechnical Engineering, March, Boise, Idaho, pp.127-134.

Robnett, Q. L., and Lai, J. S. (1982), "Fabric-Reinforced Aggregate Roads – Overview" Transportation Research Record No. 875, Transportation Research Board, Washington D.C., pp. 42-49.

Shrestha, S. C., and Bell, J. R. (1982), "Creep Behavior of Geotextiles Under Sustained Loads," Proceedings of the Second International Conference on Geotextiles, Las Vegas, Nevada, August, Vol. III, pp. 769-774 and discussion Vol. IV, pp. 120-122.

Sowers, G. F., Collins, S. A., and Miller, D. G. (1982) "Mechanism of Geotextile-Aggregate Support in Low-Cost Roads," Proceedings of the Second International Conference On Geotextiles, Las Vegas, Nevada, Vol. II, pp. 341-346.

Webster, S. L. (1992), "Geogrid Reinforced Base Courses for Flexible Pavements for Flexible Pavements for Light Aircraft, Test Section Construction, Behavior Under Traffic, Laboratory Tests, and Design Criteria," Report No. 0156267, DOT/FAA/RD-92/25, U.S. Dept. Of Transportation, Federal Aviation Administration, Washington, D.C., pp. 1-85.

White, D. W., (1991), "Literature Review on Geotextiles to Improve Pavements For General Aviation Airport," Report No. GL-91-3. U.S. Army Engineers Waterways Experiment Station, Vicksburg, Mississippi, pp. 1-46.

Wathugala, G. W., Huang, B., and Pal, S. (1996), "Numerical Simulation of Geosynthetic-Reinforced Flexible Pavements", Transportation Research Record No. 1534, Transportation Research Board, Washington D.C., pp. 58-65.

Wu, T. H., (1989), "Behavior of Soil-Geotextile Composites and its Application to Finite Element Analysis," Proceedings of Geosynthetics '89, San Diego, CA, pp. 365- 372.

APPENDIX
CALIBRATION TESTS AND FIELD MEASUREMENTS

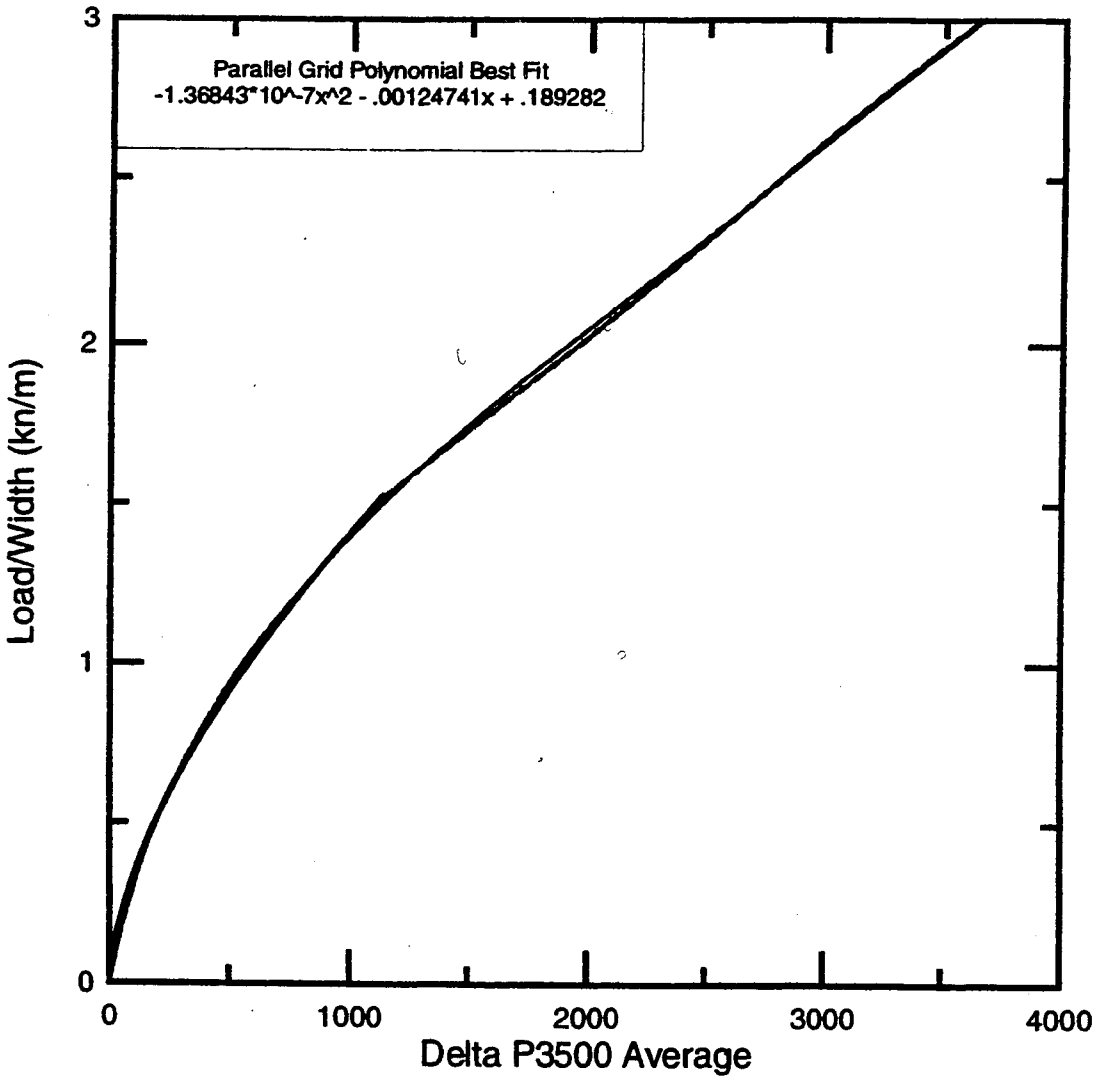

A-1 Calibration for load cells parallel to centerline.

Average curve for first loading of six calibration tests with the load cell in the parallel to centerline direction.

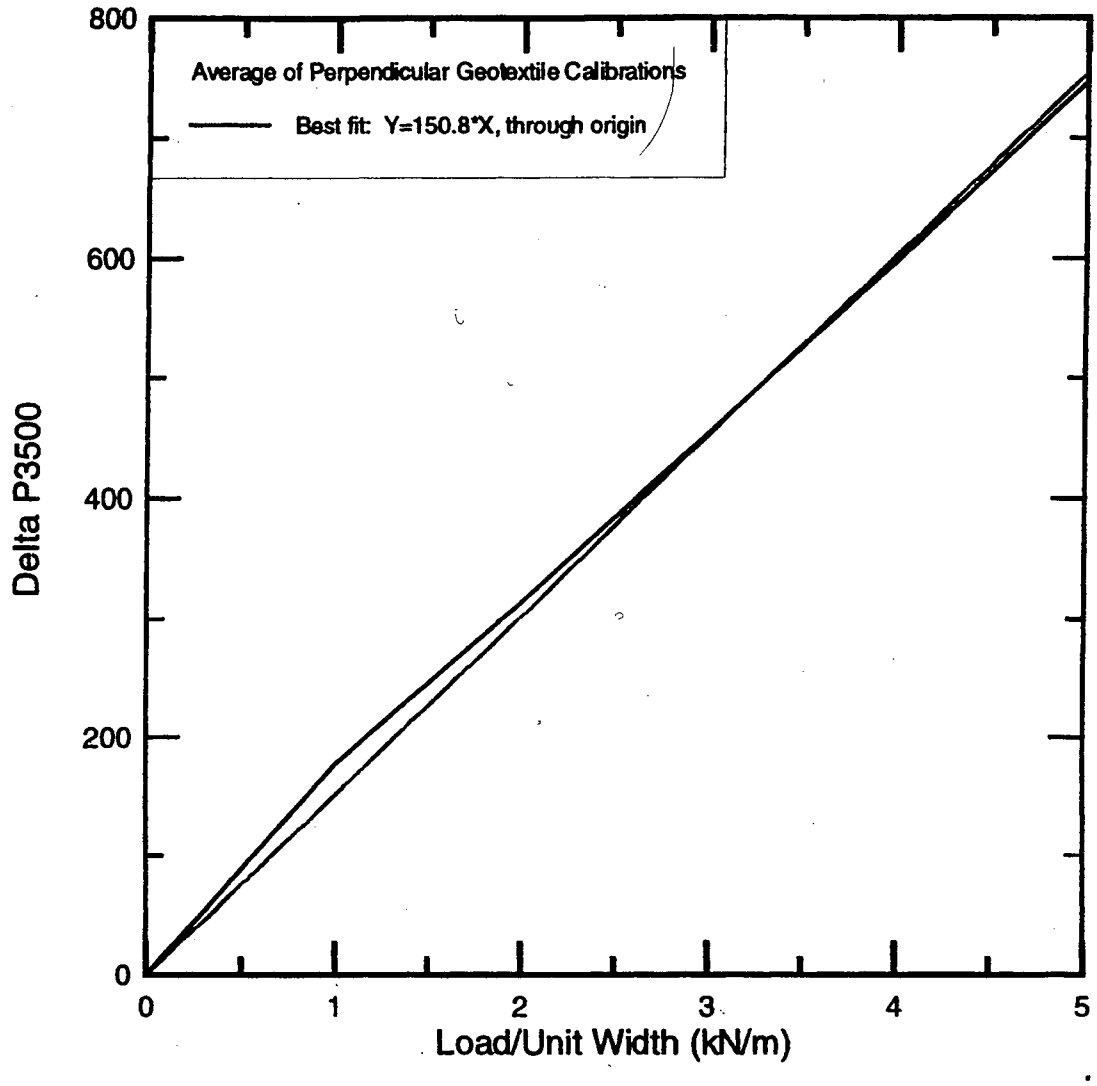

A-2 Calibration of geotextile strain gages perpendicular to centerline

Average of initial locating of six calibration tests with the strain gage placed perpendicular to the centerline.

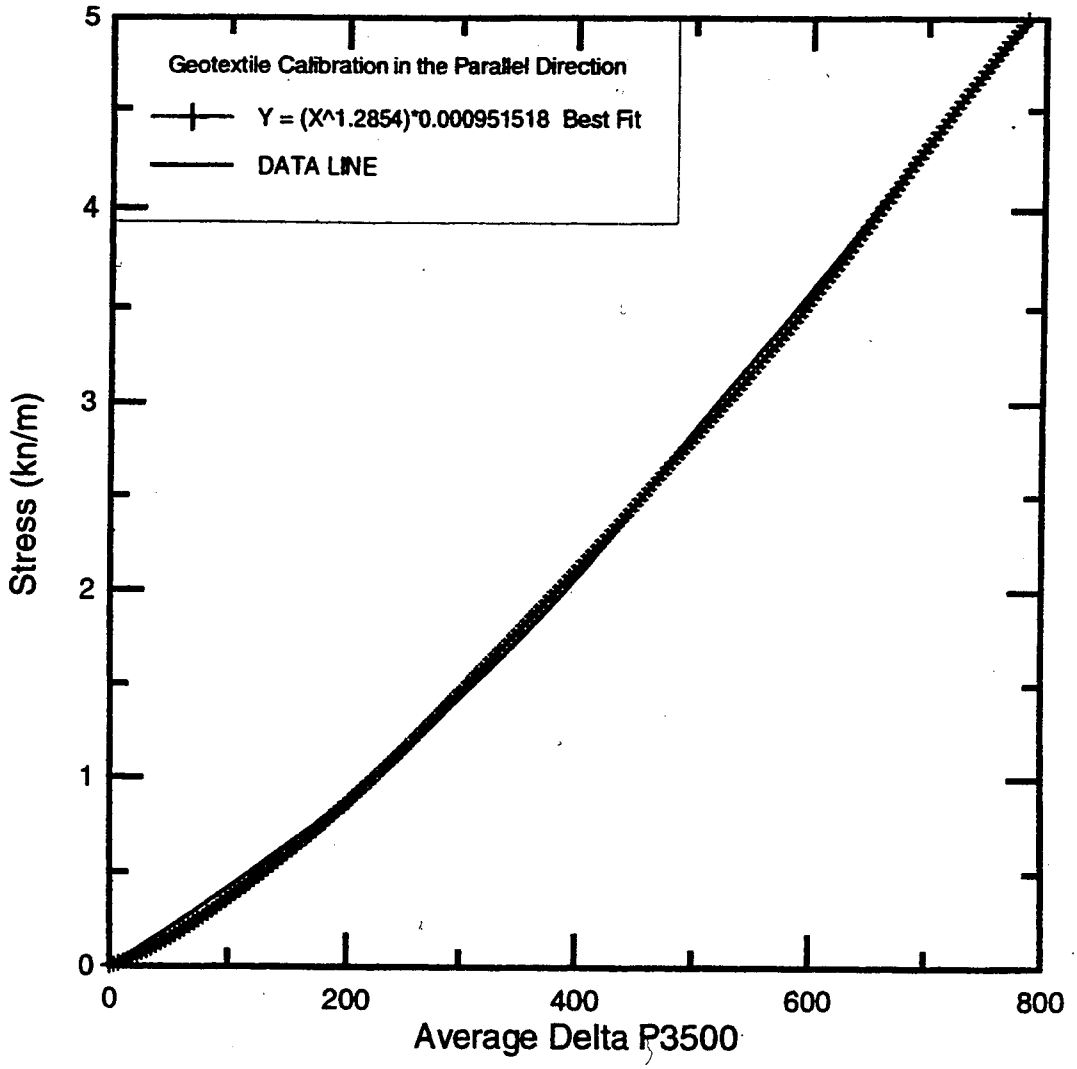

A-3 Calibration of geotextile strain gages parallel to centerline

Average of initial locating of five calibration tests with the strain gage placed parallel to the centerline.

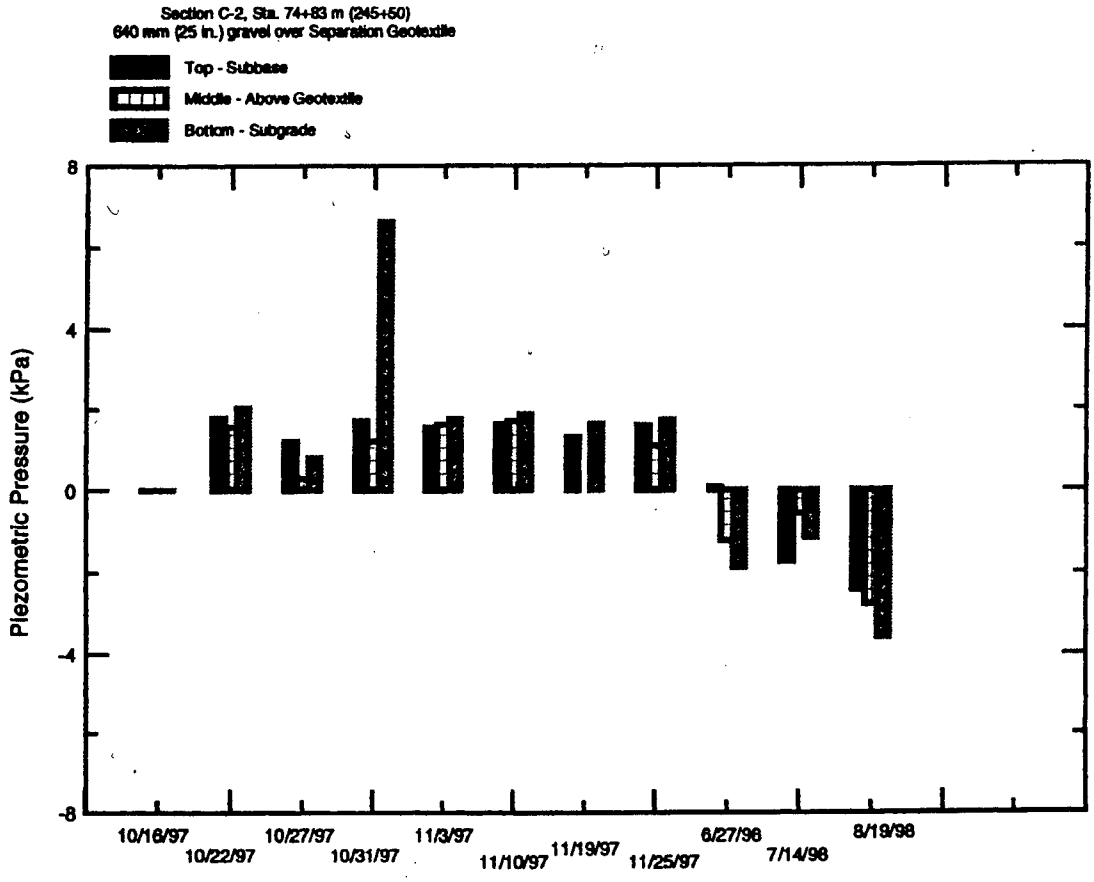

A-4 Piezometer readings for section C-2.

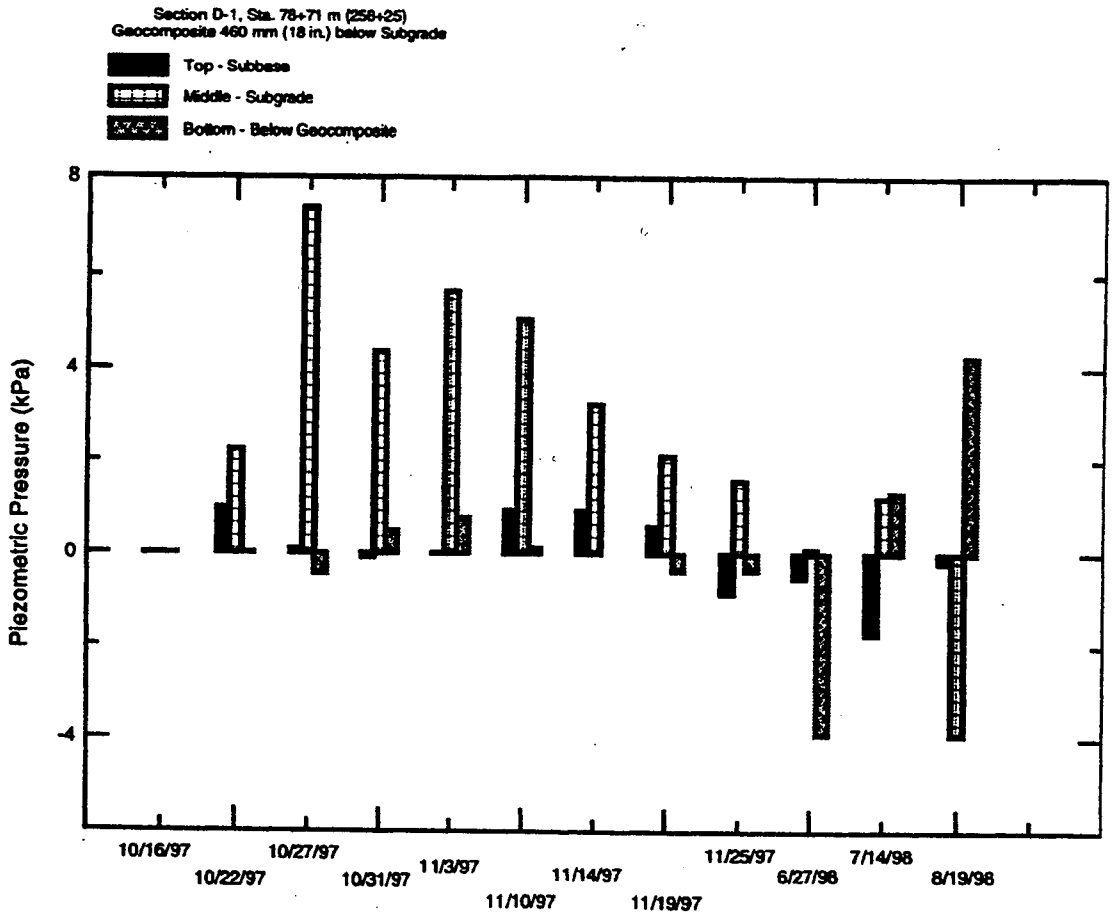

A-5 Piezometer readings from Section D-1.

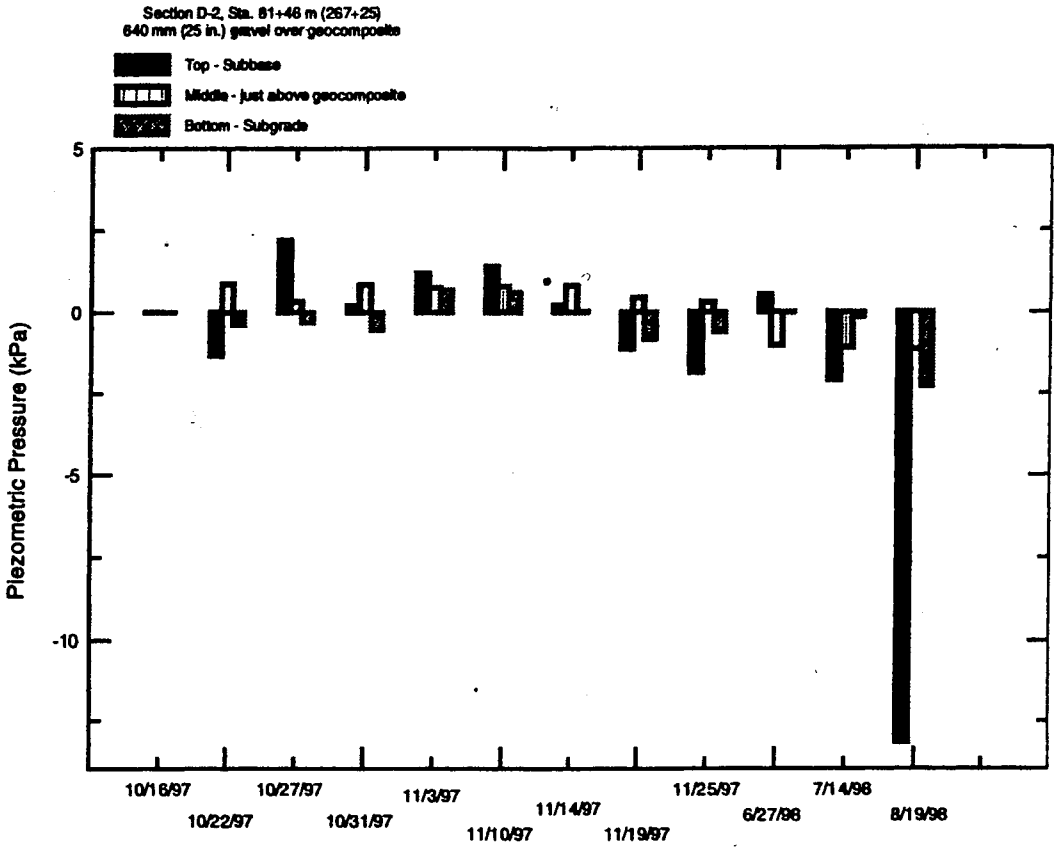

A-6 Piezometer readings from Section D-2.

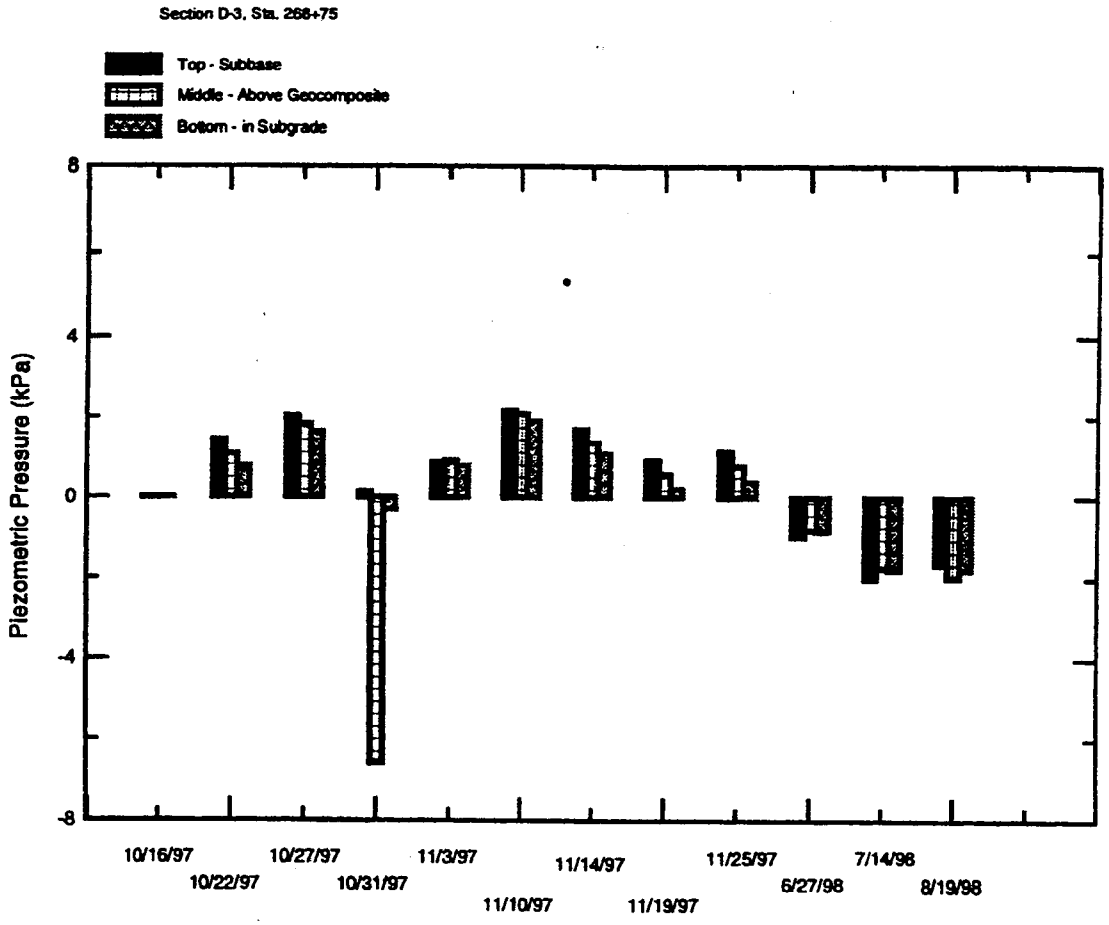

A-7 Piezometer readings from Section D-3.

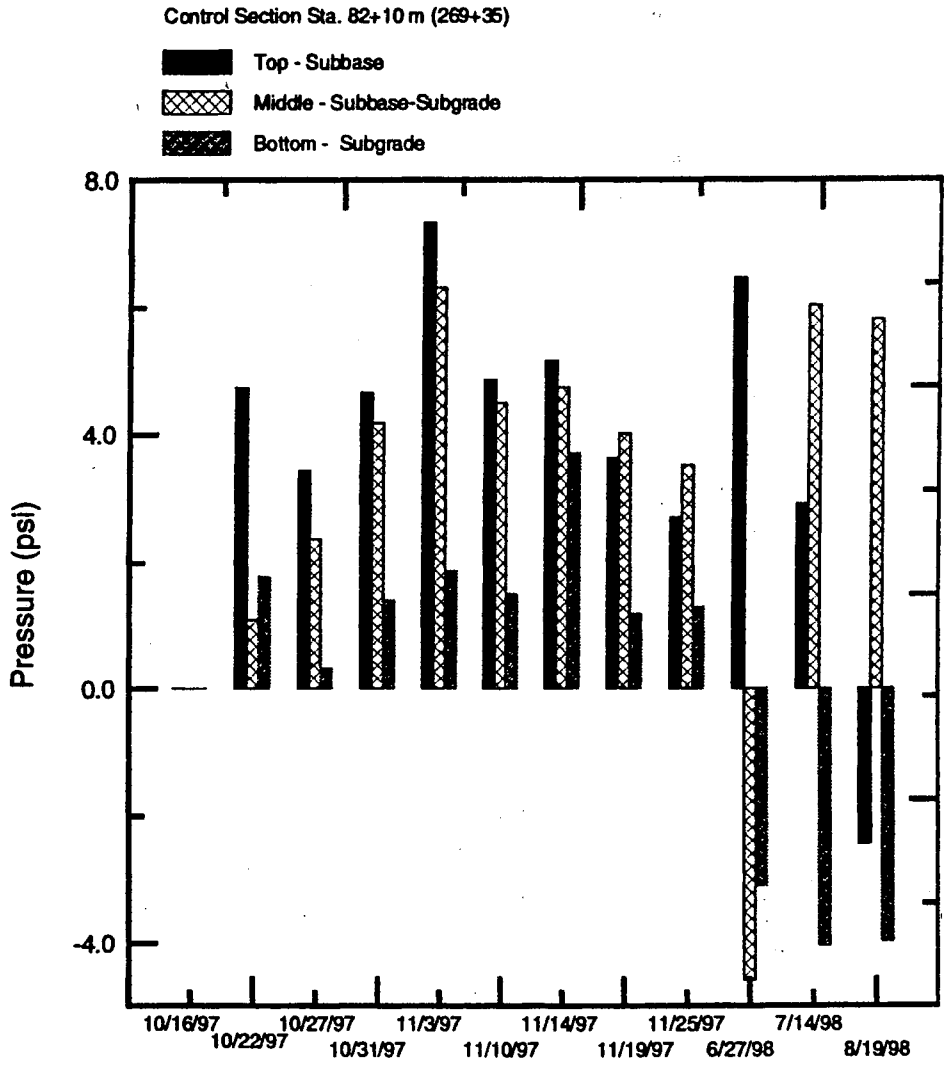

A-8 Piezometer readings for Control Section.